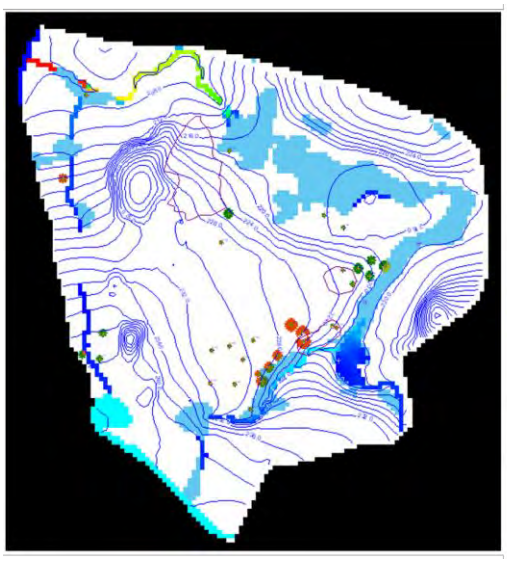
Hodge.WaterResources

# Historical Groundwater Reconstruction Study Transport of PFAS to the Grove Pond Wellfield

*Ayer, Massachusetts*






**Prepared for:**

SILENT SPRING INSTITUTE
Researching the Environment and Women's Health

320 Nevada Street, Suite 302
Newton, MA 02460

**Prepared by:**

HWR
Hodge.WaterResources, LLC

95 Arlington St.
Brighton, MA 02135

June 17, 2025

Revision: 0.0

# TABLE OF CONTENTS

**SECTION** **PAGE**

Executive Summary ..... 4
1.0 Introduction ..... 6
1.1 Project Objectives and Scope ..... 6
1.2 PFAS in General ..... 7
1.3 Previous and Ongoing Studies ..... 8
2.0 Site Description and History ..... 10
2.1 Site Description ..... 10
2.2 Historical PFAS Contamination ..... 10
2.2.1 AOC 57 ..... 10
2.2.2 AOC 74 ..... 10
2.2.3 AOC 75 ..... 11
2.2.4 AOC 32/43A ..... 11
2.2.5 AOC 5 (Shepley's Hill Landfill) ..... 11
2.2.6 MAARNG ..... 11
2.3 PFAS Source Summary ..... 12
2.4 Ayer Water Distribution System ..... 14
2.4.1 Grove Pond Pumping History ..... 14
2.4.2 PFAS Contamination at the Grove Pond Wellfield ..... 18
2.5 Summary ..... 21
3.0 Hydrogeologic Setting ..... 22
3.1 Topography and Hydrology ..... 22
3.2 Geology ..... 25
3.3 Hydrogeology ..... 28
4.0 Conceptual Site Model ..... 34
4.1 Potential Transport Pathways ..... 34
4.2 PFAS Source Area Sampling Near Grove Pond Wellfield ..... 35
4.2.1 PFOS ..... 36
4.2.2 PFOA ..... 44
4.2.3 PFHpA ..... 44
4.2.4 PFHxS ..... 44
4.2.5 PFHxA ..... 44
4.2.6 PFNA ..... 44
4.3 Transport Pathways and Groundwater Quality Sample Results ..... 44
4.4 Fingerprinting PFAS Sources ..... 45
4.5 PFAS-Specific Transport Considerations ..... 47
4.6 Reconciling Historical Information and the CSM ..... 47
4.7 CSM Summary ..... 47
5.0 Groundwater Flow Modeling ..... 49
5.1 Groundwater Flow Model Development ..... 49
5.1.1 Model Domain ..... 49
5.1.2 Model Discretization ..... 50
5.1.3 Surface Water Features as CLNs and Boundary Conditions ..... 50
5.1.4 Recharge and Evapotranspiration ..... 53
5.1.5 Hydraulic Conductivity, Specific Storage, Specific Yield, and Porosity ..... 55
5.2 Groundwater Flow Model Calibration ..... 57
5.2.1 Calibration Dataset ..... 57
5.2.2 Calibration Parameters ..... 58

5.3 Groundwater Flow Model Calibration Performance ..... 61
5.3.1 Quantitative Evaluation of Groundwater Flow Model Calibration ..... 64
5.3.2 Qualitative Evaluation of Groundwater Flow Model Calibration ..... 66
5.3.2.1 Infiltration at Grove Pond ..... 66
5.3.2.2 Cold Spring Brook ..... 66
5.3.2.3 Comparison to Former Fort Devens Regional Groundwater Flow Model ..... 67
5.4 Summary of Groundwater Flow Modeling ..... 68
6.0 Groundwater Transport Modeling ..... 69
6.1 Model Setup ..... 69
6.1.1 Transient Boundary Conditions ..... 69
6.1.2 Transport Boundary Conditions ..... 70
6.2 Transport Model Confidence Building ..... 71
6.2.1 Transport Model Source Concentrations ..... 72
6.2.2 Transport Model Retardation Factors ..... 72
6.2.3 Transport Model Dispersivity ..... 73
6.3 Transport Model Results ..... 74
6.4 Sensitivity Analysis ..... 80
7.0 Estimate of PFAS Concentrations at Grove Pond Wells ..... 83
8.0 References ..... 88

**TABLES**

Table 1-1: Previous Investigations Related to Grove Pond Wellfield ..... 9
Table 5-1: Boundary Conditions ..... 53
Table 5-2: Aquifer Properties: Specific Storage, Specific Yield, and Porosity ..... 57
Table 5-3: Recharge and Evapotranspiration Calibrated Values ..... 60
Table 6-1: Transport Model PFAS Source Strength Concentrations ..... 72
Table 6-2: Transport Model Retardation Factors ..... 73
Table 7-1: Average PFNA Concentration at Grove Pond Wellfield ..... 87

**FIGURES**

Figure 2-1: Locus Map and Site Layout ..... 13
Figure 2-2: Grove Pond Zone II Limits ..... 15
Figure 2-3: Grove Pond Wellfield Individual Well Locations with Well Depths and Screened Intervals ..... 15
Figure 2-4: Interpreted Annual Groundwater Pumping ..... 16
Figure 2-5: Grove Pond Individual Well Pumping (Monthly Average) ..... 17
Figure 2-6: Grove Pond Individual Well Pumping (Annual Average) ..... 17
Figure 2-7: PFAS6 Time Series at Grove Pond Wells ..... 18
Figure 2-8: Individual PFAS Timeseries at GP-01 ..... 19
Figure 2-9: Individual PFAS Time Series at GP-06 ..... 19
Figure 2-10: Individual PFAS Time Series at GP-07 ..... 20
Figure 2-11: Individual PFAS Time Series at GP-08 ..... 20
Figure 3-1: Topography in Vicinity of Grove Pond Wellfield (MassGIS, 2024) ..... 23
Figure 3-2: Grove Pond and Plow Shop Pond Bathymetry (Mercadante et al., 1999) ..... 24
Figure 3-3: Surficial Geology in Vicinity of Grove Pond Wellfield (MassGIS, 2024a) ..... 26
Figure 3-4: Bedrock Elevations in Vicinity of Grove Pond Wellfield ..... 27
Figure 3-5: Groundwater Surface Contouring 1992 (CDM, 1993) ..... 28
Figure 3-6: Groundwater Surface Contours from KGS (2020) ..... 29
Figure 3-7: Estimates of Hydraulic Conductivity from Zone II Study (CDM, 1993) ..... 31
Figure 3-8: Estimates of Hydraulic Conductivity from SHL Study (Geosyntec, 2020) ..... 32

Figure 4-1: Schematic of Conceptual Site Model ..... 35
Figure 4-2: Iso-Concentration Contours of PFOS in Groundwater ..... 38
Figure 4-3: Iso-Concentration Contours of PFOA in Groundwater ..... 39
Figure 4-4: Iso-Concentration Contours of PFHpA in Groundwater ..... 40
Figure 4-5: Iso-Concentration Contours of PFHxS in Groundwater ..... 41
Figure 4-6: Iso-Concentration Contours of PFHxA in Groundwater ..... 42
Figure 4-7: Iso-Concentration Contours of PFNA in Groundwater ..... 43
Figure 4-8: PFAS Radar Plots ..... 46
Figure 5-1: Model Domain ..... 50
Figure 5-2: Model Grid Discretization ..... 51
Figure 5-3: Surface Water Feature CLNs and Boundary Conditions ..... 52
Figure 5-4: Land Use Types, Recharge and Evapotranspiration Factors ..... 55
Figure 5-5: Hydraulic Conductivity Zones ..... 56
Figure 5-6: Groundwater Surface Calibration Targets ..... 58
Figure 5-7: Hydraulic Conductivity Calibrated Values ..... 59
Figure 5-8: CLN FSKIN Calibrated Values ..... 60
Figure 5-9: Calibrated Groundwater Flow Model Groundwater Elevation (Layer 1 and Layer 2) ..... 62
Figure 5-10: Calibrated Groundwater flow model Groundwater Elevation (Layer 3 and Layer 4) ..... 63
Figure 5-11: Calibration Residual Values Versus Observed Groundwater Levels ..... 65
Figure 5-12: Modeled Groundwater Levels Versus Observed Groundwater Levels ..... 65
Figure 5-13: Groundwater Head and Water Flux in Model CLNs ..... 66
Figure 5-14: Cold Spring Brook Groundwater Surface Contour Comparison ..... 67
Figure 5-15: Regional Groundwater Flow Model Results (Papadopulos, 2022) ..... 68
Figure 6-1: Transient Model Pumping Rates for Grove Pond Wells ..... 69
Figure 6-2: Transport Model PFAS Source Terms ..... 70
Figure 6-3: Modeled and Observed Iso-Concentration Contours of PFOS in Groundwater ..... 75
Figure 6-4: Modeled and Observed Iso-Concentration Contours of PFOA in Groundwater ..... 76
Figure 6-5: Modeled and Observed Iso-Concentration Contours of PFHpA in Groundwater ..... 77
Figure 6-6: Modeled and Observed Iso-Concentration Contours of PFHxS in Groundwater ..... 78
Figure 6-7: Modeled and Observed Iso-Concentration Contours of PFHxA in Groundwater ..... 79
Figure 6-8: Modeled and Observed PFOS Concentrations at GP-08 (2016-2022) ..... 80
Figure 6-9: Modeled and Observed PFOA Concentrations at GP-08 (2016-2022) ..... 81
Figure 6-10: Modeled and Observed PFHpA Concentrations at GP-08 (2016-2022) ..... 81
Figure 6-11: Modeled and Observed PFHxS Concentrations at GP-08 (2016-2022) ..... 82
Figure 6-12: Modeled and Observed PFHxA Concentrations at GP-08 (2016-2022) ..... 82
Figure 7-1: Estimated PFAS Concentrations at GP-08 (2000-2020) ..... 85
Figure 7-2: Estimated PFAS Concentrations at GP-01 (2000-2020) ..... 86

**ATTACHMENTS**

Attachment 1: Excerpt from The Public Spirit September 15, 1960

Attachment 2: PFAS Concentration Sample Results in Surface Water with Plume Contour Delineation

Attachment 3: Hydrogeologic Calibration Targets

Attachment 4: Observed and Modeled PFAS Contours for Model Layers 1, 3, and 4

Attachment 5: Observed and Modeled PFAS Concentrations at Grove Pond Wellfield Wells

Attachment 6: Estimated PFAS Concentrations at Grove Pond Wellfield

Digital Attachment 1: Previous Study Reports

## EXECUTIVE SUMMARY

Hodge.WaterResources, LLC, HydroPredictions, LLC, and HydroAnalysis LLC (the Project Team) have completed a historical reconstruction of per- and polyfluoroalkyl substance (PFAS) concentrations at the Grove Pond wellfield in Ayer, Massachusetts. The aquifer that feeds the wellfield has been investigated multiple times, including as part of a wellhead protection area (WPA) study (CDM, 1993), the Shepley's Hill Landfill remediation study (Geosyntec, 2020), and the ongoing PFAS remedial investigation (RI) at nearby former Fort Devens (KGS, 2020; Papadopulos, 2022). These studies provide an extensive body of work that the Project Team used to guide and inform the historical reconstruction of PFAS concentrations in the aquifer and at the wellfield.

The Project Team developed a conceptual site model (CSM) that identifies the Massachusetts Army National Guard (MAARNG) area as the primary source of PFAS at the Grove Pond wellfield. Based on the available historical information, our current understanding is that the original release of PFAS at the MAARNG occurred in 1960. We identify Area of Concern (AOC) 74 as a secondary PFAS source with the use of aqueous film-forming foam (AFFF) beginning in 1996. The primary transport pathway from these two sources to the Grove Pond wellfield is through groundwater. The Project Team identified AOC 57 as a tertiary source. The primary transport pathway from AOC 57 to the wellfield is groundwater discharge into Cold Spring Brook and subsequent induced infiltration back into the aquifer through the bottom of Grove Pond. The available surface water quality samples shows that surface water concentrations in Grove Pond are an order of magnitude lower than concentrations at the wells. This suggests that the majority of PFAS are arriving at the wells via groundwater transport.

We developed a coupled groundwater flow and transport model based on the CSM using the computer code MODFLOW-USG (Panday, 2013) and the graphical user interface Groundwater Vistas (ESI, 2020). Based on the geologic information collected during the previous studies, the Project Team developed a steady-state groundwater flow model of the aquifer. The model domain extends south to north from Robbins Pond to just north of Grove Pond, and west to east from just west Willow Brook to the groundwater divide east Cold Spring Brook. The Project Team calibrated the steady-state flow model to measured groundwater elevations. We then converted the model to a transient model with dynamic pumping at the Grove Pond wellfield. Annual pumping rates at each well were determined from available Massachusetts Department of Environmental Protection (DEP) records for the period from 1986 to 2022. For the years before 1986 (i.e., 1960-1985), the annual pumping rates are based on the total pumping as reported in the Town of Ayer annual reports.

The Project Team implemented transport modeling by introducing source terms at the MAARNG (South and North), AOC 74, and AOC 57. We then engaged in a confidence-building process for the transport model by comparing modeled and observed iso-concentration contours for each PFAS compound. We iteratively adjusted source term strength, aquifer dispersivity, and chemical retardation factors to optimize the match between the modeled and observed PFAS plumes.

The Project Team developed estimated groundwater concentrations at the Grove Pond wellfield for each of the five wells (i.e., GP-01, GP-02, GP-06, GP-07, and GP-08). These estimates are consistent with the CSM for the site. The Project Team is confident that the simulated PFAS concentrations at the Grove Pond wellfield from 2000 through 2022, while uncertain, are defensible based on the available information.

The estimated PFAS concentrations at the Grove Pond wellfield are an estimate of the PFAS concentrations entering the Ayer drinking water supply system. The transport modeling indicates that the

PFAS plumes were migrating towards the wells throughout 2000-2022. PFAS concentrations at the Grove Pond wellfield were slowly and steadily increasing until 2013 when wells GP-06, GP-07, and GP-08 were developed. Those wells are located west of GP-01 and GP-02, closer to the primary PFAS source, and at locations with elevated PFAS concentrations relative to wells GP-01 and GP-02. Prior to 2013 estimated PFAS concentrations from the Grove Pond wellfield range from approximately 1 to 40 nanograms per liter (ng/L) depending on the specific PFAS compound. After 2013, estimated PFAS concentrations at the Grove Pond wellfield range from 4 to 125 ng/L depending on the specific PFAS compound.

# 1.0 INTRODUCTION

Silent Spring Institute (SSI) asked Hodge.WaterResources, LLC to conduct a historical reconstruction of per- and polyfluoroalkyl substances (PFAS) concentrations at the Grove Pond wellfield in Ayer, Massachusetts. Hodge.WaterResources, LLC collaborated with HydroPredictions, LLC and HydroAnalysis LLC to complete this work. References to the Project Team indicate the collective work of these three organizations.

This historical reconstruction of PFAS is part of the Agency for Toxic Substances and Disease Registry (ATSDR) PFAS Multi-site Study (MSS). The PFAS MSS aims to better understand the health impacts of exposure to PFAS through drinking water. The PFAS MSS builds off of the Pease Study (ATSDR, 2024)), a prior study of the former Pease Air Force Base in New Hampshire. The PFAS MSS includes sites in seven different states. Within Massachusetts, the PFAS MSS is focused on two communities: Ayer and Hyannis. This historical reconstruction focuses on the Grove Pond wellfield, one of two public water supply wellfields that supply drinking water to the Ayer water distribution system.

The PFAS MSS sites jointly established the study period to be the years 2000 through 2023. PFAS samples at the Grove Pond wellfield began in late 2016, and Ayer began treating the pumped water to remove PFAS in 2020. An estimate of PFAS concentrations in the groundwater for the years 2000 through 2022 is necessary to achieve the PFAS MSS goals at the Ayer site and maintain consistency with the study for the Spectacle Pond wellfield.

## 1.1 Project Objectives and Scope

The study objective was to estimate PFAS concentrations in the Grove Pond public water supply wells from 2000 through 2022.

The following four PFAS compounds were included in this objective:

- perfluorooctane sulfonic acid (PFOS),
- perfluorooctanoic acid (PFOA),
- perfluorohexane sulfonate (PFHxS), and
- perfluorononanoic acid (PFNA).

PFOS, PFOA, PFNA, and PFHxS were selected because they are the primary focus for exposure reconstruction with pharmacokinetic modeling through the MSS.

For the purposes of analysis, the Project Team expanded the list of PFAS evaluated in this report to include:

- perfluorinated heptanoic acid (PFHpA) and
- perfluorohexanoic acid (PFHxA).

PFHpA and PFHxA were added because they have elevated concentrations at three of the four active wells at the Grove Pond wellfield. References to PFAS in this report are a reference to this set of six PFAS compounds.

The Project Team set out to estimate annual PFAS concentrations in groundwater at the wells by simulating PFAS transport in the aquifer supplying water to the Grove Pond wellfield. Prior to developing the model, the Project Team investigated available information about the aquifer, potential sources of PFAS

contamination, and the Grove Pond wellfield pumping history. The Project Team used this information to develop a conceptual site model (CSM), and a groundwater flow and transport model to estimate PFAS concentrations at the wells.

The state of the science related to PFAS is evolving. In contrast to many other contaminants, the chemical and physical processes involved in PFAS fate and transport are more complex and not fully understood. These limitations result in PFAS fate and transport modeling uncertainty. For the Grove Pond wellfield, PFAS transport uncertainty is coupled with site-specific uncertainty. Information about the sources of the dominant PFAS plumes near the Grove Pond wellfield is limited. The Project Team was not able to ascertain definitive dates or quantities of the known releases. Given the general uncertainty in PFAS transport and the site-specific uncertainty, we concluded that quantifying the uncertainty is not possible. As an alternative, the Project Team engaged in a "confidence building" process (Hassan, 2004). Confidence building ensures against incorrect conclusions based on model results and provides a defensible foundation for decision-making.

### 1.2 PFAS in General

PFAS are a category of synthetic chemicals that include carbon-fluorine bonds. Thousands of different PFAS chemicals have been created since the 1950s (US EPA, 2024a). PFAS have been ubiquitous in manufacturing for many decades. Some of the most common uses include as a surfactant in aqueous film-forming foam (AFFF), as a water/grease repellant for textiles, and as component materials for a wide range of industrial products.

PFAS are commonly called "forever chemicals" due to their persistence in the environment. The properties that make PFAS useful also make them resistant to biodegradation. PFAS are found in water, soil, and air around the world. Some of the most common sources of PFAS in the environment are applications of AFFF, wastewater treatment plants (WWTP), and landfills. These common sources are not an exhaustive list. The ubiquitous nature of PFAS in industrial operations means that any industrial activity has the potential to be a source of PFAS in the environment.

The behavior of PFAS in the environment is different from conventional contaminants. Most of the PFAS that have been detected in the environment have a chemical structure that consists of a hydrophobic (not attracted to water) head and a hydrophilic (attracted to water) tail (ITRC, 2024a). This structure leads PFAS to accumulate at the interface between different media. These interfaces include the groundwater surface (i.e., the interface between air and water) and the interface between soils and groundwater. The accumulated PFAS are typically in the aqueous phase because most PFAS have high aqueous solubility (ITRC, 2024a). The occurrence of pure phase PFAS in the environment is rare (ITRC, 2024a). Polyfluorinated precursor PFAS can transform and typically form perfluoroalkyl acids (ITRC, 2024a).

Partitioning at the soil-water interface is thought to be primarily controlled by sorption through electrostatic interactions and sorption to organic matter via hydrophobic interactions (ITRC, 2024a). The vast number and variable chemical structure of PFAS mean that the partitioning behavior of PFAS has not been fully determined. Conventional approaches to fate and transport modeling may not be as conceptually correct as for conventional contaminants, but these approaches remain the best way to evaluate PFAS fate and transport.

## 1.3 Previous and Ongoing Studies

The aquifer that feeds the Grove Pond wellfield has been investigated for multiple purposes in the past and is part of an active investigation of PFAS from the former Fort Devens historical operations. Table 1-1 lists and describes the work of five previous studies. These studies serve as the foundation for the work described in this report. Digital copies of these documents are included with this report as Digital Attachment 1.

***Table 1-1: Previous Investigations Related to Grove Pond Wellfield***

| Study Title | Reference | Description |
|---|---|---|
| Town of Ayer, Massachusetts Grove Pond Wells Hydrogeologic Investigation and Zone II Aquifer Mapping | CDM, 1993 | This study delineated the wellhead protection area for the Grove Pond wellfield. It included geologic investigations, boring logs, and construction details for Well 1 (GP-01) and Well 2 (GP-02). It also included estimates of hydraulic conductivity based on pumping tests and a three-dimensional groundwater model of the aquifer. |
| FINAL Base-Wide Preliminary Assessment for Evaluation of Perfluoroalkyl Substances, Former Fort Devens Army Installation, BRAC Legacy Sites, Devens Massachusetts | KGS, 2017 | The United States Army Corps of Engineers (USACE) New England District is conducting an extensive investigation into PFAS contamination of groundwater resulting from past activities at Fort Devens. This preliminary assessment includes summaries of historical activities and records research to identify releases of PFAS to the environment, including the aquifer that feeds the Grove Pond wellfield. |
| Shepley's Hill Landfill Groundwater Flow Model Revision Report, Former Fort Devens Army Installation, Devens, Massachusetts | Geosyntec, 2020 | The Shepley's Hill Landfill is located west of Grove Pond. This study developed a groundwater model to evaluate remediation options for arsenic contamination in groundwater originating from the landfill. The study included geologic investigations, water level measurements, hydraulic conductivity testing, and the development of a three-dimensional groundwater model that extends from approximately one mile west of Grove Pond to just east of the eastern edge of Grove Pond. |
| Area 1 Preliminary Site Characterization Summary, Per- and Polyfluoroalkyl Substances (PFAS) Remedial Investigation, Former Fort Devens Army Installation, Devens, MA | KGS, 2020 | Area 1 is the portion of the USACE investigation that includes the Grove Pond wellfield. The work completed includes water level monitoring, and PFAS sampling in groundwater and soil. The study included limited geological investigations. |
| Regional Groundwater Flow Model of the Former Fort Devens, Massachusetts | Papadopulos, 2022 | This groundwater modeling study used water levels and geologic investigations from KGS (2020) and previous modeling of Fort Devens to develop a calibrated steady-state model of groundwater flow throughout the Fort Devens region. The model domain for this groundwater model extends from the southern limit of South Post (approximately 10 miles south of Grove Pond) to approximately two miles north of Grove Pond. The model domain also extends from two miles west of the Nashua River to approximately two miles east of Grove Pond. |

# 2.0 SITE DESCRIPTION AND HISTORY

## 2.1 Site Description

The town of Ayer is located in eastern Massachusetts approximately 30 miles northwest of Boston. The town provides drinking water to most of its residents through a water distribution system. The source waters for the town's distribution system are the Grove Pond wellfield and Spectacle Pond wellfield with each wellfield located adjacent to their respective ponds. Figure 2-1 shows the location of Grove Pond. Cold Spring Brook drains to Grove Pond which in turn flows to Plow Shop Pond. A small dam at the western end of Plow Shop Pond controls the water levels in Plow Shop Pond and Grove Pond. Water that flows over the dam enters Nonacoicus Brook. Willow Brook drains Robbins Pond and joins Nonacoicus Brook prior to the brook flowing into the Nashua River. This set of streams and ponds provides a natural demarcation of the region of interest for evaluating PFAS contamination at the Grove Pond wellfield.

## 2.2 Historical PFAS Contamination

The region of interest is part of the northeastern corner of Fort Devens. Fort Devens was originally established in 1917 and became a permanent military installation in 1932. Fort Devens remained active until 1990 (KGS, 2017, pg. 2-1). Military training occurred at Fort Devens. These activities included the use and storage of various products including ordnance (i.e., explosive material), jet fuel and other petroleum products, AFFF, and many other industrial products (KGS, 2020). As a permanent installation, Fort Devens also included many municipal activities such as the operation of landfills (e.g., Shepley's Hill Landfill), a wastewater treatment facility, and water supply wells. KGS (2020) identified potential PFAS sources within the region of interest. Some of the potential sources are named Areas of Concern (AOCs) while others are identified by a site-specific name. The potential sources that the Project Team determined to be relevant in this study are shown in Figure 2-1 and described below.

### 2.2.1 AOC 57

AOC 57 is located between Barnum Road and Cold Spring Brook southeast of former Building 3713. In 1977, an estimated 50 to 100 gallons of fuel oil were spilled, some of which entered a storm drain (KGS, 2020, pg. 3-1). Investigations in 1992 identified polycyclic aromatic hydrocarbons and petroleum hydrocarbons. Remediation activities were completed between 1994 and 2003 (KGS, 2020, pg. 3-2). PFAS Remedial Investigation (RI) sampling in 2018 identified elevated PFAS concentrations in soil, groundwater, surface water, and sediments (KGS, 2020).

### 2.2.2 AOC 74

AOC 74 is located near Barnum Road behind former Building 3773. At the time of Fort Devens' closure, the Fort Devens Fire Department became the Devens Fire Department, part of the organization MassDevelopment. As a part of this transition, firefighting training moved from the Fort Devens airfield to the former Building 3773. The training conducted at the site included the use of AFFF (KGS, 2020, pg. 4-1). The exact timeline of the firefighting training activities is not well documented. The Project Team understands that firefighting training and the use of AFFF at AOC 74 did not begin until 1996, when Fort Devens was closed. Until that time, firefighting training had occurred at the Moore Army Airfield (KGS, 2017, pg. 2-9). After the base closed, the firefighting training was moved to Building 3773 (i.e., AOC 74) (KGS, 2017, Appendix C, pg. 1). To the best of our knowledge, firefighting training at AOC 74 ceased in or around the year 2000. Sample results from 2018 show elevated PFAS concentrations in soil, groundwater, surface water, and sediments (KGS, 2020).

### 2.2.3 AOC 75

AOC 75 is located off Saratoga Street and was the site of former Building T-1445. KGS (2020, pg. 5-1) indicate that a large fire occurred at some point in the late 1980s or early 1990s. AFFF was reportedly used to extinguish this fire. No estimate of the amount of AFFF was reported by KGS (2020), but they did note that storm drains located adjacent to the former building T-1445 drained to Cold Spring Brook, and AFFF may have been transported via storm drain to the brook (KGS, 2020, pg. 5-2). Sample results from 2018 show elevated PFAS concentrations in soil, groundwater, surface water, and sediments (KGS, 2020).

### 2.2.4 AOC 32/43A

AOC 32/43A is located on the west side of Cook Street. AOC 32/43A is also referred to as the Defense Reutilization and Marketing Office (DRMO). In the years 1964 through 1995, the area was used to store various materials including equipment containing lead-acid batteries, reusable parts from vehicles, and tires (KGS, 2017, pg. 2-17). There is no history of PFAS-specific contamination at this location (e.g., the use of AFFF), and KGS (2017, pg. 2-17) concluded that there was no exposure pathway for contamination to reach soil or groundwater based on current land uses. The area was not included in the Area 1 Site Characterization (KGS, 2020).

### 2.2.5 AOC 5 (Shepley's Hill Landfill)

AOC 5 is the Shepley's Hill Landfill (SHL). KGS indicates that SHL was definitively in operation by the 1940s but was potentially in use as much as one hundred years earlier (KGS, 2017, pg. 2-18). Shepley's Hill Landfill sits on 84 acres located west of Grove Pond, and the SHL stores 1.3 million cubic yards (cy) of waste, of which as much as 11% is below the water table (KGS, 2017, pg. 2-18). Closure of the landfill was completed in 1993, but subsequent investigations identified contamination originating from the landfill in soil, sediments, surface water, and groundwater. The contamination includes inorganics (e.g., arsenic) and volatile organic compounds (VOCs) (KGS, 2020, pg. 2-18). More recent (i.e., 2018-2019) sample results does not indicate elevated PFAS concentrations in the vicinity of the landfill. KGS concluded that there was no exposure pathway for contamination to reach soil or groundwater based on current land uses.

### 2.2.6 MAARNG

The Massachusetts Army National Guard (MAARNG) area is not discussed in the base-wide preliminary assessment of PFAS, but it is discussed in detail in the Area 1 Site Characterization. The MAARNG is immediately southwest of Grove Pond and outside the boundary of the Fort Devens. The MAARNG was historically used for vehicle maintenance and storage and the history of the area includes a potential fire and firefighting response. KGS (2020, pg. 6-1) states:

> "The facility currently and previously has relied on former Fort Devens fire department for support. There was reportedly a fire in a warehouse in the western portion of the facility in the early 1960's. It is unknown if AFFF was used to extinguish the fire, but due to the early date, it is unlikely. There are no other known use, storage, or disposal of AFFF at the MAARNG property."

Sample results from 2018 show elevated PFAS concentrations in soil, groundwater, surface water, and sediments (KGS, 2020). The Project Team identified additional historical information about the fire reported at the MAARNG by KGS (2020). An article from The Daily Spirit, a local newspaper at the time, indicates that a fire at a warehouse located near the northeast gate of Fort Devens occurred on Thursday, September 8, 1960. The article states:

> "Ayer and Shirley firefighters remained at the scene of the fire for more than three hours pouring water on the burning ruins. Equipment and parts for tanks and military vehicles owned and stored in the warehouse by the Massachusetts National Guard were destroyed, and the building was a total loss." (The Daily Spirit, September 15, 1960).

A copy of the original article is included with this report as Attachment 1.

Based on the description from The Daily Spirit and a review of historical aerial imagery, the Project Team determined the likely location of the warehouse fire. That location is shown in Figure 2-1. In subsequent investigations, the Project Team concluded that evidence of PFAS in groundwater extended from the fire location downhill/downgradient to a structure immediately next to Grove Pond. According to CDM (1993), the structure is the pumphouse for the Fort Devens wellfield. As of 1993, the Fort Devens wellfield was only used as a source of "emergency supply" and only turned on occasionally. Given the elevated concentrations near the structure, the Project Team included the area from the warehouse fire to the pumphouse in our delineation of the MAARNG as a potential PFAS source.

### 2.3 PFAS Source Summary

The Grove Pond wellfield is located near and downgradient of multiple locations where PFAS was released to the environment. The multiple potential releases at different points within the upgradient region complicates the identification and delineation of PFAS sources leading to the PFAS contamination at the Grove Pond wellfield. In Section 4.0 of this report, the Project Team demonstrates how the observed PFAS concentrations suggest that the closest and oldest PFAS sources are likely to be the primary sources of PFAS contamination at the Grove Pond wellfield.

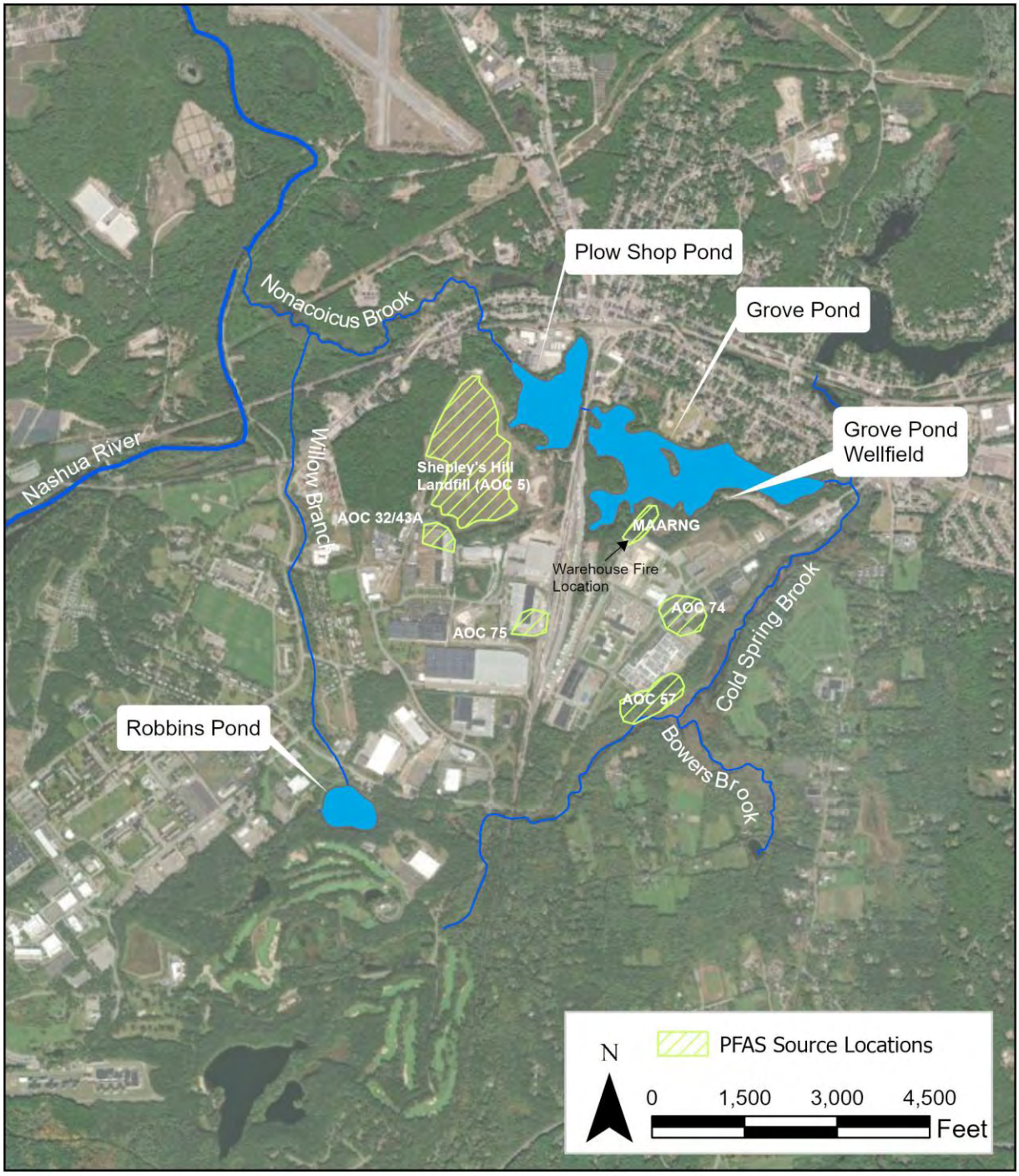



***Figure 2-1: Locus Map and Site Layout***

## 2.4 Ayer Water Distribution System

The primary source of drinking water in Ayer is groundwater. The water distribution system includes two wellfields: the Grove Pond wellfield and the Spectacle Pond wellfield. Both wellfields pump from sand and gravel aquifers. The Grove Pond aquifer is an unconfined aquifer, and the Spectacle Pond aquifer is a semi-confined aquifer. The first Grove Pond well was developed in 1943 (CDM, 1993, pg. 1-2). Since the completion of that first well, additional wells have been drilled. A total of five wells are present at the Grove Pond wellfield. The first Spectacle Pond well was developed in 1975, and a second well was completed in 1985 (Tata & Howard, 1999, pg. 3-4).

The town of Ayer completed a Zone II study for the Grove Pond wellfield in 1993 (CDM, 1993). A Zone II study is an investigation that establishes the wellhead protection area (WPA) that should be protected from groundwater contamination to prevent drinking water contamination. The Grove Pond Zone II study included sub-surface investigations such as observation well drilling and groundwater sampling, pumping tests, and groundwater modeling. The WPA represents the region of the contributing aquifer where groundwater flows towards the well. The WPA for the Grove Pond wellfield is shown in Figure 2-2. The WPA encompasses many of the potential PFAS contamination sources discussed in the previous section but excludes most of Shepley's Hill Landfill. In addition to the northeastern corner of Fort Devens, the WPA includes undeveloped land east of Cold Spring Brook and residential areas north of Grove Pond.

### 2.4.1 Grove Pond Pumping History

GP-01 was developed in 1943 and GP-02 in 1952. These two wells were in service when the Zone II study was completed (CDM, 1993). In 2014, three new wells were added to the Grove Pond wellfield. These new wells are identified as Wells 6 (GP-06), 7 (GP-07), and 8 (GP-08). After these new wells were developed, GP-01 was used only intermittently, and GP-02 was decommissioned. Figure 2-3 shows the location of each of these wells along the southern shore of Grove Pond and the depth below the ground surface where the well is screened (i.e., the depth at which water is withdrawn). GP-07 and GP-08 are screened approximately 10 ft deeper than the other wells.

The Grove Pond wells have been pumped at different rates based on capacity, demand, and maintenance over the years. In addition to the variability of pumping at the Grove Pond wellfield, the Town of Ayer made significant changes to their pumping operations over the years, again in response to capacity, demand, and maintenance. The Project Team collected all available pumping records from the Massachusetts Department of Environmental Protection (DEP). These records date back to 1986. The Project Team relied on annual pumping estimates included within the town's annual reports to understand the intensity of pumping at each wellfield prior to 1986. Figure 2-4 shows the interpreted annual average pumping rate at the two wellfields. The Spectacle Pond wellfield came online in 1977, and the Grove Pond wellfield was rarely used from then until 1998. From that year forward, both wellfields supplied water for the town.

Individual well pumping at Grove Pond is not available prior to 1986. Starting in 1986, monthly pumping records are available for each well. Figure 2-5 shows the monthly average pumping rates, and Figure 2-6 shows the annual average pumping rates. These figures show that the town routinely varied pumping from well to well.

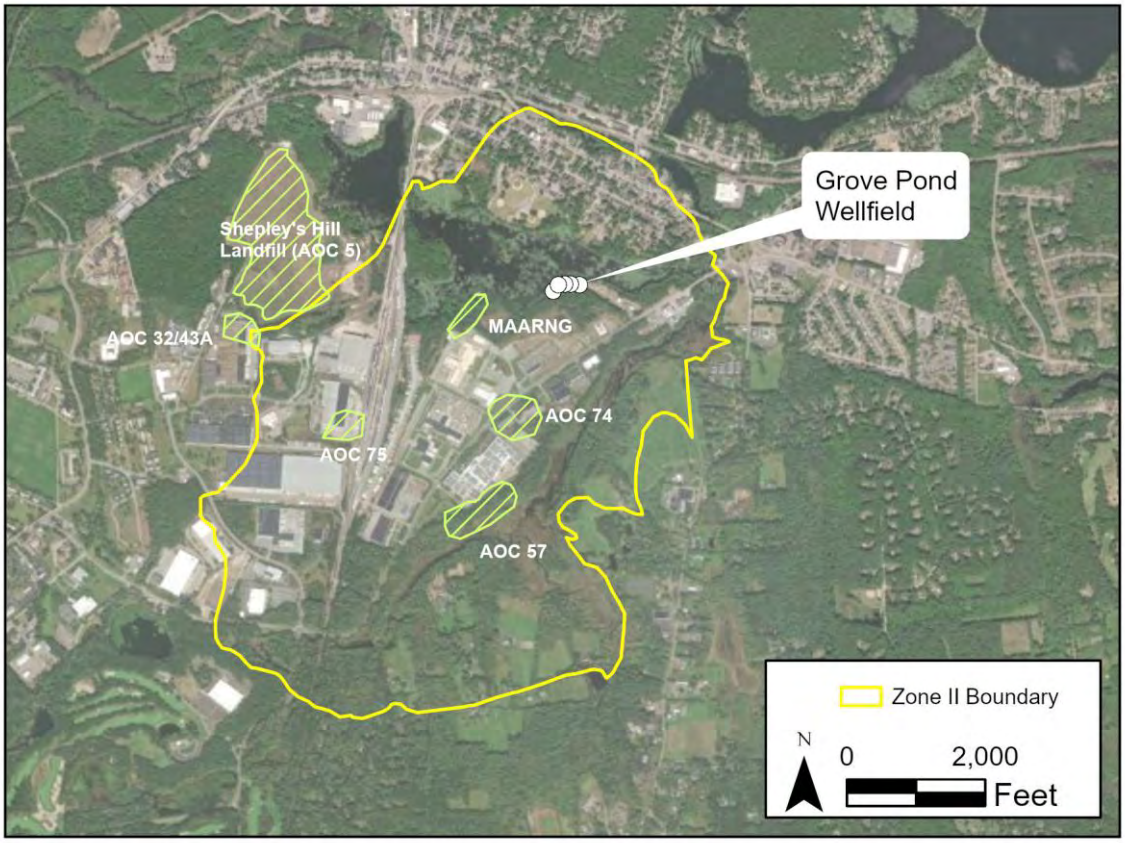



***Figure 2-2: Grove Pond Zone II Limits***

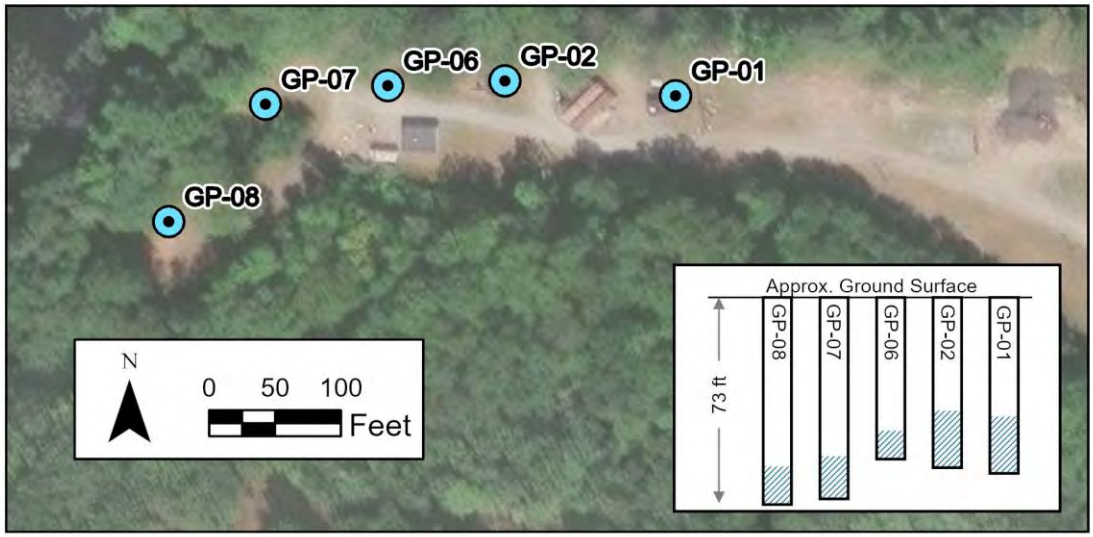



***Figure 2-3: Grove Pond Wellfield Individual Well Locations with Well Depths and Screened Intervals***

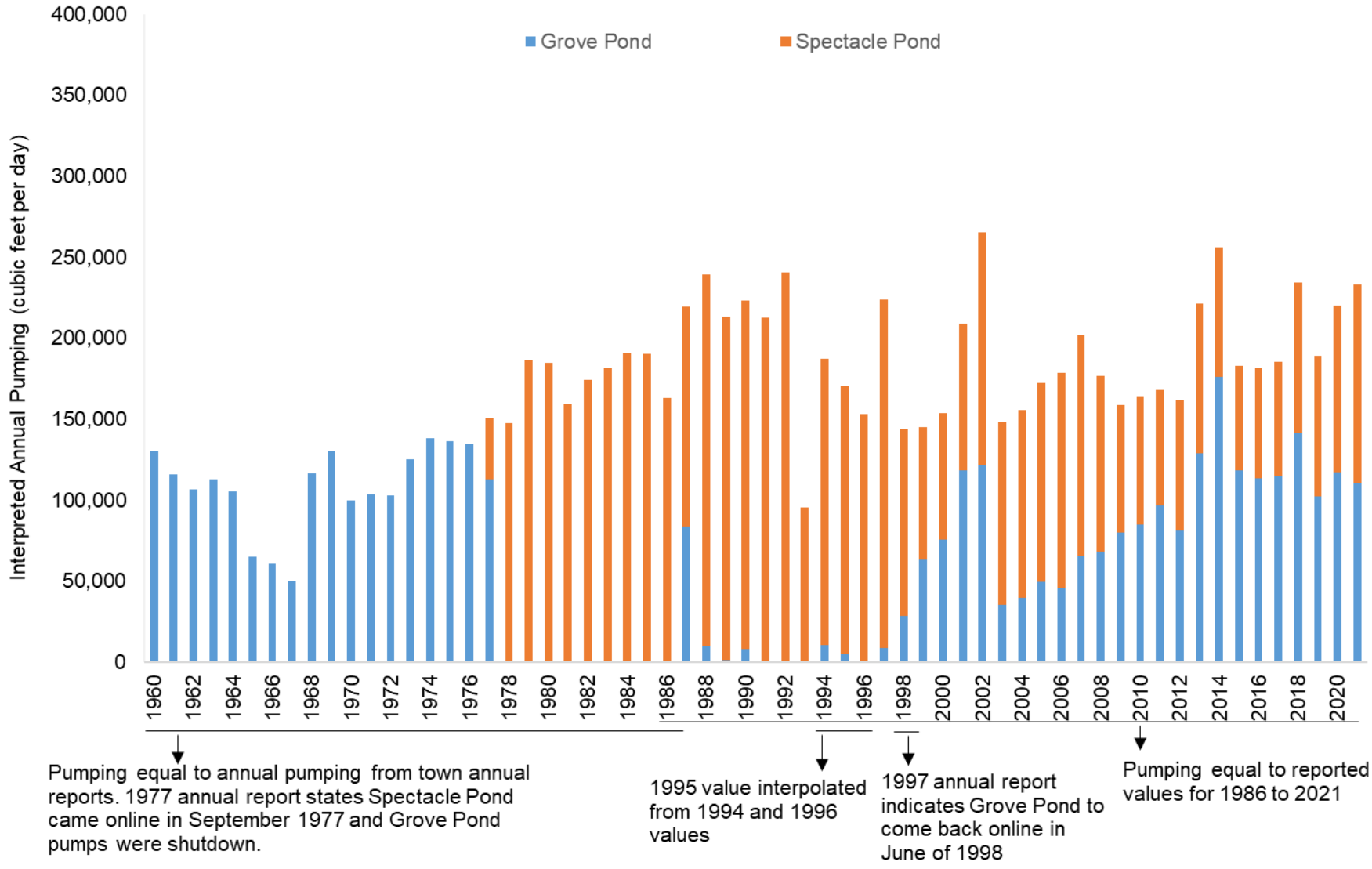



***Figure 2-4: Interpreted Annual Groundwater Pumping***

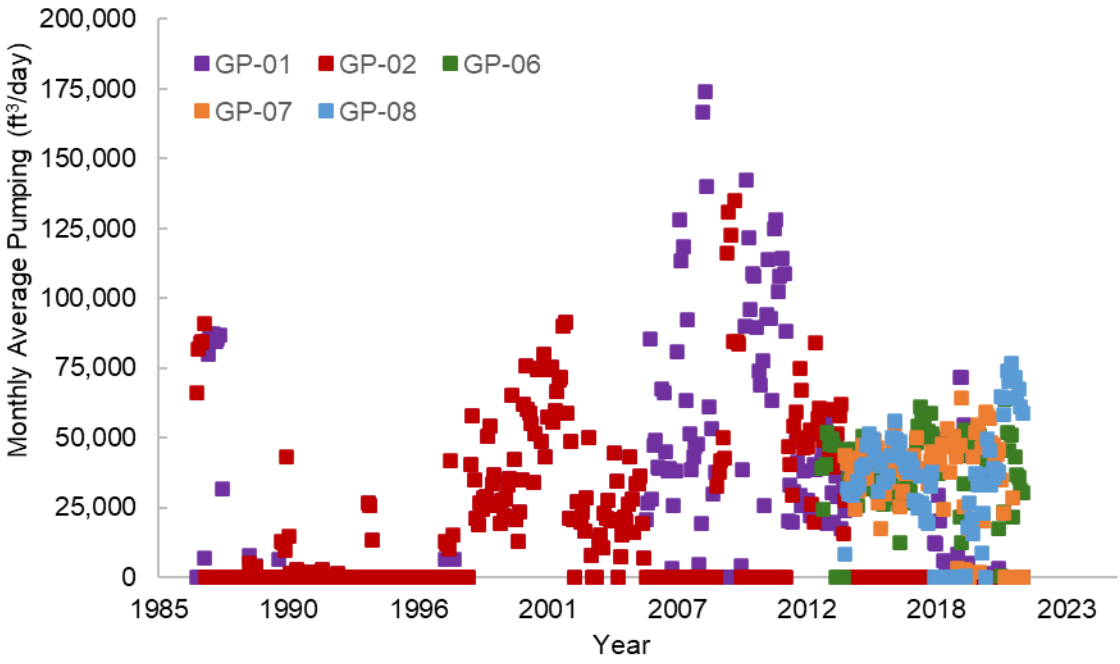



***Figure 2-5: Grove Pond Individual Well Pumping (Monthly Average)***

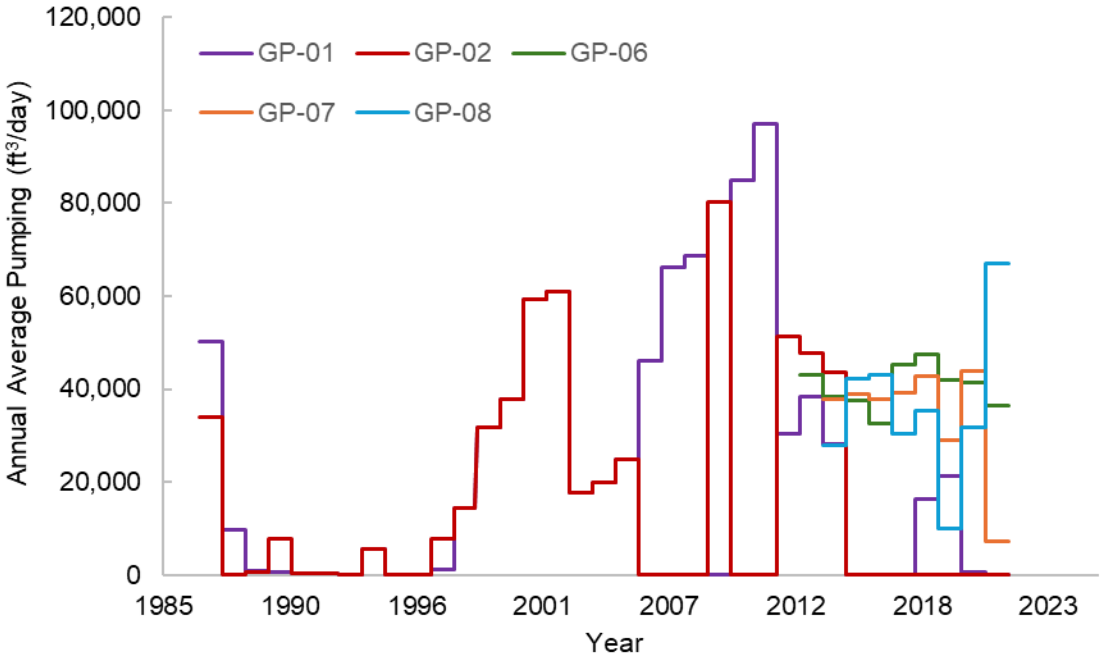



***Figure 2-6: Grove Pond Individual Well Pumping (Annual Average)***

### 2.4.2 PFAS Contamination at the Grove Pond Wellfield

Ayer first detected PFAS in drinking water at the Grove Pond wellfield in 2016 (Ayer, 2025), and PFAS was subsequently detected at the Spectacle Pond wellfield in 2018. Since that time, Ayer has been regularly monitoring PFAS concentrations in both the raw (i.e., prior to treatment) and finished (i.e., after treatment) drinking water. Figure 2-7 shows the PFAS6 concentrations recorded at the Grove Pond wellfield between mid-2018 and mid-2022 as reported to the state (EEA, 2022). PFAS6 refers to the six compounds regulated by the Commonwealth of Massachusetts. These compounds are: PFOS, PFOA, PFHxS, PFNA, PFHpA, and PFDA (perfluorodecanoic acid). GP-08 consistently has the highest PFAS6 concentrations. Concentrations at GP-08, GP-01, and GP-06 are variable, but do not exhibit a consistent trend either increasing or decreasing. Concentration at GP-07 demonstrates variability but also has a clear downward trend with PFAS6 concentrations decreasing to less than 40 nanograms per liter (ng/L) by mid-2020 and remaining below that value thereafter. Figure 2-9 through Figure 2-11 show the concentrations of individual PFAS compounds at each well. PFDA is excluded from this set of figures, and PFHxA is included. The decision to evaluate PFHxA instead of PFDA is based on the goals of this study.

PFHxA is consistently one of the highest concentrations across the wells other than at GP-01. PFOA is present in higher concentrations at the eastern wells (i.e., GP-01 and GP-06), and PFHpA is present in higher concentrations at the western wells (i.e., GP-07 and GP-08). During the time period of PFAS sampling, GP-02 was inactive, but each of the other wells was being actively pumped to some degree with GP-06 having the highest average annual pumping rate.

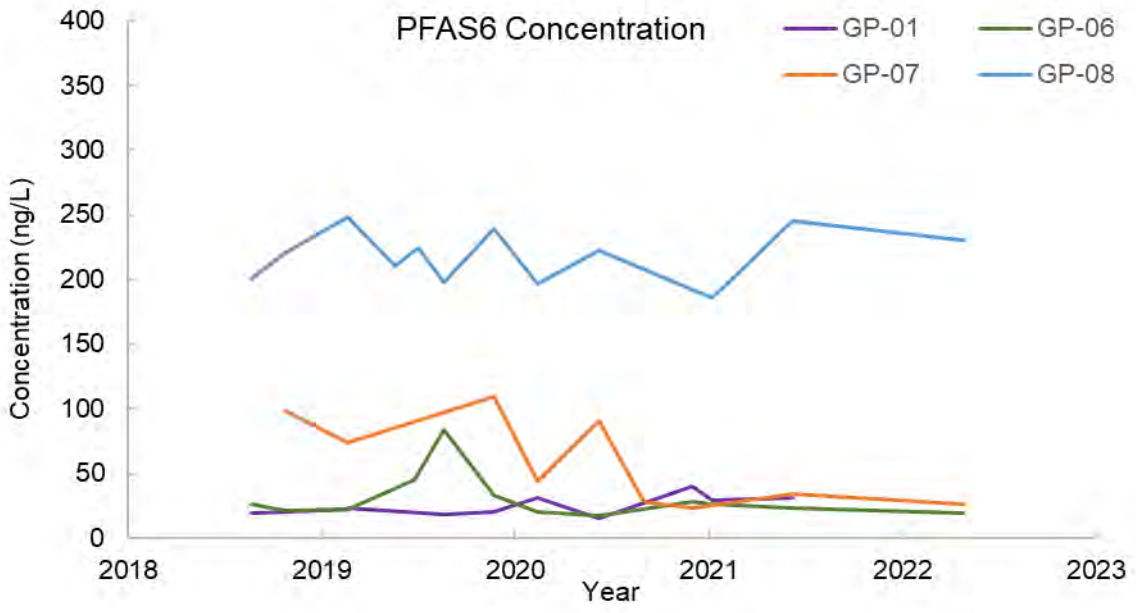



***Figure 2-7: PFAS6 Time Series at Grove Pond Wells***

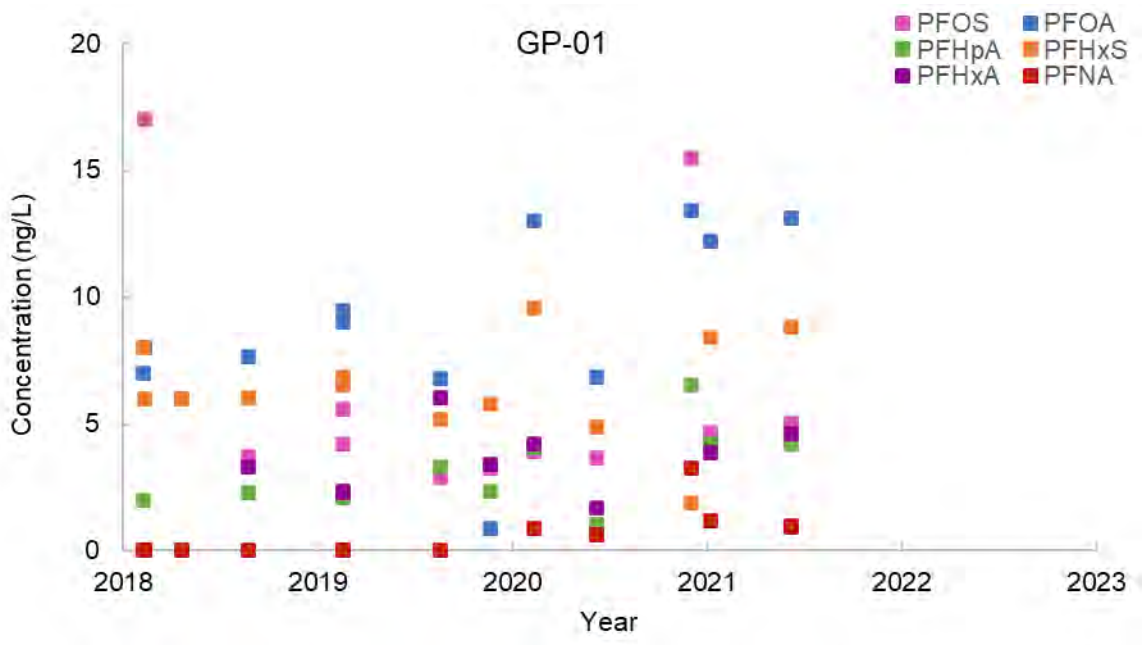



***Figure 2-8: Individual PFAS Timeseries at GP-01***

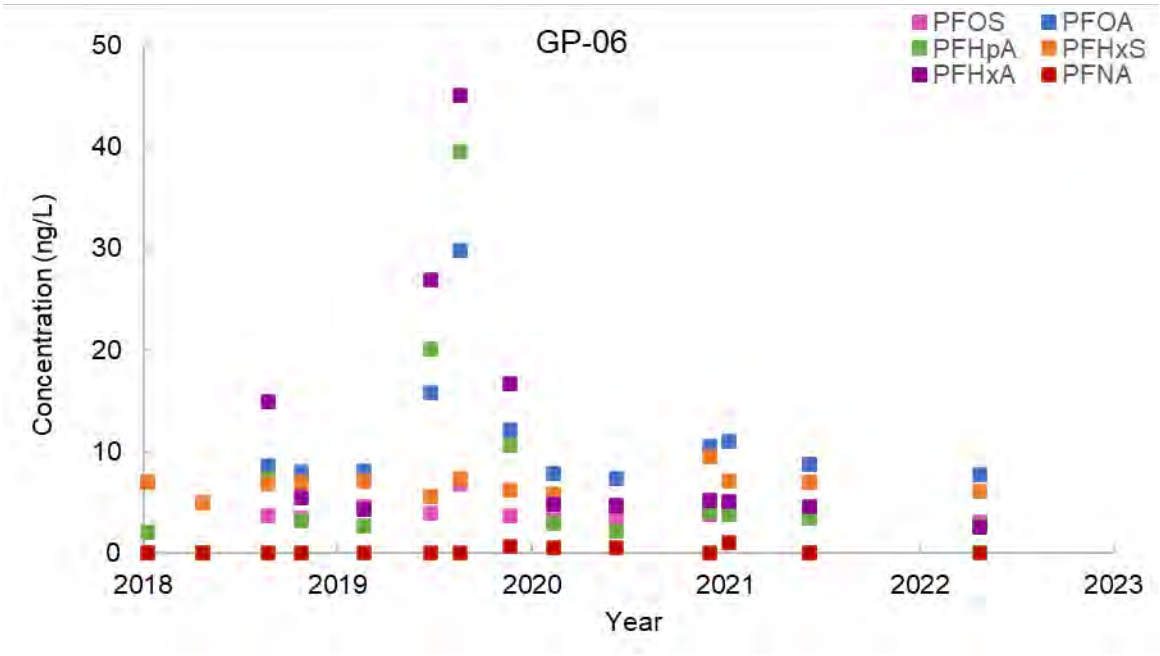



***Figure 2-9: Individual PFAS Time Series at GP-06***

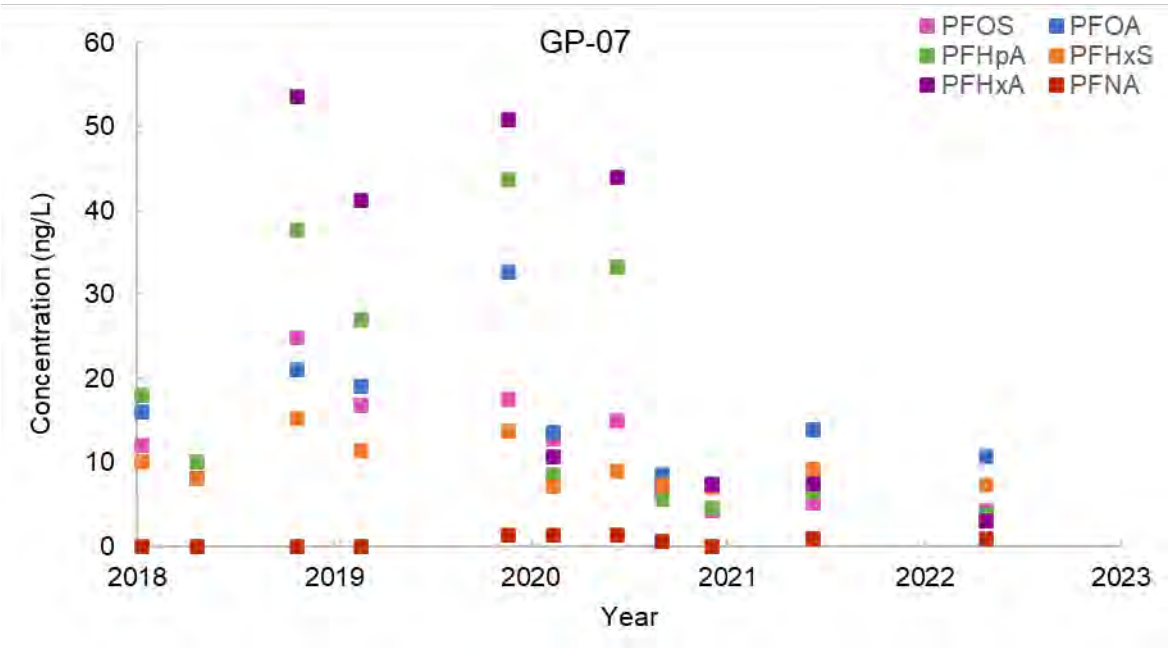



***Figure 2-10: Individual PFAS Time Series at GP-07***

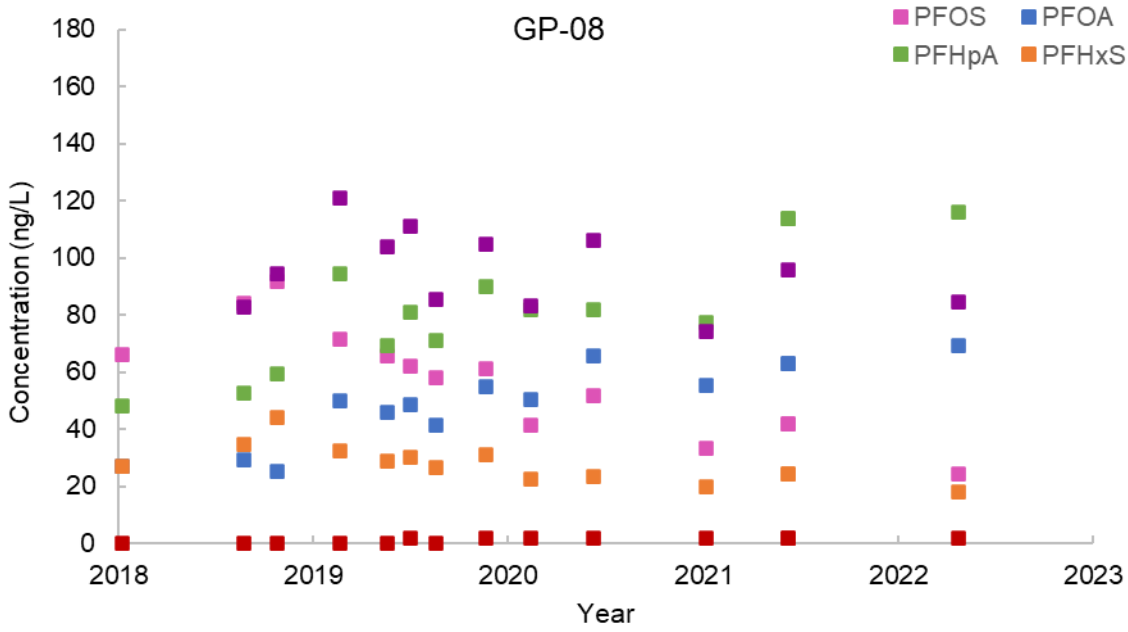



***Figure 2-11: Individual PFAS Time Series at GP-08***

## 2.5 Summary

The town of Ayer has been pumping groundwater from the Grove Pond wellfield since the middle of the 20th century. Evidence of PFAS contamination in the wells dates back to 2016, but the nearest potential sources are substantially older with the earliest potential source dating to 1960. In the next section of the report, we present the hydrogeologic setting for the Grove Pond wellfield. We then evaluate the available groundwater quality data in the context of the site history and hydrogeologic setting to develop a conceptual site model as the foundation for the numerical groundwater model of the Grove Pond wellfield aquifer.

# 3.0 HYDROGEOLOGIC SETTING

Previous and ongoing investigations provide a substantial amount of information to aid our understanding of the Grove Pond aquifer's hydrogeology. The Grove Pond Zone II study (CDM, 1993) included sub-surface investigations such as observation well drilling, groundwater sampling, pumping tests, and groundwater modeling. In addition to the Zone II study, the Grove Pond wells and aquifer are a part of the PFAS investigation work that is currently ongoing at the Fort Devens Army Installation (KGS, 2020) and part of the modeling for the Shepley's Hill Landfill (Geosyntec, 2020).

## 3.1 Topography and Hydrology

The topography near Grove Pond generally slopes from the south to the north. Figure 3-1 shows ground surface contours in feet referenced to the North American Vertical Datum 1988 (NAVD88). The figure also shows the primary surface water features. Robbins Pond is located approximately 6,000 ft south-southwest of Grove Pond and approximately 100 ft higher elevation. Willow Brook drains Robbins Pond to the north. Bowers Brook and Cold Spring Brook flow into Grove Pond, and Grove Pond is connected to Plow Shop Pond through a culvert. The western end of Plow Shop Pond includes an overflow to Nonacoicus Brook. Nonacoicus Brook and Willow Brook join prior to flowing into the Nashua River.

Grove Pond and Plow Shop Pond are shallow ponds. The maximum water depth in Grove Pond is approximately 3 ft. Plow Shop Pond is deeper than Grove Pond and has a maximum water depth of approximately 8 ft. Aerial imagery shows algal blooms present in many historical images of the ponds, suggesting they may be relatively stagnant. Figure 3-2 shows the bathymetry of both ponds and the approximate sediment thickness as of 1999 (Mercadante et al., 1999). The topography, observed groundwater levels, previous modeling investigations, and PFAS sample results of groundwater and surface water all indicate that Cold Spring Brook and Willow Brook are in direct contact with groundwater and that groundwater provides a consistent baseflow of surface water draining to Grove Pond. Similarly, Grove Pond and Plow Shop Pond are hydraulically connected to the underlying aquifer. Pumping at the Grove Pond wellfield induces surface water infiltration into the aquifer and to the public water supply (PWS) wells.

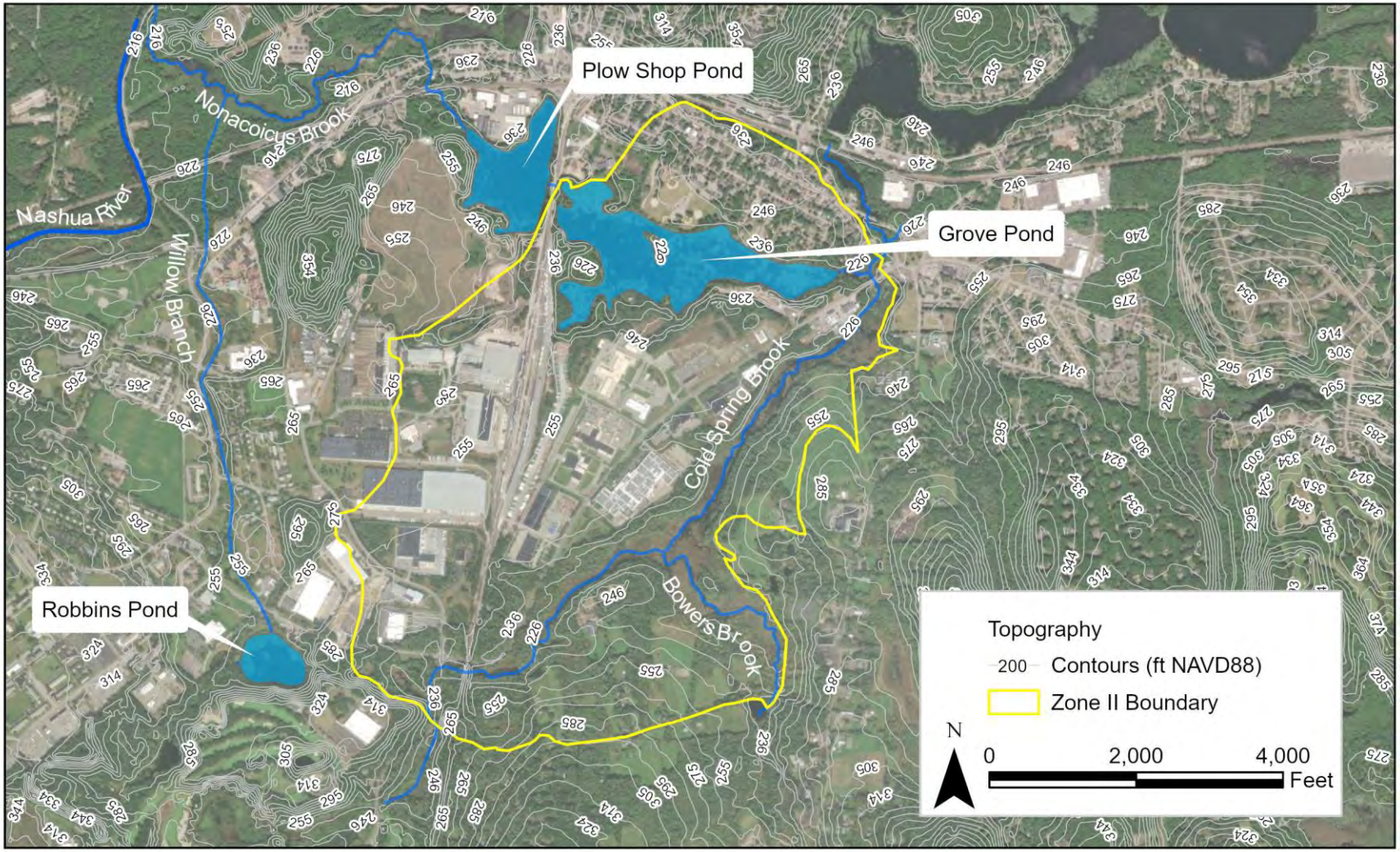



***Figure 3-1: Topography in Vicinity of Grove Pond Wellfield (MassGIS, 2024)***

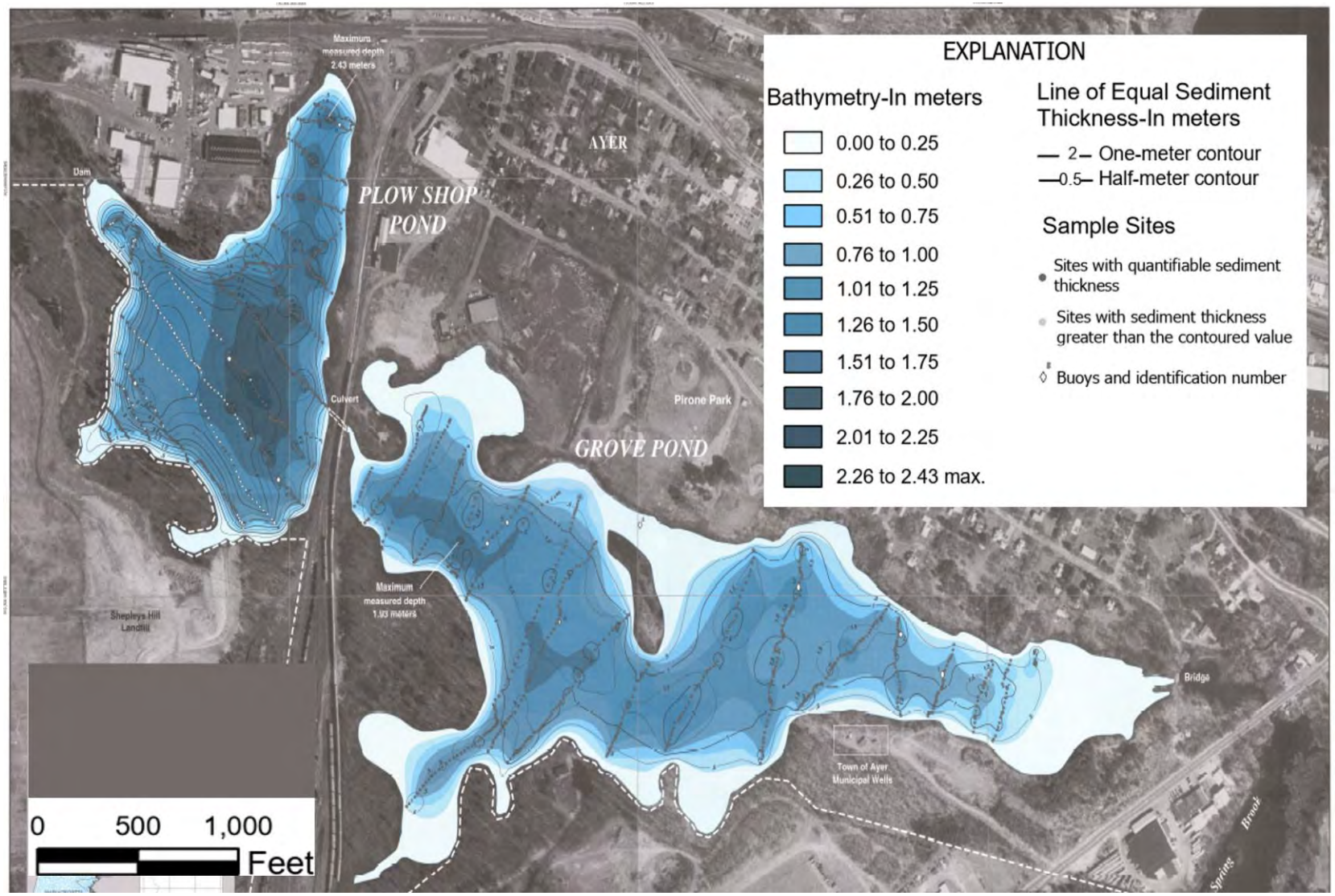



***Figure 3-2: Grove Pond and Plow Shop Pond Bathymetry (Mercadante et al., 1999)***

## 3.2 Geology

CDM (1993, pg. 3-3) describes the surficial geology near Grove Pond as primarily glacial terrace deposits composed of coarse sand, pebbles, and gravel. The surrounding area consists of glacial till deposits that range from 20 ft to 100 ft. The glacial till is primarily present as coarse to fine sand with gravel and trace silt. Subsequent studies (e.g., the Shepley's Hill Study) support this description. Figure 3-3 shows the surficial geologic characterization completed by the United States Geological Survey (USGS) and available from MassGIS (2024a). The USGS characterization is consistent with the description developed by CDM with glacial deposits making up most of the region south of Grove Pond and the Grove Pond wellfield. Figure 3-3 indicates the presence of multiple bedrock outcrops located west of Shepley's Hill Landfill and north of Grove Pond. The USGS characterization also shows thick till east of Cold Spring Brook. These outcrops and till are natural barriers to flow that direct groundwater and limit the spread of groundwater contamination.

Bedrock elevations vary substantially in the vicinity of Grove Pond. Bedrock outcrops and deep depressions are both present. The Project Team used bedrock surface depth measurements from the Massachusetts Well Database (MassDEP, 2024), the Shepley's Hill Landfill (SHL) modeling study (Geosyntec, 2020), and the USACE Remedial Investigation (KGS, 2020) to develop a bedrock surface for the CSM and the groundwater model. Figure 3-4 shows the bedrock surface contours with the boring/well locations from the various data sources. The Project Team compared our surface to surfaces developed by KGS (2020) and Geosyntec (2020) and concluded that the bedrock surfaces are functionally equivalent.

Figure 3-4 clearly shows the presence of a bedrock depression approximately 4,000 ft south of Grove Pond. The general slope of the bedrock is towards the north consistent with both the slope of the surface topography at the site and the direction of groundwater flow. CDM (1993) identified the bedrock as metamorphic bedrock, and both CDM (1993) and KGS (2020) concluded that the groundwater flow through the bedrock is small relative to the groundwater flow in the overburden.

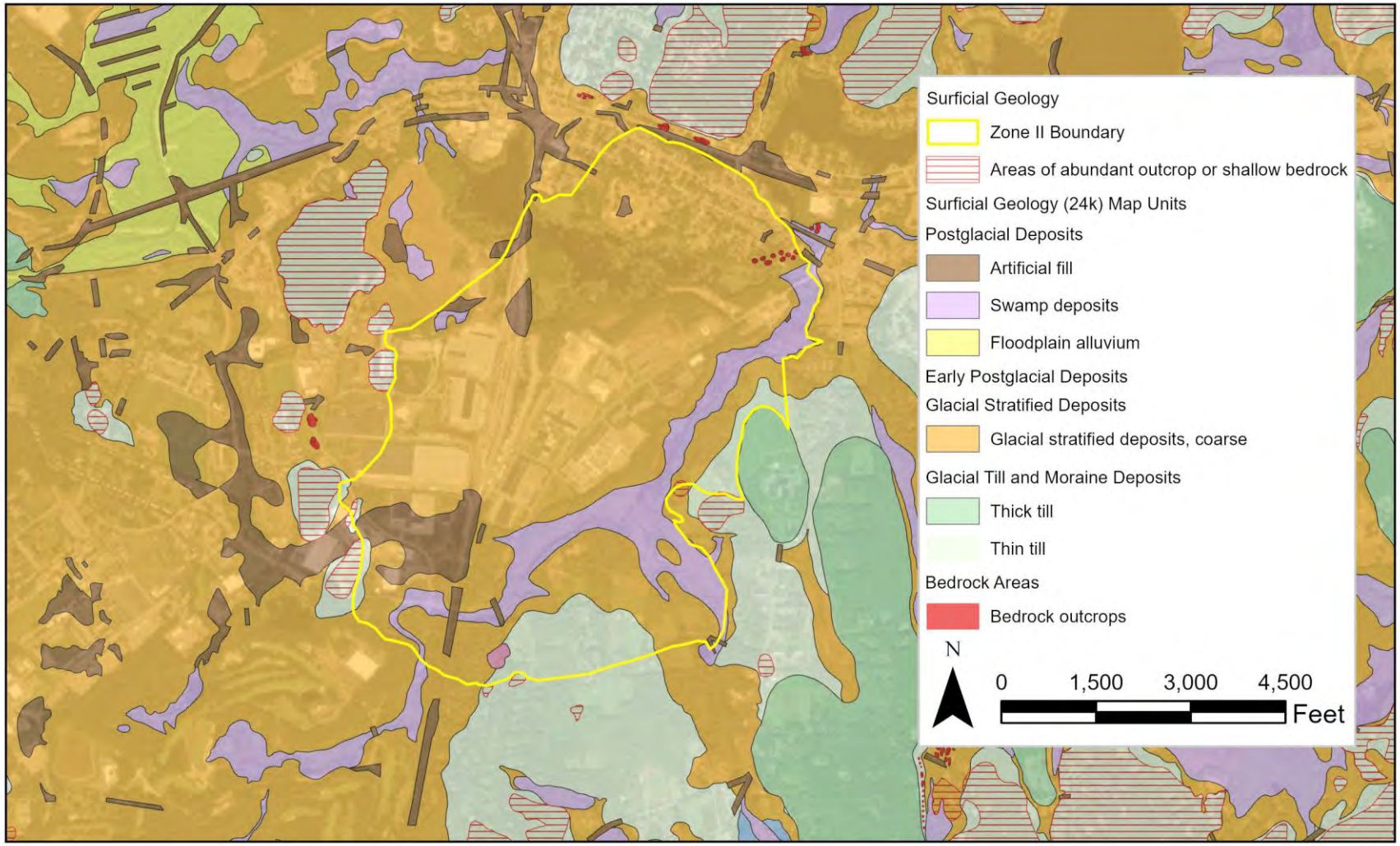



***Figure 3-3: Surficial Geology in Vicinity of Grove Pond Wellfield (MassGIS, 2024a)***

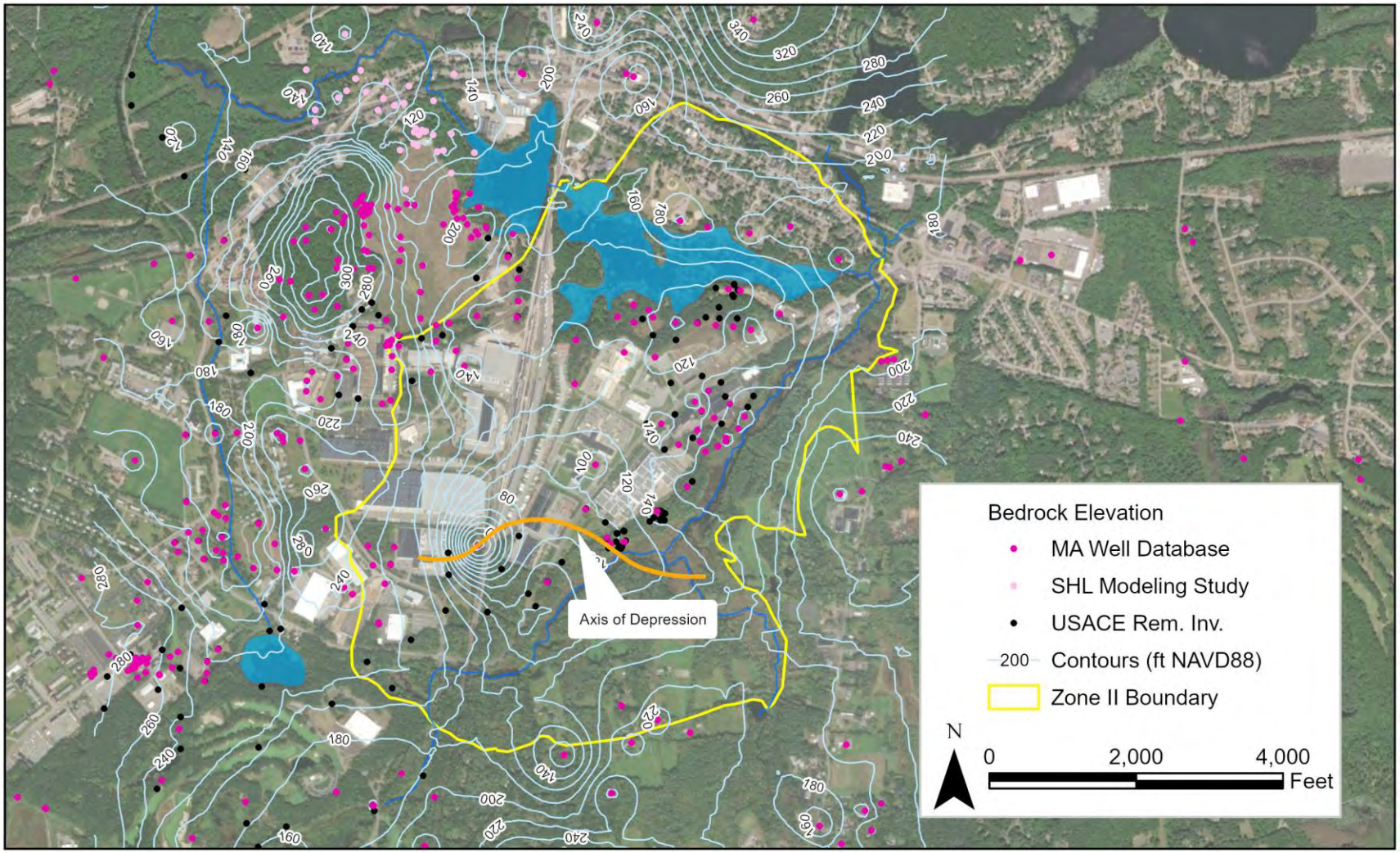



***Figure 3-4: Bedrock Elevations in Vicinity of Grove Pond Wellfield***

### 3.3 Hydrogeology

CDM (1993), Geosyntec (2020), and KGS (2020) investigated the piezometric head in the aquifer that feeds the Grove Pond wellfield. The aquifer is an unconfined aquifer. The piezometric head measured at wells approximates the water table elevation. Figure 3-5 is an excerpt from CDM (1993) showing groundwater contours from a pumping test conducted in June 1992. The piezometric head generally mimics the contours of the ground surface, sloping downward from the south-southwest towards the north. Near Robbins Pond, the groundwater table is approximately 243 ft National Geodetic Vertical Datum of 1929 (NGVD29). The water table at Grove Pond is approximately 216 ft NGVD29. The contours show a cone of depression from the pumping test around the Grove Pond wells. KGS (2020) identified similar groundwater levels 25 years later as a part of the ongoing Fort Devens PFAS investigation. Figure 3-6 shows excerpts from their report. Groundwater generally slopes from the south-southwest towards the north with similar groundwater elevations at Grove Pond. The primary difference between the 2020 contours and the 1993 contours is the higher level of detail along Cold Spring Brook. The 2020 contours clearly indicate the connection between the brook and the aquifer.

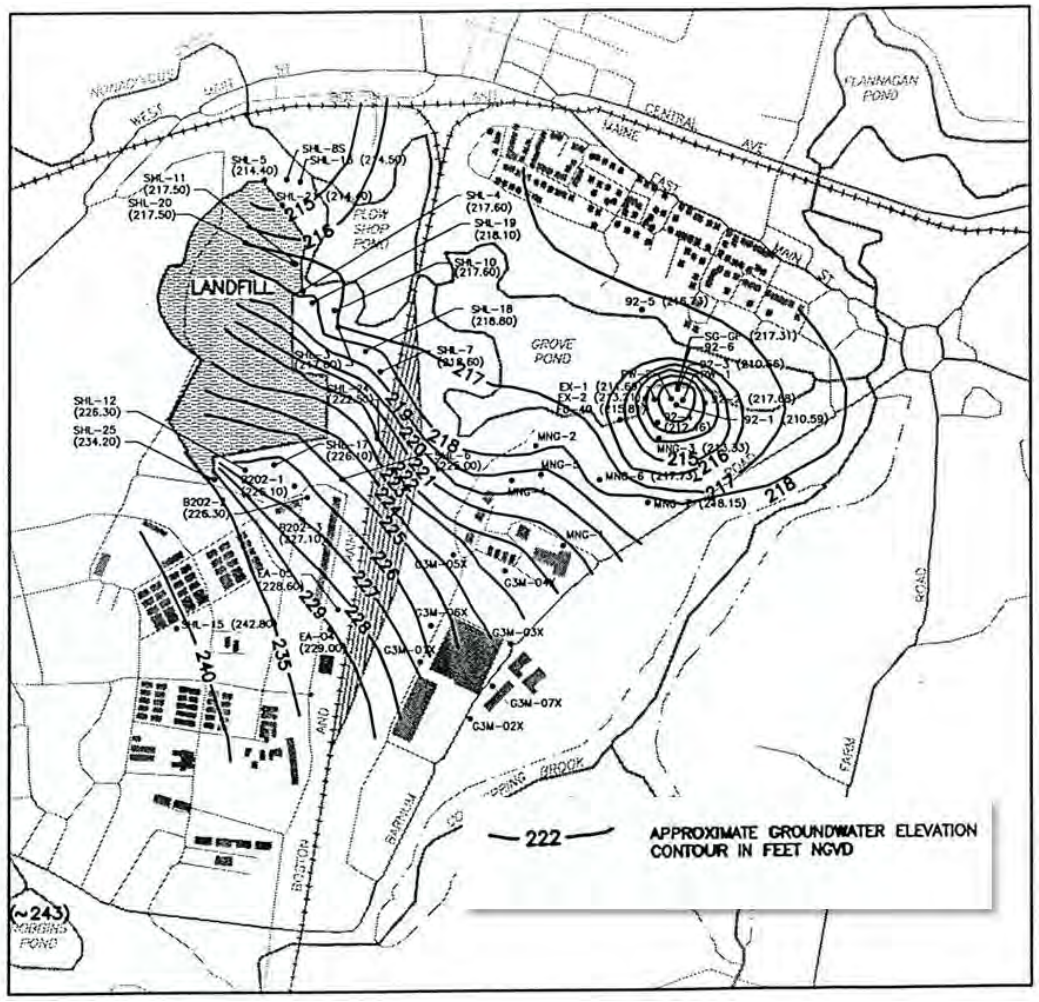



***Figure 3-5: Groundwater Surface Contouring 1992 (CDM, 1993)***

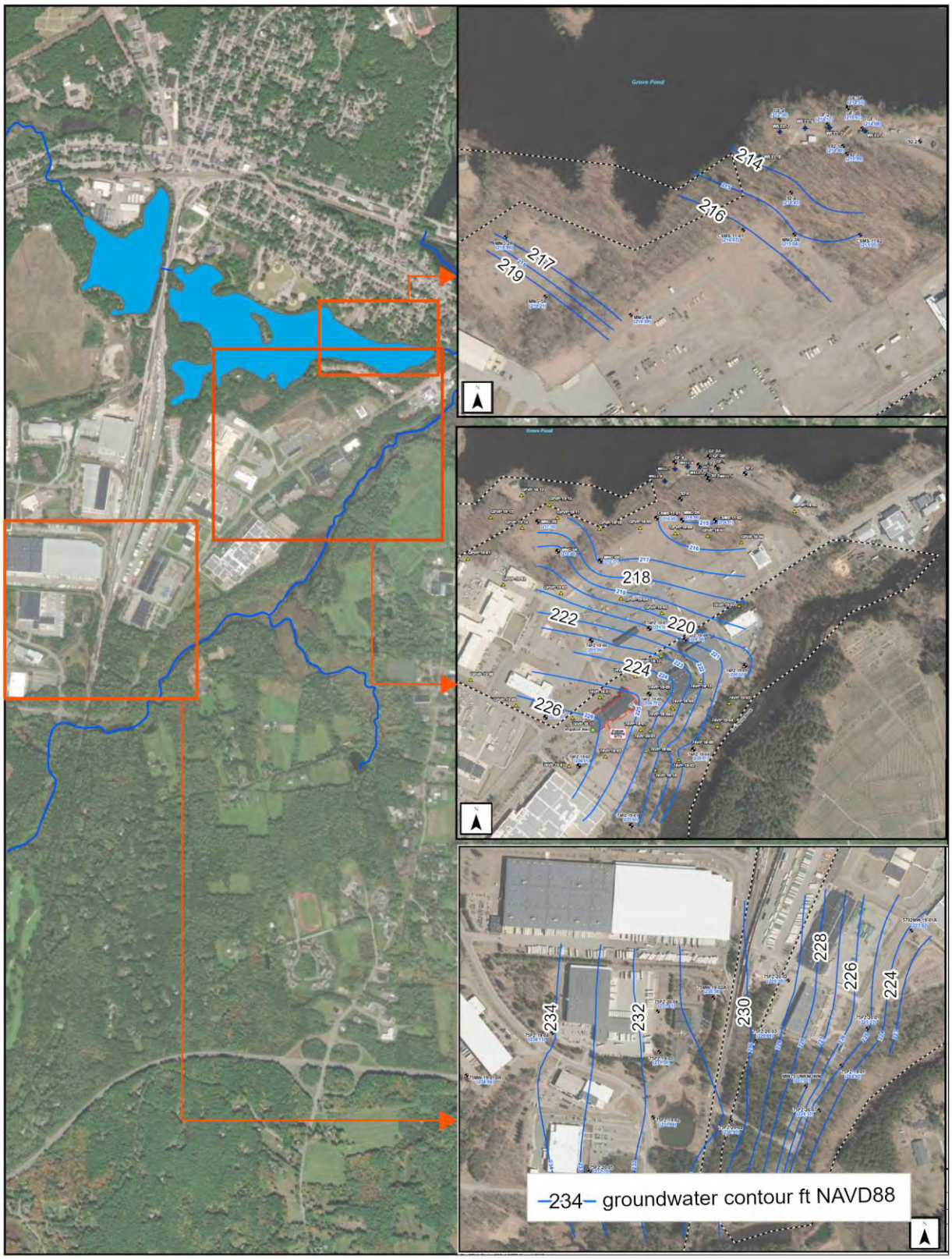



***Figure 3-6: Groundwater Surface Contours from KGS (2020)***

Horizontal groundwater flow can be generally presumed to be perpendicular to groundwater contours (i.e., lines of constant head) in non-fractured media. Thus, the direction of groundwater flow is generally towards Grove Pond from the south-southwest. The rate of groundwater flow is a function of the hydraulic gradient (i.e., piezometric head differential between two points along the line of flow divided by the distance between the points) and the hydraulic conductivity of the media. Hydraulic conductivity is a coefficient with units of length per time that is used in Darcy's law to represent the ease with which water passes through porous media (Freeze and Cherry, 1979). Both CDM (1993) and Geosyntec (2020) conducted testing to estimate the hydraulic conductivity of the aquifer that feeds the Grove Pond wellfield.

CDM (1993) evaluated surficial geology, grain size distributions from boring logs, and calculated transmissivity and storativity based on a pumping test at the Grove Pond wellfield. They established a range of hydraulic conductivity values based on grain size. "Fine to medium sand deposits" were assigned a hydraulic conductivity range of 10 to 60 ft/day, and "sand and gravel deposits (such as those around Grove Pond and Plow Shop Pond)" were assigned a hydraulic conductivity range of 200 to 300 ft/day (CDM, 1993). CDM also established ranges for vertical hydraulic conductivity of sediments beneath surface water bodies. They assigned a range of 1 to 5 ft/day for the brooks and a range of 0.2 to 0.5 ft/day for Grove Pond. CDM used these ranges as starting points for their steady-state groundwater model calibration. Figure 3-7 shows the calibrated hydraulic conductivity zones used by CDM to determine the WPA. Their model domain was subdivided into three layers with some vertical variation in the hydraulic conductivity. In general, the horizontal hydraulic conductivity is approximately an order of magnitude lower south of Grove Pond than directly beneath Grove Pond.

Geosyntec (2020) used the results of slug tests (i.e., a single-well test used to measure the hydraulic conductivity of the material immediately surrounding a monitoring well) to determine appropriate hydraulic conductivity values for use in their own groundwater model. The slug tests were primarily conducted at wells surrounding Shepley's Hill Landfill, but their model domain and estimated hydraulic conductivity covers the area east of the landfill, including Cold Spring Brook. Figure 3-8 shows an excerpt from the Shepley's Hill Landfill modeling study. Similar to CDM, Geosyntec sub-divided the aquifer into zones with regions defined based on hydraulic conductivity. Geosyntec's zones cover a larger area and include more and smaller zones, especially around the landfill. Geosyntec assigned a hydraulic conductivity value of approximately 166 ft/day to the zone directly beneath Grove Pond and a hydraulic conductivity value of approximately 32 ft/day to the zone south-southwest of Grove Pond.

CDM (1993) and Geosyntec (2020) assigned different hydraulic conductivity values in their modeling work, but the relative trend is consistent. The aquifer beneath Grove Pond has a hydraulic conductivity that is approximately one order of magnitude greater than the aquifer portion that is south-southwest of Grove Pond. Both studies assumed a ratio of horizontal-to-vertical anisotropy of ten-to-one for hydraulic conductivity. The Project Team reviewed their work, as described in the reports, and agreed with their conclusions.

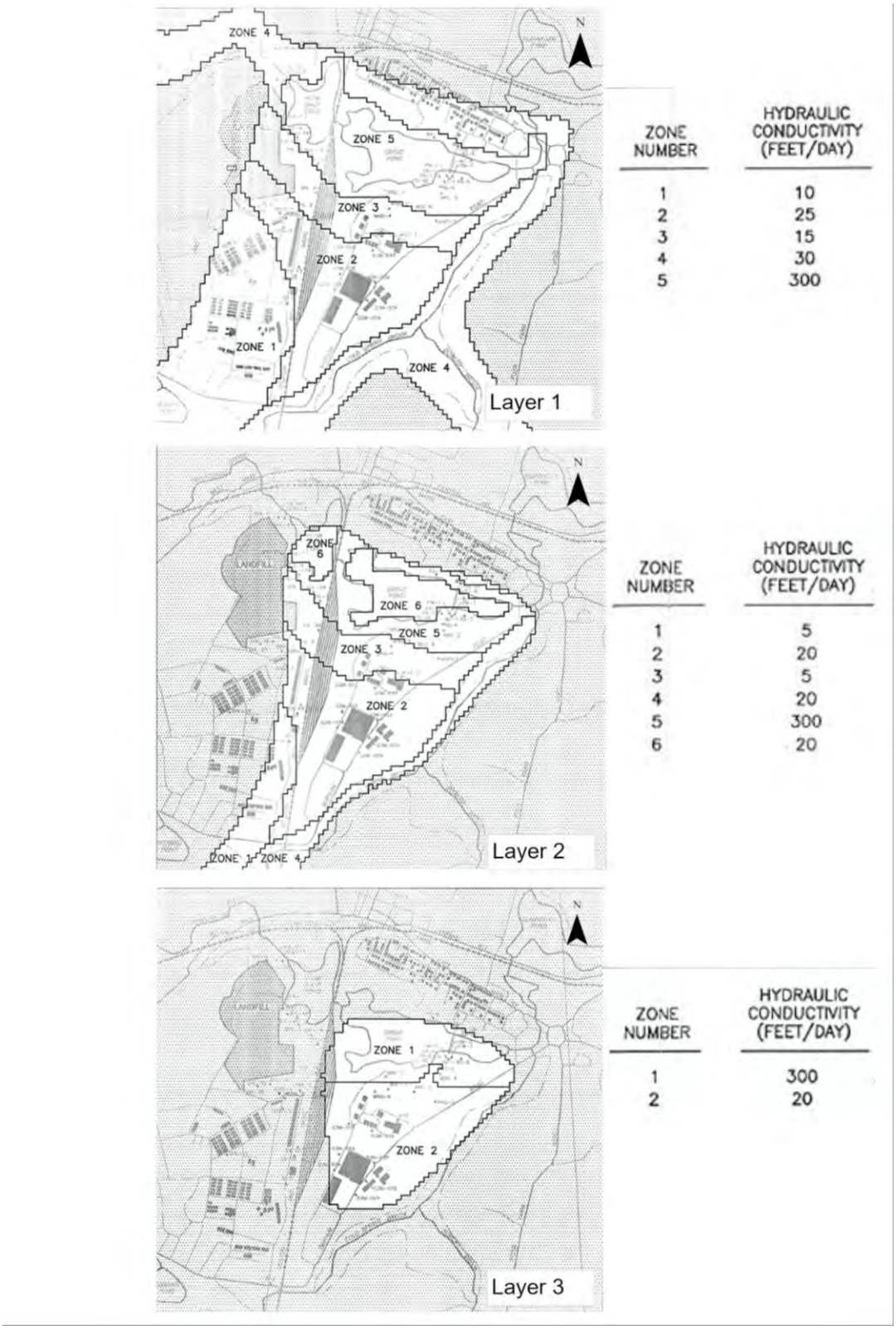
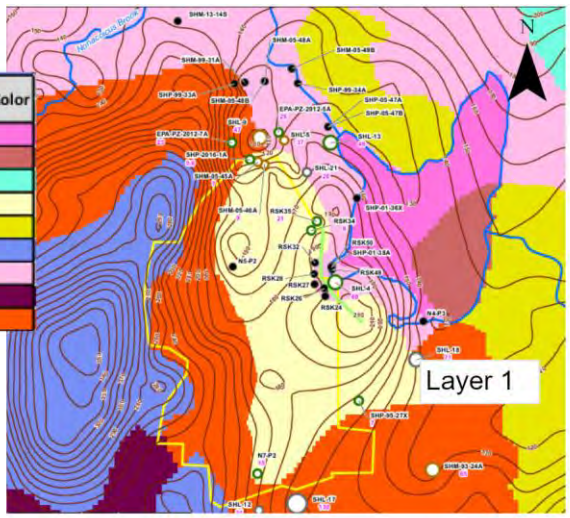
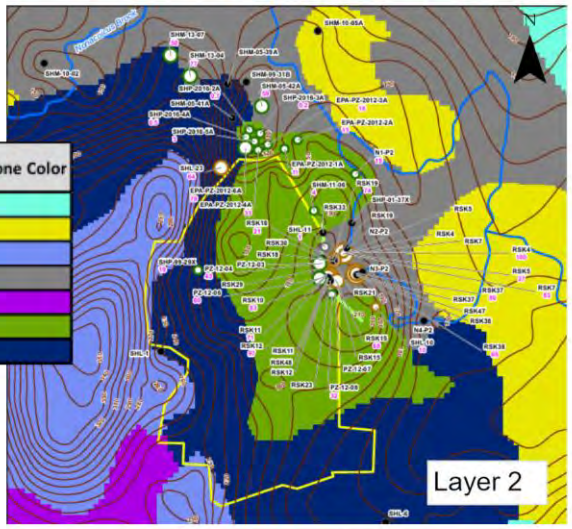



***Figure 3-7: Estimates of Hydraulic Conductivity from Zone II Study (CDM, 1993)***

| Zone Number | Hydraulic Conductivity (ft/d) | | | Zone Color |
|---|---|---|---|---|
| | Kx | Ky | Kz | |
| 1 | 4.9 | 4.9 | 4.9 | |
| 2 | 16.6 | 16.6 | 16.6 | |
| 3 | 31.7 | 31.7 | 3.2 | |
| 4 | 21.0 | 21.0 | 5.3 | |
| 6 | 165.9 | 165.9 | 16.6 | |
| 10 | 1.0 | 1.0 | 0.1 | |
| 11 | 48.8 | 48.8 | 12.2 | |
| 12 | 22.5 | 22.5 | 2.3 | |
| 15 | 130.0 | 130.0 | 32.5 | |




| Zone Number | Hydraulic Conductivity (ft/d) | | | Zone Color |
|---|---|---|---|---|
| | Kx | Ky | Kz | |
| 3 | 31.7 | 31.7 | 3.2 | |
| 6 | 165.9 | 165.9 | 16.6 | |
| 10 | 1.0 | 1.0 | 0.1 | |
| 21 | 39.2 | 39.2 | 9.8 | |
| 22 | 59.0 | 59.0 | 5.9 | |
| 24 | 6.0 | 6.0 | 1.5 | |
| 25 | 19.0 | 19.0 | 4.8 | |




| Zone Number | Hydraulic Conductivity (ft/d) | | | Zone Color |
|---|---|---|---|---|
| | Kx | Ky | Kz | |
| 3 | 31.7 | 31.7 | 3.2 | |
| 6 | 165.9 | 165.9 | 16.6 | |
| 10 | 1.0 | 1.0 | 0.1 | |
| 31 | 135.0 | 135.0 | 33.8 | |
| 32 | 135.0 | 135.0 | 13.5 | |
| 34 | 30.0 | 30.0 | 7.4 | |
| 35 | 24.1 | 24.1 | 6.0 | |

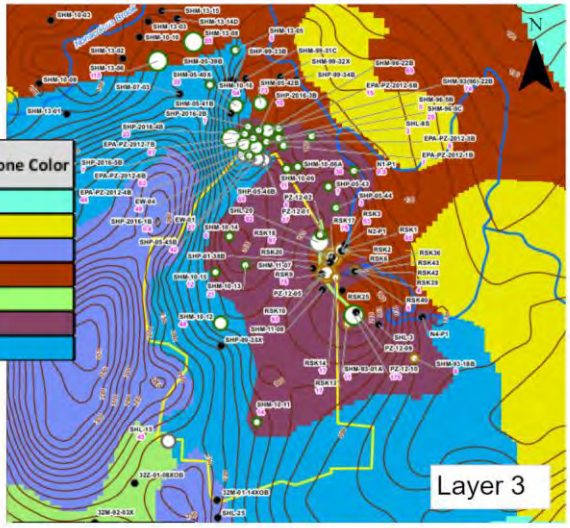



***Figure 3-8: Estimates of Hydraulic Conductivity from SHL Study (Geosyntec, 2020)***

Groundwater recharge is the volumetric difference between the water entering the aquifer at the water surface and water exiting the aquifer at the water surface (Freeze and Cherry, 1979). Recharge is typically less than precipitation because water is lost to surface runoff and evapotranspiration. CDM (1993) stated that the average rainfall in the vicinity of Grove Pond was 44 inches/year (in/yr) and that approximately 50% of that was lost to the atmosphere through evapotranspiration. They estimated annual recharge to be between 14-18 in/yr (CDM, 1993, pg. 41). Geosyntec (2020) subdivided the region surrounding Shepley's Hill Landfill into recharge zones and determined recharge based on estimates of total precipitation infiltrating the ground in that zone. The estimated aquifer recharge ranged from 6% to 75% of the precipitation and ranged from 0.9 in/yr (0.0002 ft/day) to 55 in/yr (0.0125 ft/day) (Geosyntec, 2020, Table 6-3). The latter value exceeds typical annual precipitation owing to unusual conditions. Geosyntec completed their model calibration based on a transient model run, and the maximum recharge value is from a model stress period with a monthly rainfall of 4.6 in/month (equivalent to 55 in/yr).

# 4.0 CONCEPTUAL SITE MODEL

The Project Team reviewed the site information, PFAS release history, and the hydrogeology of the aquifer in order to develop a CSM. The CSM represents our understanding of the sources and transport of PFAS compounds that drive the PFAS concentrations at the Grove Pond wellfield.

## 4.1 Potential Transport Pathways

Groundwater flows from the south-southwest towards Grove Pond. Bedrock, which extends to the surface to the north of Grove Pond forms a natural no-flow boundary. The presence of low hydraulic conductivity glacial till to the east also effectively forms a natural no-flow boundary. The aquifer is hydraulically connected with Willow Brook in the west and Cold Spring Brook in the east. During periods of low stream flow, groundwater flows out of the aquifer and into these streams. Water that enters Cold Spring Brook will flow into Grove Pond and to Plow Shop Pond before entering Nonacoicus Brook and flowing to the Nashua River. Grove Pond and Plow Shop Pond are also hydraulically connected with the aquifer. In the vicinity of the Grove Pond wellfield, the net direction of flow is out of Grove Pond into the underlying aquifer and into the wells. The net direction of flow in Plow Shop Pond is groundwater flowing into the pond from the aquifer.

The aquifer is between 70 ft and 100 ft thick immediately below Grove Pond and gets thinner moving south-southwest away from Grove Pond. The thickest part of the aquifer also has the highest hydraulic conductivity (order of magnitude 100 ft/d). Most of the rest of the aquifer, as bounded by the bedrock outcrops to the west and Cold Spring Brook to the east, is composed of stratified glacial deposits that have relatively lower hydraulic conductivity (order of magnitude 10 ft/d). Peat and other swamp deposits result in a strip of lower hydraulic conductivity along and beneath Cold Spring Brook.

Based on this CSM, the Project Team identified the area bounded by Robbins Pond, Willow Brook, Plow Shop Pond, Grove Pond, and Cold Spring Brook as the region of interest for PFAS iso-concentration contouring and groundwater flow modeling. Figure 4-1 shows a diagram of the natural boundaries and flow/transport directions.

There are multiple potential sources within the region of interest, but there is limited information about the exact timing or amount of PFAS that may have been released at each potential source. While the site history does not provide a clear indication of primary PFAS sources, the RI (KGS, 2020) provides a comprehensive assessment of the distribution of PFAS in groundwater, surface water, and soil within the region of interest as of the winter of 2018-2019. The Project Team conducted extensive analysis on this dataset (subsequently referred to as the site investigation and remedial investigation (SIRI) dataset) to further refine the CSM regarding PFAS transport to the Grove Pond wellfield.

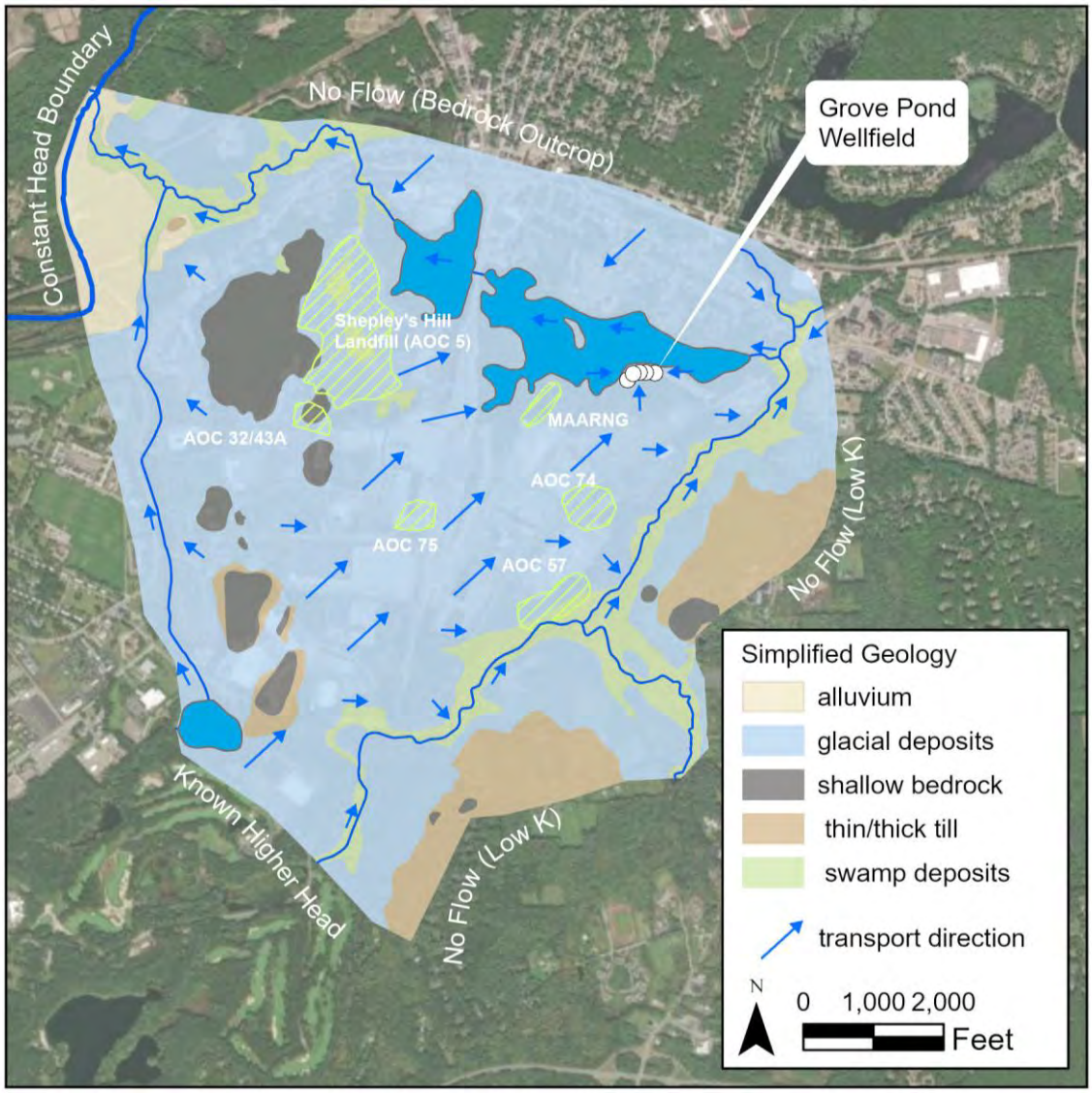



***Figure 4-1: Schematic of Conceptual Site Model***

## 4.2 PFAS Source Area Sampling Near Grove Pond Wellfield

The Preliminary Site Characterization for the Per- and Polyfluoroalkyl Substances Remedial Investigation at Fort Devens Army Installation (Devens) (KGS, 2017) identified many AOCs on and near Fort Devens. KGS and the USACE grouped the AOCs into three areas. Area 1 is the region upgradient of the Grove Pond wellfield. The RI for Area 1 is summarized by KGS (2020). The field investigations included "…sampling of existing monitoring wells, groundwater vertical profiling, soil sampling, and surface water and sediment sampling…" (KGS, 2020, pg. 1-2). The Project Team reviewed the Area 1 Preliminary Site Characterization Summary (KGS, 2020) and identified the AOCs relevant to this study that are discussed in Section 2.2 of this report. We also determined that additional analysis of the field investigation sample results would be necessary to achieve the goals of this study. We requested and received all groundwater level measurements and PFAS sample results from the USACE for the site investigation (SI) and RI and received the dataset in November 2022. The SIRI dataset includes groundwater sample, surface water

sample, and soil sample results collected between September 2018 and July 2022 at Fort Devens. We did not receive any subsequent sample results or other monitoring data. KGS (2020) provides a full discussion of the sampling that is relevant to Area 1 and completed prior to June of 2020. The Project Team used a subset of the SIRI dataset to understand the location and extent of various PFAS plumes based on groundwater samples collected in the winter of 2018-2019 and summer of 2019 to visualize PFAS plumes in groundwater.

Figure 4-2 through Figure 4-7 show a set of PFAS plume maps with one map for each of the six PFAS compounds evaluated in this study (i.e., PFOS, PFOA, PFHpA, PFHxS, PFHxA, and PFNA). Each map shows groundwater contours on a modified logarithmic scale (i.e., 10 ng/L, 50 ng/L, 100 ng/L, 500 ng/L, 1,000 ng/L, and 5,000 ng/L). The Project Team developed the iso-concentration contours based on the field investigation results, numerical contouring methods, and the hydraulic gradient of the groundwater table.

In addition to the iso-concentration contour lines, each map shows the sampling locations, which are the basis for the contours, as dots with the sample values shown adjacent to each location. The locations are color-coded. Green dots represent groundwater samples collected during the winter of 2018-2019, and blue dots represent groundwater samples collected during the summer of 2019. Many of the sampling locations in the SIRI dataset include measurements at multiple vertical locations. We subdivided these vertical positions based on the layers of the groundwater model that is described in Section 5.0 of this report. The contouring shown in these figures are from layer two which represents groundwater concentrations at or near the air-water interface. The Project Team completed the contouring for all depths, but we present the results near the air-water interface because they represent the highest PFAS concentrations.

The SIRI dataset includes soil samples collected at multiple depths for the same location. All of the soil sample results are from above the ground water surface and represent concentrations in the unsaturated zone, typically within the first 10 feet below the ground surface. Soil sample results are shown in Figure 4-2 through Figure 4-7 as red dots, and the concentrations are the maximum soil concentration regardless of depth below ground surface at each sampling location.

The Project Team made the decision to focus the figures on the primary and secondary PFAS sources (i.e., MAARNG and AOC 74). We evaluated groundwater sample results in the vicinity of AOC 57, AOC 75, and Shepley's Hill Landfill (AOC 5). The evaluation confirmed their ancillary influence on PFAS at the Grove Pond wellfield, and we developed this set of figures that focus on the primary and secondary source.

The Project Team recognizes that observed concentrations of perfluoroalkyl acids may be affected by precursor transformations, especially for perfluorocarboxylic acids (PFCAs) (e.g., PFHxA, PFHpA, and PFOA). We note that the highest concentrations are in the immediate vicinity of the source. We cannot rule out the formation of PFCAs from precursor transformations at the source given the available information in the SIRI dataset.

#### 4.2.1 PFOS

Elevated concentrations of PFOS are present immediately northeast of AOC 74. The plume is spreading both towards the north and towards the east. Groundwater sample results downgradient of Shepley's Hill Landfill and AOC 75 indicate elevated concentrations, but lower concentrations than are observed in the immediate vicinity of the MAARNG. AOC 57 sample results are low relative to AOC 74 and the MAARNG. The MAARNG source area has the highest concentrations of PFOS at the northern end immediately next to Grove Pond. The PFOS plume extends from the northern tip of the MAARNG eastward toward the Grove

Pond wellfield, but the plume originating at AOC 74 does not reach the Grove Pond wellfield. A third plume originating from an unknown source south of MAARNG appears to be migrating northward towards the MAARNG, but the highest concentrations of the plume (on the order of 100 ng/L) do not appear to connect to the plume originating from the MAARNG. The MAARNG appears to be the largest source of PFOS to the Grove Pond wellfield.

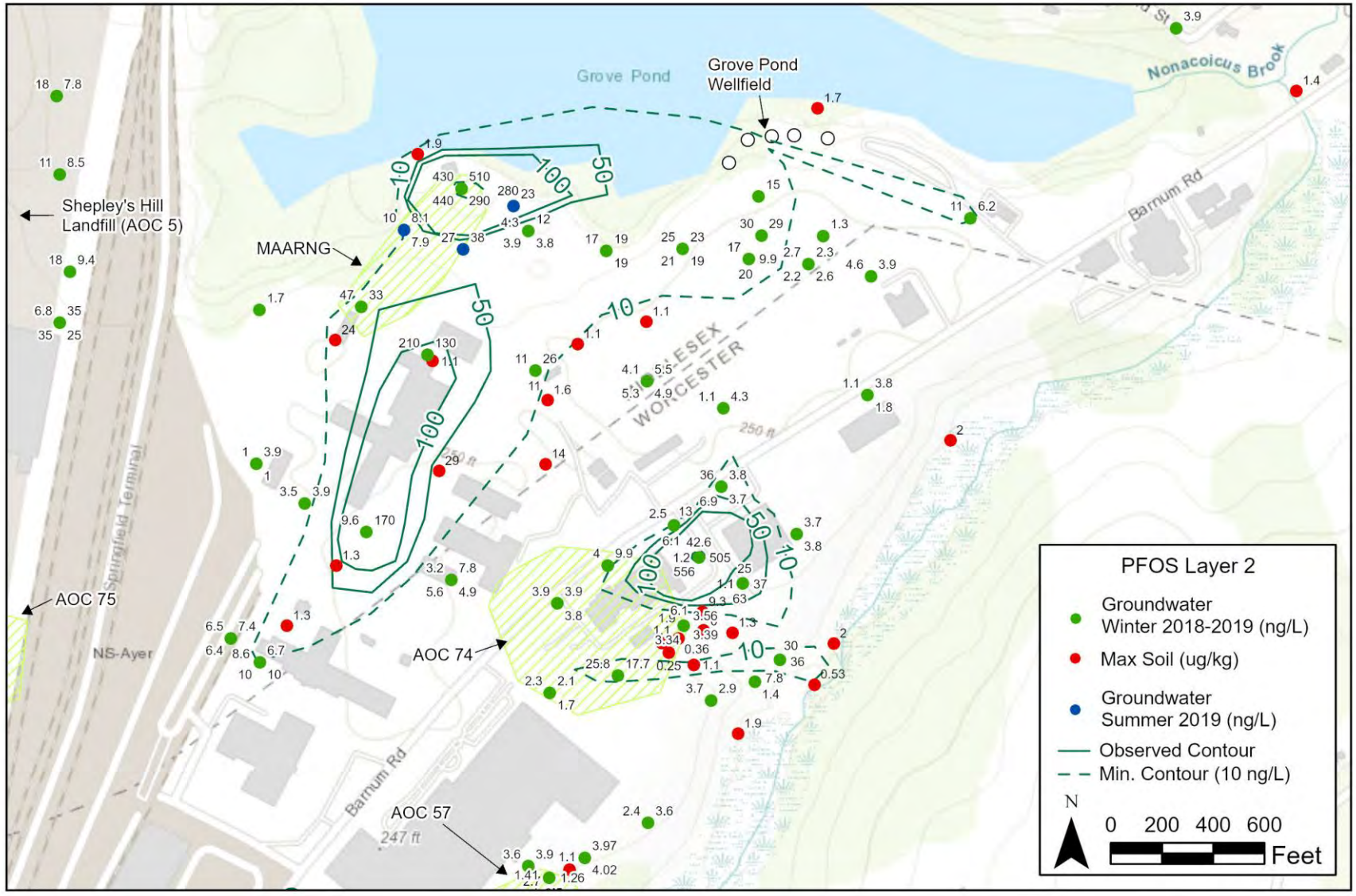



***Figure 4-2: Iso-Concentration Contours of PFOS in Groundwater***

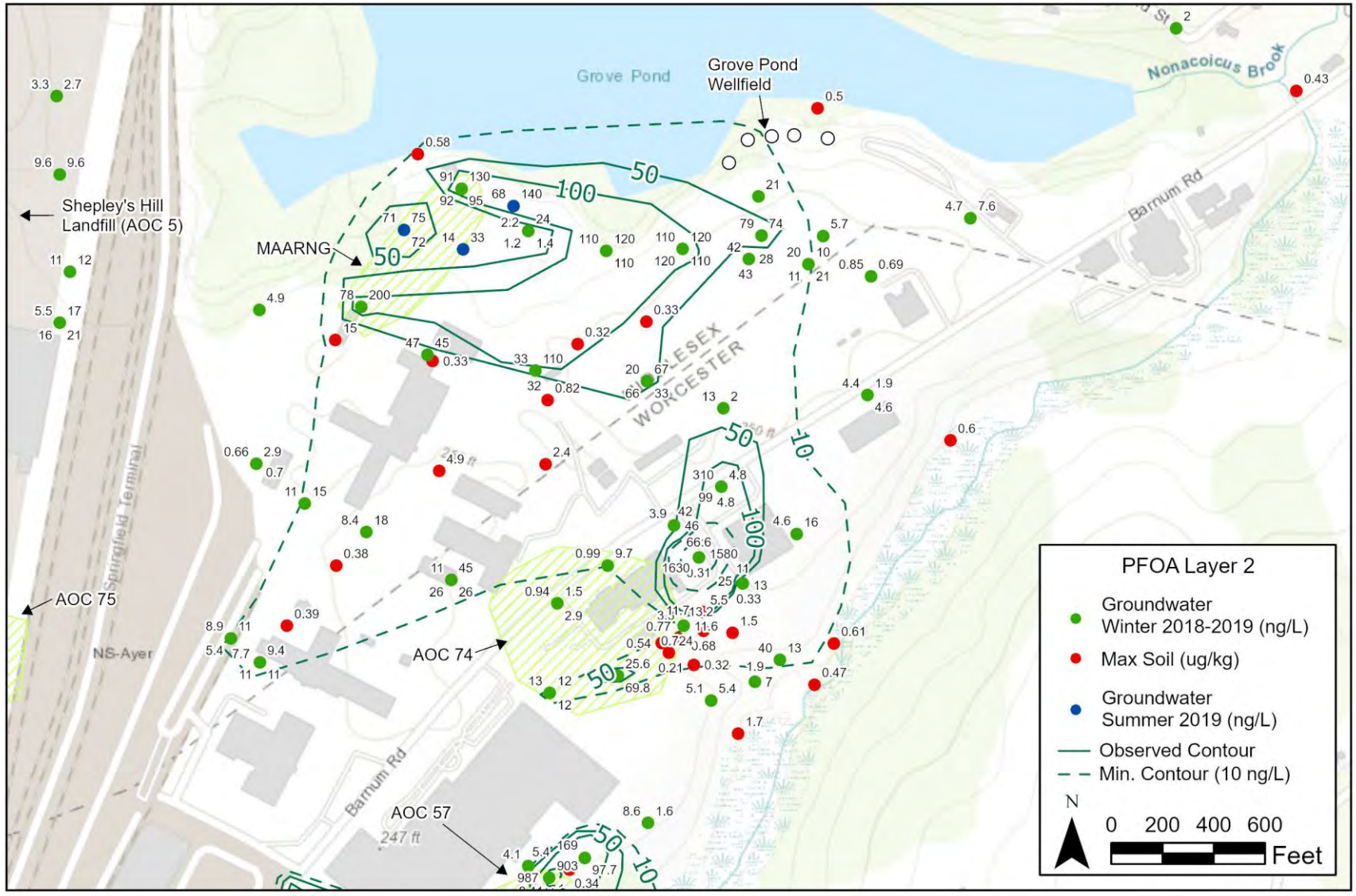



***Figure 4-3: Iso-Concentration Contours of PFOA in Groundwater***

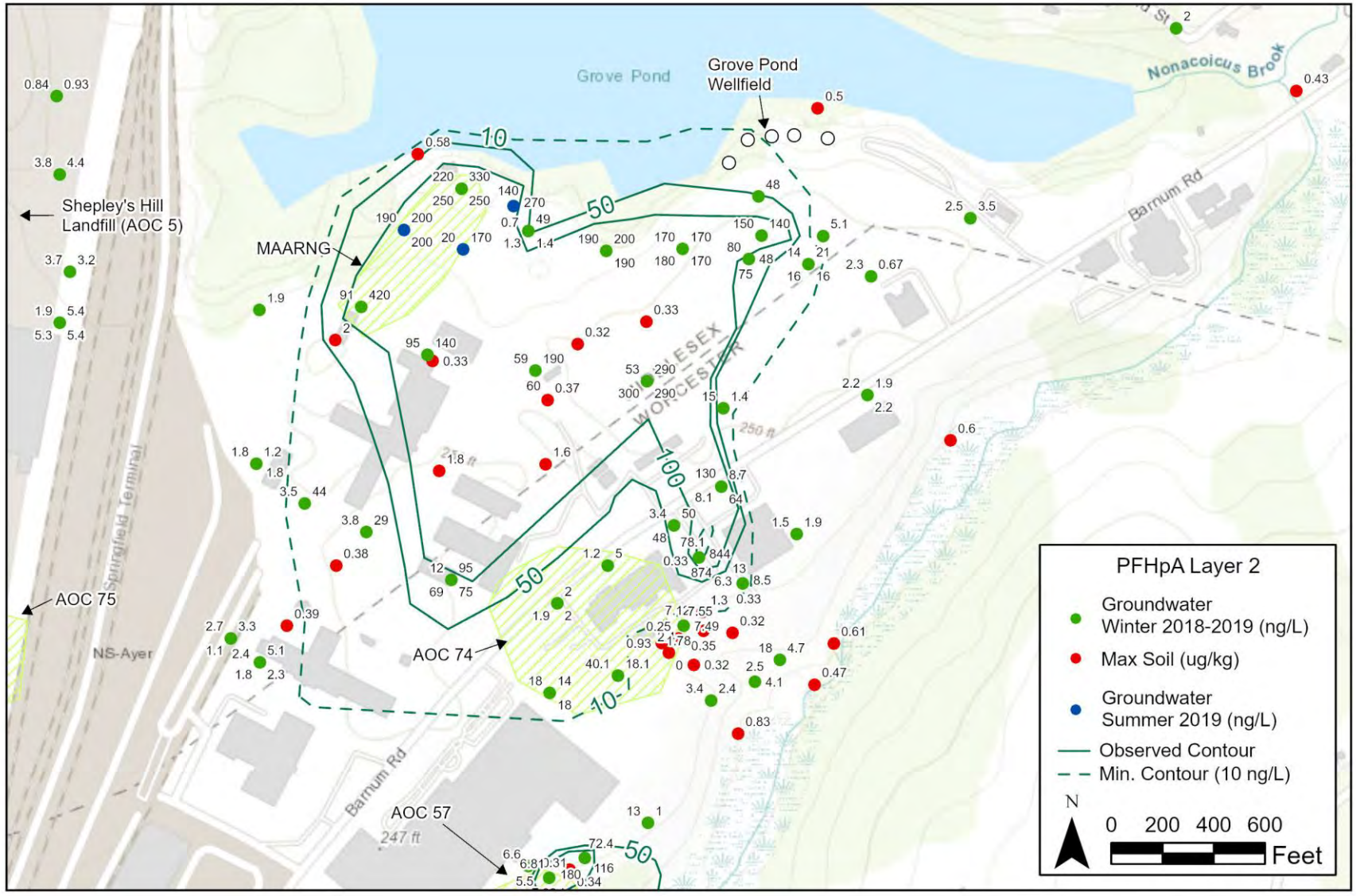



***Figure 4-4: Iso-Concentration Contours of PFHpA in Groundwater***

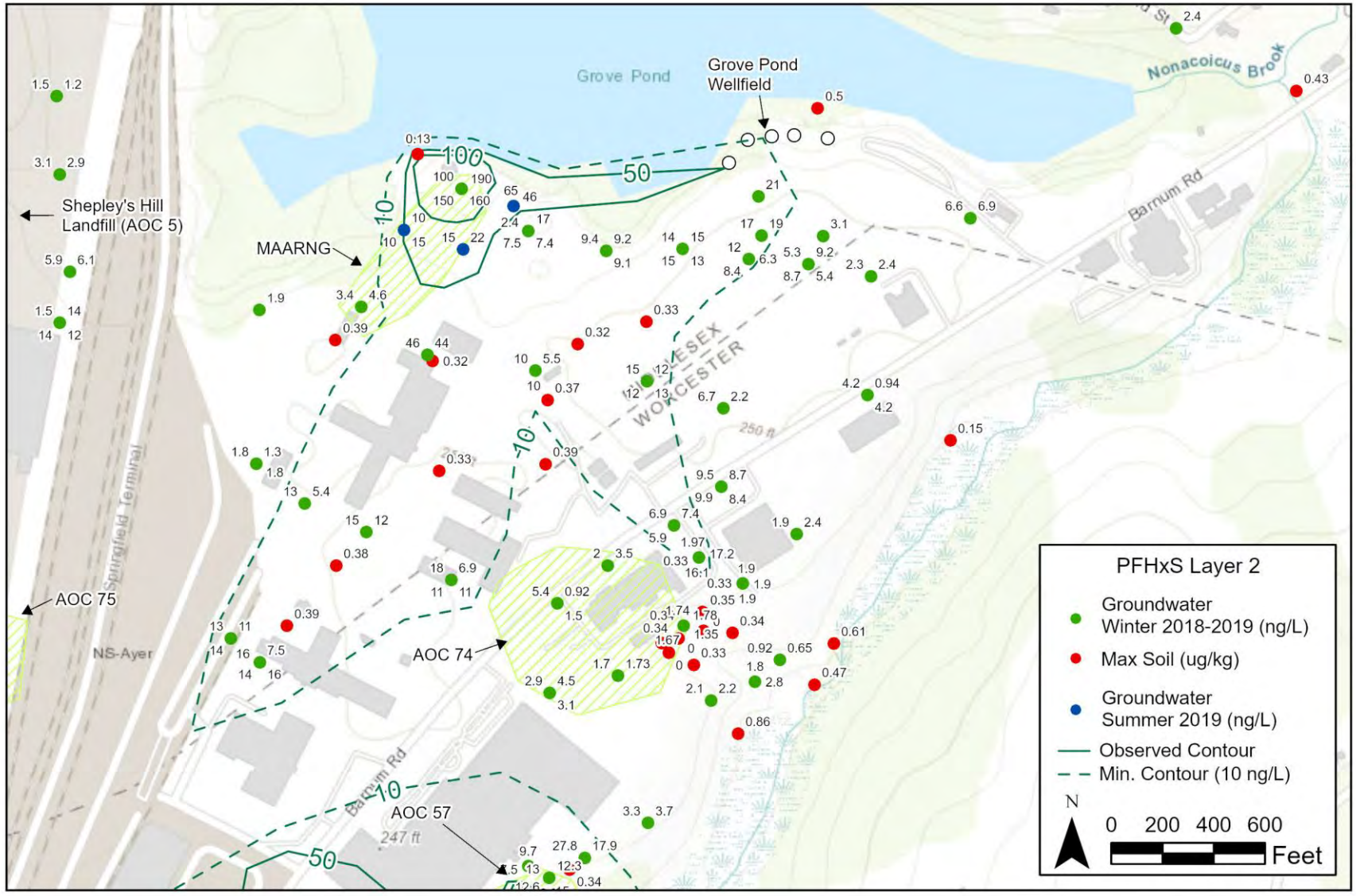



***Figure 4-5: Iso-Concentration Contours of PFHxS in Groundwater***

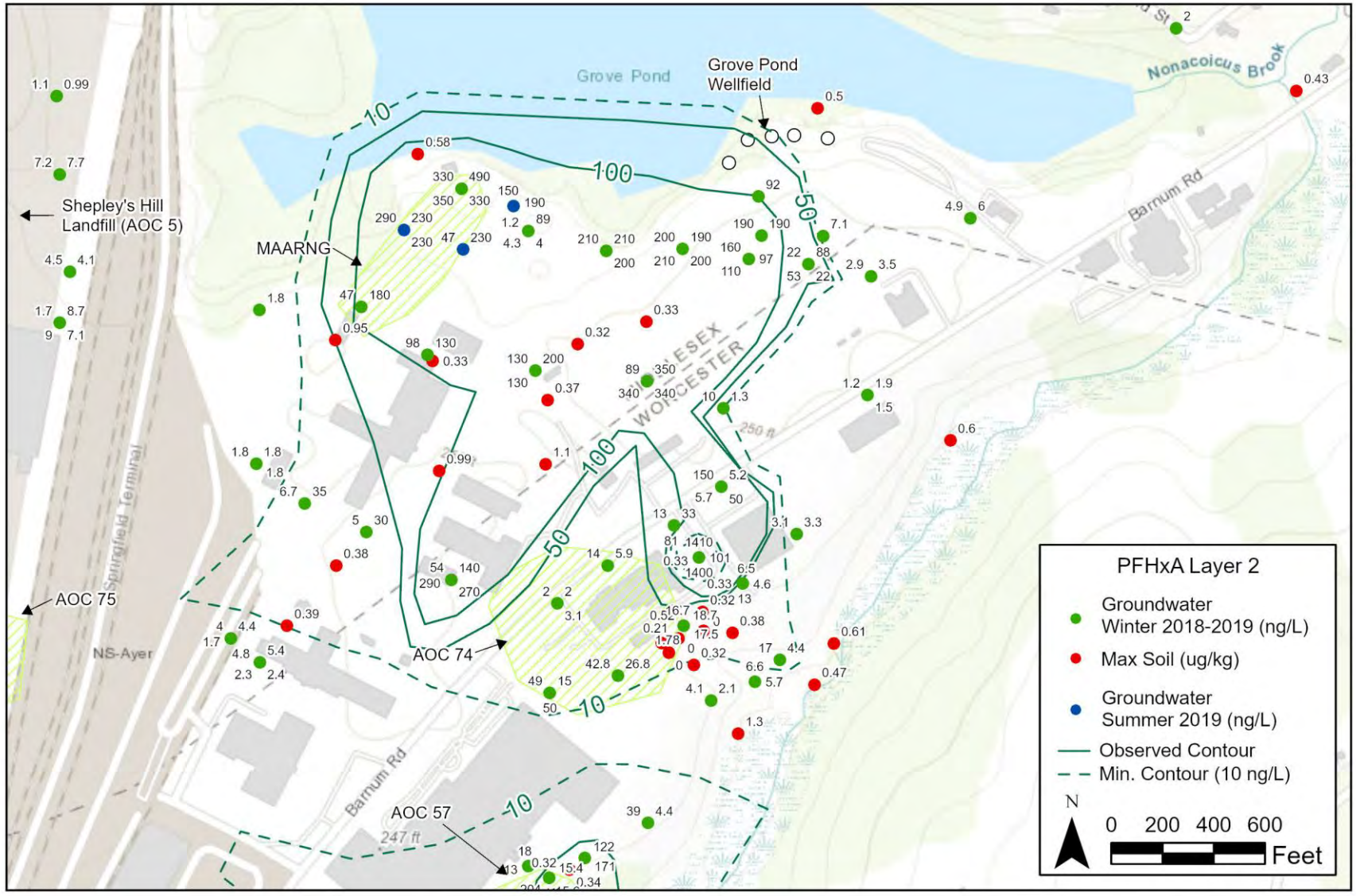



***Figure 4-6: Iso-Concentration Contours of PFHxA in Groundwater***

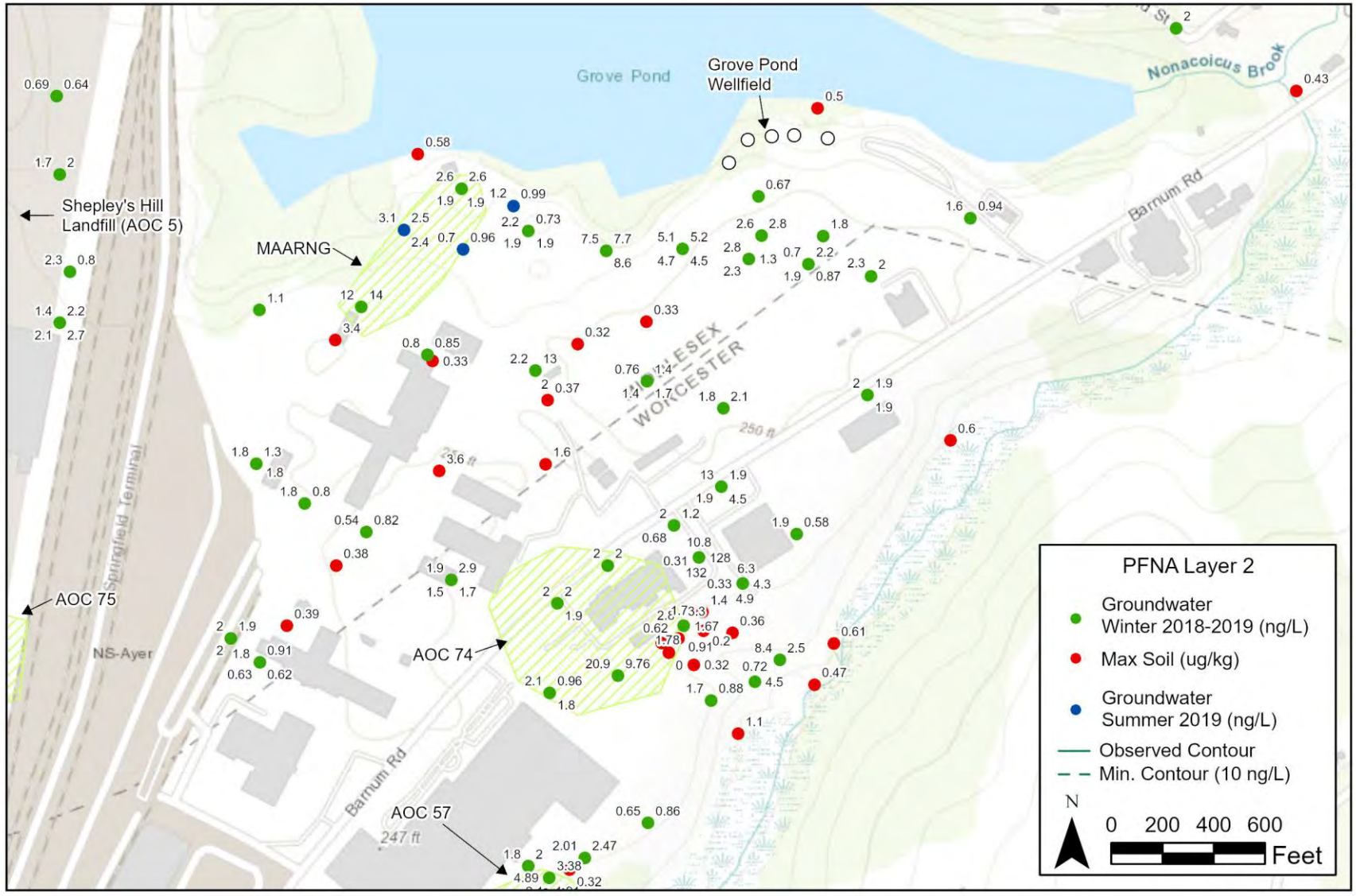



***Figure 4-7: Iso-Concentration Contours of PFNA in Groundwater***

#### 4.2.2 PFOA

Elevated concentrations of PFOA are present northeast of AOC 74 with the plume extending northward. Elevated concentrations are also present at AOC 57 with the plume extending eastward towards Cold Spring Brook. There is no evidence of a PFOA plume originating from AOC 75 or Shepley's Hill Landfill that is migrating towards the Grove Pond wellfield. Elevated PFOA concentrations are present in the MAARNG from both the southern end and the northern end of the delineated area. The plume is migrating eastward toward the Grove Pond wellfield. The MAARNG plume appears to be the dominant source of PFOA at the Grove Pond wellfield, but the plume from AOC 74 may also be contributing PFAS to the wells.

#### 4.2.3 PFHpA

Elevated concentrations of PFHpA are present northeast of AOC 74. The plume extends northwards and appears to combine with a broader plume originating from the MAARNG. This combined plume spans the area between AOC 74 and the MAARNG. There are also indications of a possible unidentified source to the south of the combined plume to the west of AOC 74. The Project Team believes that this is evidence of additional, but smaller, releases of PFAS that amount to background concentrations for the purposes of this study. Elevated concentrations at AOC57 are migrating eastward to Cold Spring Brook. Groundwater quality sample results do not indicate a PFHpA plume originating from Shepley's Hill Landfill or AOC 75.

#### 4.2.4 PFHxS

AOC 74 does not have elevated concentrations of PFHxS near the groundwater surface. Elevated concentrations are present south of AOC 57 (not shown in Figure 4-5), and the plume is migrating eastward towards Cold Spring Brook. There does not appear to be a PFHxS plume originating from Shepley's Hill Landfill or AOC 75 that is migrating towards the Grove Pond wellfield. The most elevated concentrations of PFHxS are present at the northern end of the MAARNG. That plume is migrating eastward towards the Grove Pond wellfield.

#### 4.2.5 PFHxA

Elevated concentrations of PFHxA are present northeast of AOC 74. The plume is migrating northward and appears to be combining with a plume originating from the MAARNG and migrating eastward. A third unidentified source to the south, similar to PFHpA, appears to be combining with these plumes as well. Elevated concentrations are present at AOC 57 and that plume is migrating eastward towards Cold Spring Brook. There does not appear to be a PFHxA plume originating from Shepley's Hill Landfill or AOC 75 that is migrating towards the Grove Pond wellfield.

#### 4.2.6 PFNA

PFNA concentrations at the Grove Pond wellfield have been consistently at or below detection limits. The groundwater quality measurements in the SIRI dataset are also low. Only two well sampling locations have sample results greater than 100 ng/L. Both of these locations are immediately north of AOC 74. In general, there are no PFNA plumes originating from any of the potential PFAS sources that are impacting the Grove Pond wellfield.

The Project Team evaluated the same dataset for deeper groundwater quality samples and that evaluation yields findings that are consistent with what is shown in Figure 4-2 through Figure 4-7.

### 4.3 Transport Pathways and Groundwater Quality Sample Results

The combination of the potential transport pathways and groundwater quality sample results provide a clear picture of PFAS transport. Shepley's Hill Landfill (AOC 5) and AOC 75 are not the source of significant

PFAS concentrations at the Grove Pond wellfield. The MAARNG appears to be the primary source of PFAS at the wellfield. AOC 74 is a secondary source. PFAS plumes from AOC 74 are migrating towards the Grove Pond PWS wells, but either have not reached the wellfield or have combined with the MAARNG plumes prior to reaching the wellfield.

PFAS plumes from AOC 57 are all migrating eastward towards Cold Spring Brook and not northward to the Grove Pond wellfield. Cold Spring Brook is in hydraulic contact with the aquifer. The brook acts as a groundwater sink (i.e., groundwater discharges to the brook), but Cold Spring Brook also feeds Grove Pond and Plow Shop Pond. The available information indicates that surface water from Grove Pond infiltrates through the pond sediments and is drawn into the wells due to pumping. This mechanism suggests that AOC 75 is also contributing to PFAS concentrations at the Grove Pond wellfield. The Project Team investigated this potential by mapping measured surface water concentrations from the SIRI dataset along with the groundwater iso-concentration contours from above. Attachment 2 to this report provides a set of six maps, one for each of the six PFAS, showing the same concentration contours from Figure 4-2 through Figure 4-7 and the surface water sample results.

These figures show that the highest surface water concentrations for each PFAS occur east of AOC 57, clearly suggesting that PFAS-contaminated groundwater is entering Cold Spring Brook from this PFAS source. The figures also show that PFAS concentrations decrease as you approach Grove Pond. This pattern suggests that PFAS concentrations are being diluted by the inflow of uncontaminated groundwater into Cold Spring Brook. Surface water samples collected in Grove Pond are typically an order of magnitude lower than the surface water concentrations adjacent to AOC 57.

The concentrations of PFAS in surface water samples from Grove Pond are typically one to two orders of magnitude lower than the concentrations being measured at the Grove Pond wellfield. For example, the typical concentrations of PFHxA are approximately 40-50 ng/L at GP-07 and approximately 80-100 ng/L at GP-08, and typical concentrations for PFHxA are approximately 5 ng/L in Grove Pond surface water. The Project Team concludes that AOC 57 via Cold Spring Brook may be a tertiary source of PFAS at the Grove Pond wellfield but is not a primary source.

### 4.4 Fingerprinting PFAS Sources

The Project Team has identified a primary source of PFAS (i.e., the MAARNG) and a secondary source of PFAS (i.e., AOC 74) of PFAS at the Grove Pond wellfield. The identification of sources is based on the SIRI dataset of groundwater quality sample results and the demonstrated migration of PFAS plumes from each potential source. We completed this identification analysis evaluating each of the PFAS analytes individually. The Project Team also conducted a fingerprinting analysis using radar plots. The purpose of the fingerprinting analysis is to compare the relative concentrations of the six PFAS at each source location to the relative concentrations of the six PFAS at the Grove Pond wellfield. Figure 4-8 shows a map of sampling locations representative of the MAARNG (i.e., GPVP-19-01 and GPVP-19-02 for the southern end and GPVP-18-11 and GPVP-18-12 for the northern end), sampling locations representative of AOC 74 (i.e., 74VP-18-05, 74VP-18-08, and 74VP-18-12), and the Grove Pond PWS wells (i.e., GP-01, GP-06, GP-07, and GP-08). The figure also shows a radar plot for each location. The radar plots for the monitoring wells show each sample depth for the location as a separate-colored line. The radar plots for the Grove Pond PWS wells show each sample date as a separate-colored line.

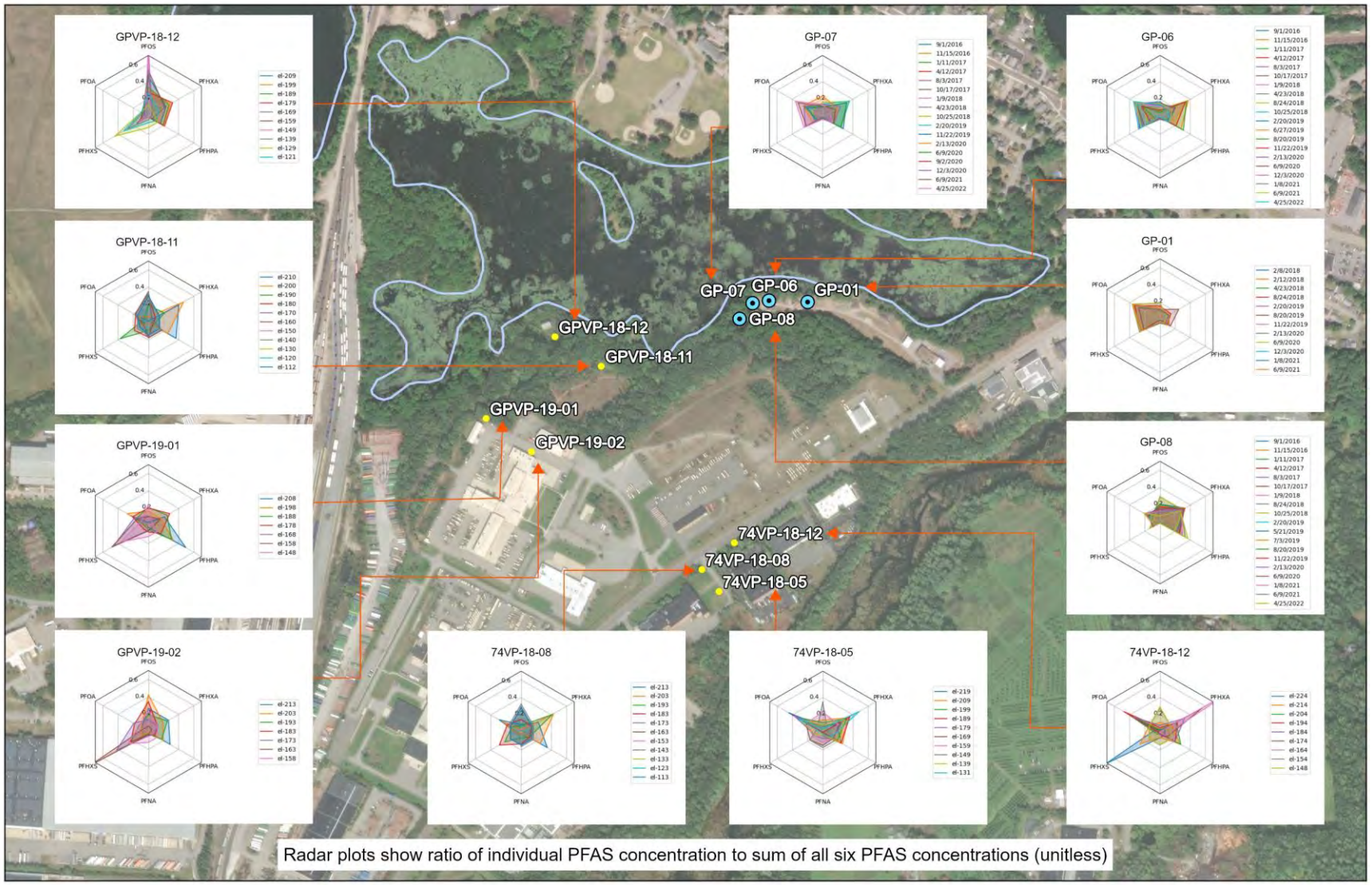



***Figure 4-8: PFAS Radar Plots***

The fingerprinting of PFAS sample results shown in Figure 4-8 is inconclusive. Multiple PFAS are present at each source, and multiple PFAS are present at the Grove Pond wells. No clear fingerprint or pattern is present to indicate that a particular source is dominant at the Grove Pond wellfield. In the absence of a fingerprint "match," the Project Team concludes that the primary and secondary source identifications based on plume delineation are not contradicted by this analysis and are appropriate for use in the CSM.

## 4.5 PFAS-Specific Transport Considerations

Thus far, the CSM has evaluated PFAS as a conventional dissolved phase pollutant. PFAS have chemical properties that are not fully understood and are being actively investigated (ITRC, 2024a). Many of the PFAS-specific transport behaviors are well summarized by the Interstate Technology Regulatory Council (ITRC) (2024a). These behaviors include a tendency for PFAS to accumulate at both the air-water interface (i.e., the groundwater surface and the vadose zone) and the ability of PFAS to partition to solid phase materials like soils and sediments. These tendencies slow down, or retard, the transport of PFAS relative to the flow of groundwater.

## 4.6 Reconciling Historical Information and the CSM

The Project Team conducted a thorough review of the available groundwater sample results. We identified the MAARNG as the primary source of PFAS affecting the Grove Pond wellfield. Groundwater quality samples indicate plumes of PFAS to be migrating from the MAARNG to the Grove Pond wellfield. The highest groundwater concentrations are centered on the area of the 1960 fire and the Fort Devens pumphouse.

KGS (2020) mention the 1960 fire, but they consider it unlikely that AFFF was used to extinguish the fire. They also indicate there is no known "use, storage, or disposal of AFFF at the MAARNG property" (KGS, 2020, pg. 6-1). AFFF was first manufactured in the mid-1960s (ITRC, 2025a). The Project Team agrees that AFFF was not used to extinguish the 1960 fire, but the warehouse that burned down was in the "ordnance depot section" and some of what was destroyed included "Equipment and parts for tanks and military vehicles" (The Daily Spirit, September 15, 1960). By 1960, PFAS was already part of the manufacturing of many industrial products (ITRC, 2025b). The Project Team believes that the likely source of PFAS is the industrial material that was a part of the fire.

Groundwater transport for PFAS is known to be substantially retarded. The shape and the size of the plumes originating from the MAARNG necessarily require an early release date. The groundwater modeling presented in subsequent sections of this report demonstrates that a PFAS release date of 1960 results in PFAS plumes that are consistent with groundwater concentrations in 2019.

## 4.7 CSM Summary

As a part of developing the CSM, the Project Team evaluated transport pathways based on hydrogeology and PFAS plume migration. We were able to develop an internally consistent CSM in which the MAARNG is the primary PFAS source affecting the Grove Pond wellfield and AOC 74 is a secondary source. PFAS are transported to the Grove Pond wellfield through groundwater. AOC 57 is a tertiary contributor to PFAS at the Grove Pond wellfield. PFAS from AOC 57 are transported via surface water and diluted substantially before potentially being drawn through sediments in Grove Pond and into the wells. All groundwater transport of PFAS is expected to be substantially retarded.

This CSM helps characterize the type of modeling tools necessary to estimate historical PFAS concentrations at the Grove Pond wellfield. The model must be a coupled hydrogeologic-transport model

that can also incorporate the influence of surface water transport and infiltration into the aquifer. The CSM also informs the period of modeling necessary to estimate historical PFAS concentrations. The best available information suggests that the release of PFAS in the MAARNG occurred as early as 1960 and at AOC 74 as early as the mid-1990s. In the next section of this report, the Project Team discusses the selected modeling tools, the development of the model, and the application of that model to estimate PFAS concentrations at the Grove Pond wellfield in the years 2000 to 2022.

# 5.0 GROUNDWATER FLOW MODELING

The Project Team considered the needs of the CSM against the available modeling options and selected MODFLOW-USG (Panday et al., 2013). MODFLOW is a groundwater model originally developed and currently maintained by the United States Geological Survey (USGS). “MODFLOW is considered an international standard for simulating and predicting groundwater conditions and groundwater/surface-water interactions” (USGS, 2024). MODFLOW-USG is a version of MODFLOW, developed by Panday (2013), that allows unstructured grids and includes multiple physical and chemical processes based on a control-volume finite-difference formulation. Some of the processes included in MODFLOW-USG are contaminant transport and groundwater-surface water interactions using connected linear networks (CLNs). CLNs allow for surface water features to not just act as boundary conditions to influence groundwater flow but for surface water to “flow” in the model domain and transport contaminants through surface water features. It is the incorporation of CLNs that led the Project team to use MODFLOW-USG. Indeed, the groundwater flow model is based on a structured grid not an unstructured grid.

MODFLOW-USG meets all requirements as described in the CSM and allows for the estimation of PFAS concentrations at the Grove Pond wellfield.

## 5.1 Groundwater Flow Model Development

The Project Team initially developed a steady-state groundwater flow model and calibrated that model to groundwater elevation measurements from the SIRI dataset. Model development included defining and discretizing the model domain both horizontally into cells and vertically into layers. We assigned boundary conditions and aquifer properties to the model and simulated the relevant surface water features as CLNs.

### 5.1.1 Model Domain

Figure 5-1 shows the model area and the active model domain. The black rectangle is the model area, and the red line marks the active model domain. The active model domain represents the presence of bedrock outcrops north of Grove Pond and low hydraulic conductivity glacial till east of Cold Spring Brook as natural no-flow boundaries. The Project Team considered using the bedrock outcrops east of Willow Brook as a natural no-flow boundary, but we concluded that the incorporation of Willow Brook was necessary for model performance. The western limit of the active model domain is sufficiently west of the area of interest not to compromise model performance and allows for the incorporation of the Nashua River as a boundary condition. A general head boundary defines the southern limit of the active model domain.

The ground surface serves as the top of the groundwater model. Given the low hydraulic conductivity of the bedrock underlying the aquifer, the Project Team assumed the bedrock to be a no-flow boundary which serves as the bottom of the model. Both the top and bottom of the model domain were smoothed as a part of model development, but the smoothed surfaces appropriately represent the ground surface as depicted in Figure 3-1 and the bedrock surface as depicted in Figure 3-4.

The model coordinate system is Massachusetts State Plane in units of feet, and the vertical datum for the model is NAVD88 in units of feet.

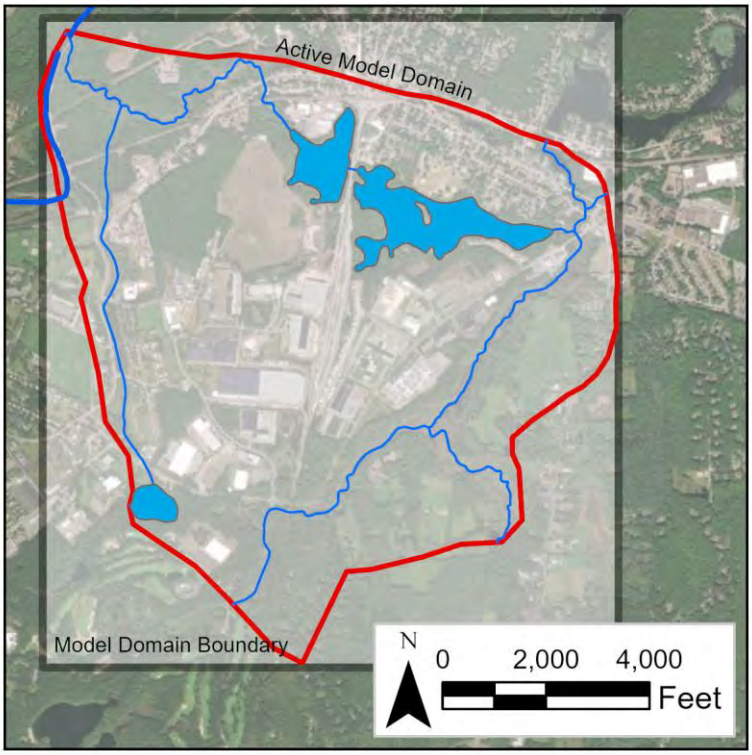



***Figure 5-1: Model Domain***

### 5.1.2 Model Discretization

MODFLOW-USG is an unstructured-grid version of MODFLOW, but utilizing an unstructured grid is not necessary to achieve the objectives for this modeling. The Project Team subdivided the horizontal model domain into a uniform finite-difference grid with cell dimensions of 100 ft by 100 ft. We subdivided the vertical model domain into four layers. The aquifer that feeds the Grove Pond wellfield is described as glacial stratified deposits. There is insufficient information about the location and thickness of strata within the primary aquifer/overburden to subdivide the model based on those strata. The Project Team used four layers of equal thickness (i.e., each layer representing 25% of the distance from the ground surface to the bedrock). This approach is consistent with the approach taken by CDM (1993) when establishing the WPA and by Geosyntec (2020) when evaluating Shepley's Hill Landfill. Figure 5-2 shows both the horizontal model discretization and the vertical discretization at three different cross sections through the model grid. Bedrock outcrops (high points) are accounted for as are bedrock depressions.

### 5.1.3 Surface Water Features as CLNs and Boundary Conditions

The model domain includes multiple ponds, brooks, and rivers. These surface water features are incorporated into the model as CLNs. A CLN is a set of model cells that are connected. This means that water can pass from one cell to another through a different transport mechanism than groundwater flow. Cold Spring Brook, Bowers Brook, Willow Brook, and Nonacoicus Brook are included in the model as separate CLNs. In cases where the brooks connect (e.g., Bowers Brook flowing into Cold Spring Brook), the CLNs are linked at a common cell to allow one CLN to flow into another CLN. Plow Shop Pond and Grove Pond are grouped together in a single CLN. The Nashua River is also included in the model as a CLN, but in contrast to all other CLNs, the water surface elevation is fixed at 205 ft NAVD88. The Nashua River serves as a constant head boundary condition in the model. Figure 5-3 shows each CLN.

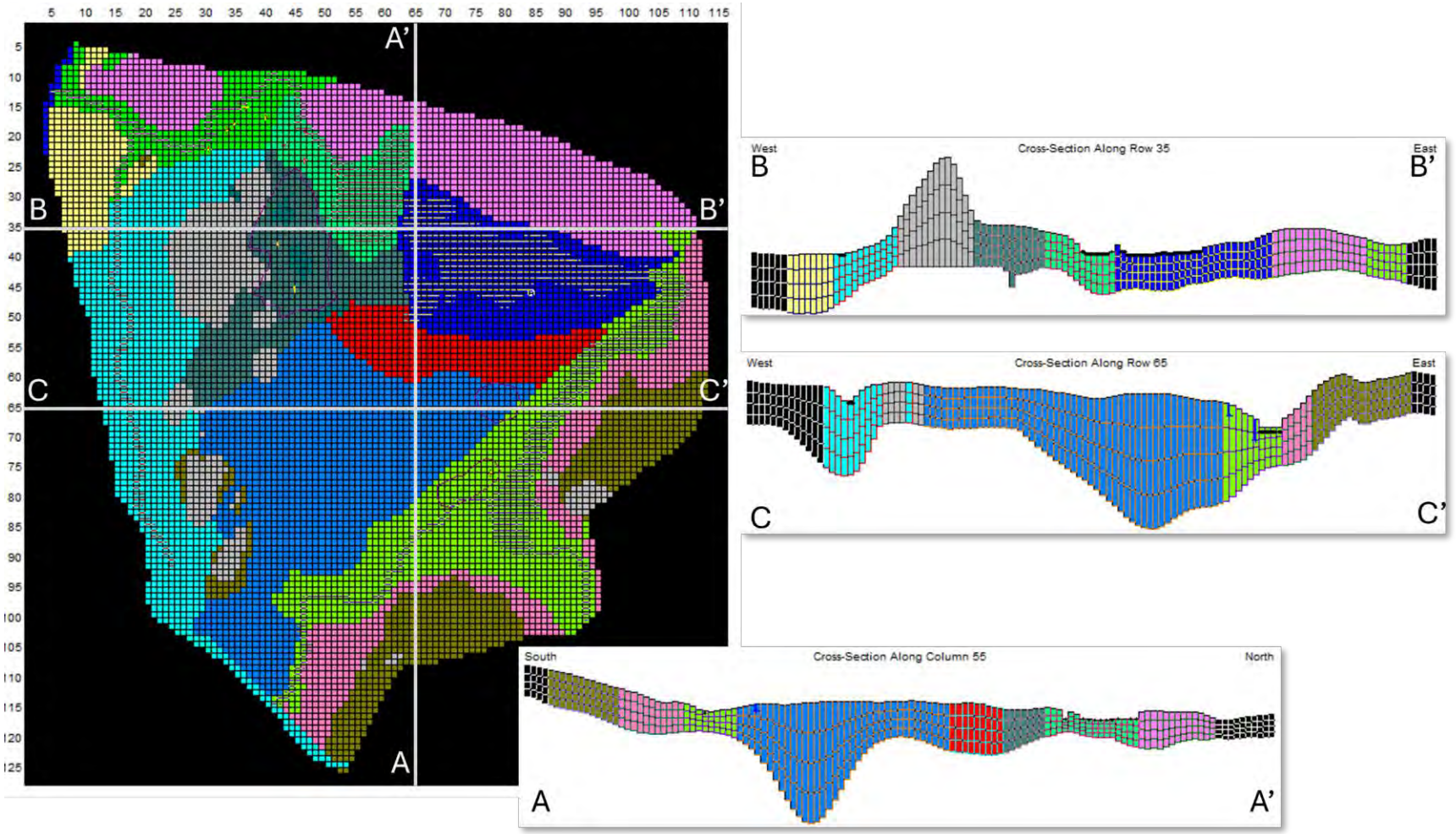



***Figure 5-2: Model Grid Discretization***

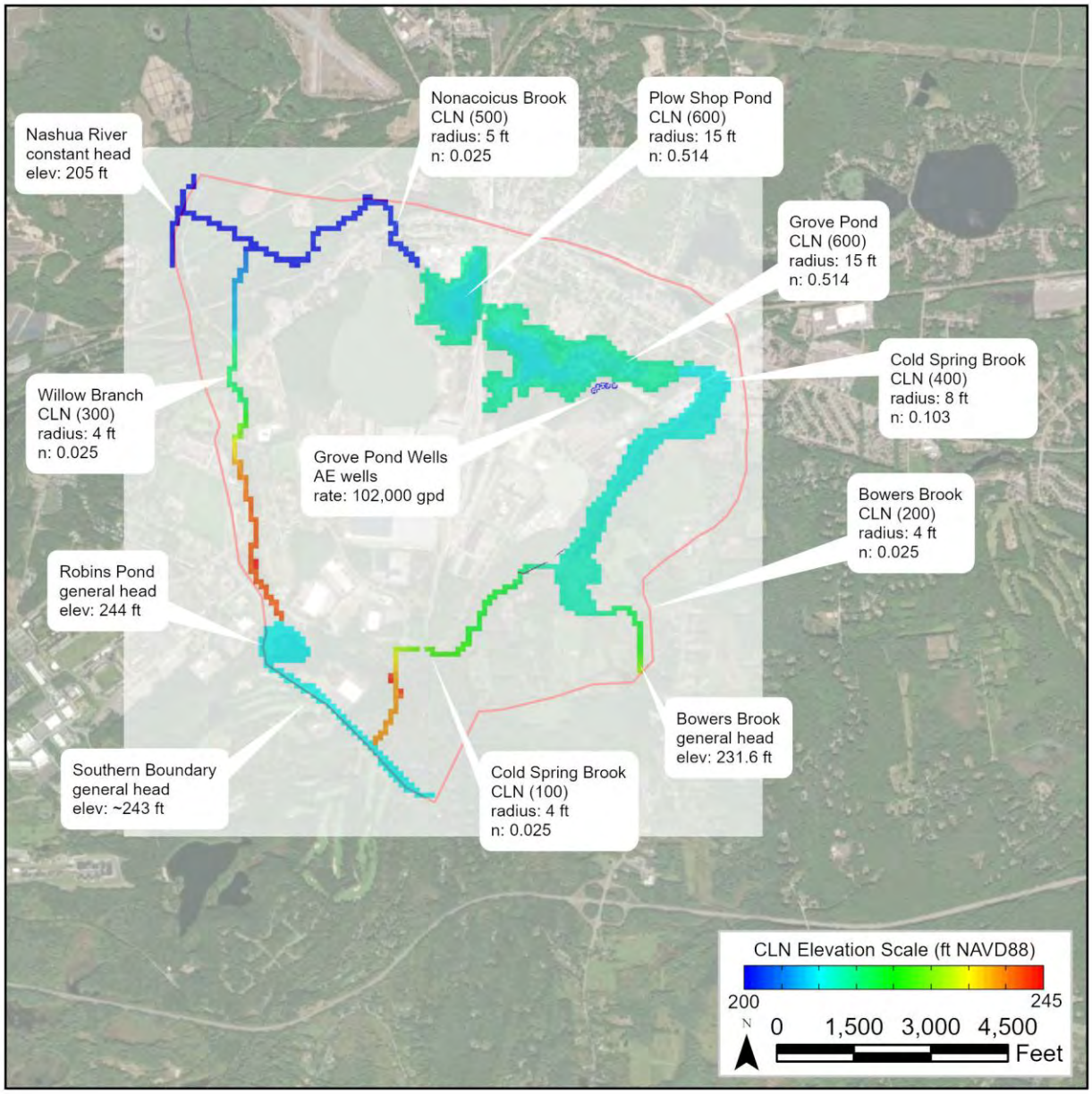



***Figure 5-3: Surface Water Feature CLNs and Boundary Conditions***

Each CLN requires a set of parameters to be specified including: radius, Manning's n, and FSKIN. The radius and the Manning's n value are measures of how easily water can flow from one cell to another. Those values are shown in Figure 5-3. The units for Manning's n values are not typically reported, but Manning's n is not a dimensionless parameter. The Manning's n values that are shown in the figure are in metric units (i.e., units when values reported without unit), but the values used in the model are English units and in the same time scale as the model (i.e., days). The final Manning's n values are based on guidance from Panday et al. (2013). The FSKIN value is a measure of the ability of water to leave the CLN and enter the groundwater grid cell. In the case of streams, FSKIN is conceptually equivalent to the vertical hydraulic conductivity through the stream bed. The Project Team used FSKIN as a calibration parameter.

The Nashua River is incorporated into the model as a CLN and acts as a constant head boundary condition. There are three additional boundary conditions in the model: a general head boundary condition along the edge of the active model domain that runs from northwest to southeast just south of Robbins Pond, a general head boundary at the upper limit of Bowers Brook, and the five pumping wells in the Grove Pond wellfield. The location of each boundary condition is shown in Figure 5-3. Table 5-1 summarizes all of the boundary conditions, the boundary type, the selected value, and the rationale for the value selected. Model calibration compared model results to groundwater table elevations from March 2020. To the extent possible, boundary condition values were selected to represent that same time period.

***Table 5-1: Boundary Conditions***

| Location | Type | Value | Rationale |
|---|---|---|---|
| Nashua River | Constant Head | 205 ft NAVD88 | Geosyntec (2020) conducted analysis to correlate Nashua River stage to downstream USGS stream gauging station in East Pepperell (ID: 01096500). They concluded that the Nashua River stage is 33.1 ft above East Pepperell. Average stage in East Pepperell in March 2020 was 171.7 ft NAVD88. Resulting Nashua River stage is 204.8 or approximately 205 ft NAVD88. |
| Southwest Model Domain Boundary | General Head | 243 ft NAVD88 | SIRI dataset includes water levels in the vicinity of this boundary in March of 2020. The approximate average from these measurements is 243 ft NAVD88. This value also matched well to water levels reported in CDM (1993). |
| Robbins Pond | General Head | 244 ft NAVD88 | SIRI dataset includes water levels in the immediate vicinity of Robbins Pond in March of 2020. |
| Head of Bowers Brook | General Head | 231.6 ft NAVD88 | Appropriate value determined during model calibration. |
| Grove Pond Wellfield | Wells | GP-01: 0 $ft^3/d$<br>GP-02: 0 $ft^3/d$<br>GP-06: 47,100 $ft^3/d$<br>GP-07: 43,300 $ft^3/d$<br>GP-08: 8,600 $ft^3/d$ | Daily average pumping rates as reported to MA DEP for March 2020. |

### 5.1.4 Recharge and Evapotranspiration

Boundary conditions act as sources (i.e., adding water to the model) and sinks (i.e., removing water from the model). Recharge is an additional source within the model and evapotranspiration is an additional sink within the model. Recharge is the rate at which precipitation enters an aquifer. Evapotranspiration is the rate at which water exits the aquifer through the physical processes of evaporation at the air-water interface

and the transpiration of water by plant life at the ground surface. Recharge and evapotranspiration are functions of climate, ground cover (e.g., pervious or impervious), and soil properties. The Project Team used recharge and evapotranspiration as calibration parameters, but we established a range of reasonable values based on site-specific information.

The average rainfall at a weather station located approximately 0.5 miles from Grove Pond during 2018 and 2019 was 48.2 inches/year (NOAA, 2023). These years were selected so as to coincide with available groundwater elevation measurements. The Project Team applied a 50% reduction to the annual precipitation to account for the water lost to surface runoff that never reaches the aquifer. The Project Team also applied a scaling factor based on land use types. We used land cover data from MassGIS (2024b) as the basis for the land use types but simplified that dataset to five representative land cover types. Figure 5-4 shows the land use types within the model domain and the recharge scaling factor.

The Northeast Regional Climate Center (NRCC) provides evapotranspiration values for Worcester, Massachusetts. Worcester is approximately 22 miles southwest of Ayer. The range of values is from 0.3 inches/month to 4.1 inches/month (NRCC, 2024).

Figure 5-4 includes scaling factors for evapotranspiration based on land use cover. The evapotranspiration scaling factors were limited to two categories based on whether the land cover prevented a direct connection to the atmosphere (i.e., impervious/surface water) or not. Both recharge and evapotranspiration were used as calibration parameters for the model. The Project Team adjusted the recharge/evapotranspiration value for the full model domain, and the full model domain values were subsequently multiplied by the scaling factors shown in Figure 5-4.

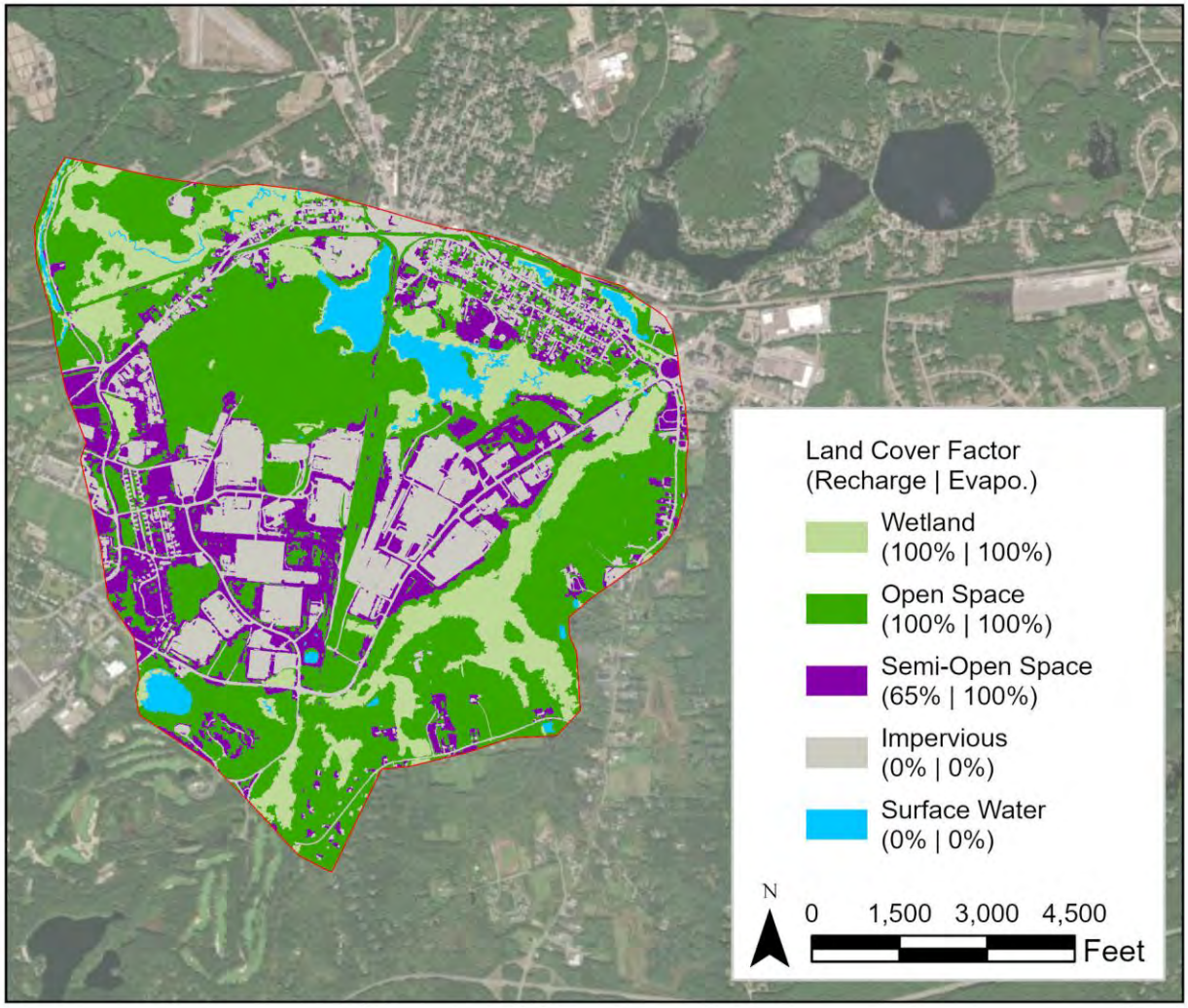



***Figure 5-4: Land Use Types, Recharge and Evapotranspiration Factors***

### 5.1.5 Hydraulic Conductivity, Specific Storage, Specific Yield, and Porosity

In addition to subdividing the model domain into grid cells and layers, the Project Team subdivided the model domain into hydraulic conductivity zones. We created these zones based on available information about the surficial geology, hydraulic conductivity zones from CDM (1993), and hydraulic conductivity zones from Geosyntec (2020). Figure 5-5 shows each hydraulic conductivity zone. The individual hydraulic conductivity values for each zone were used as calibration parameters.

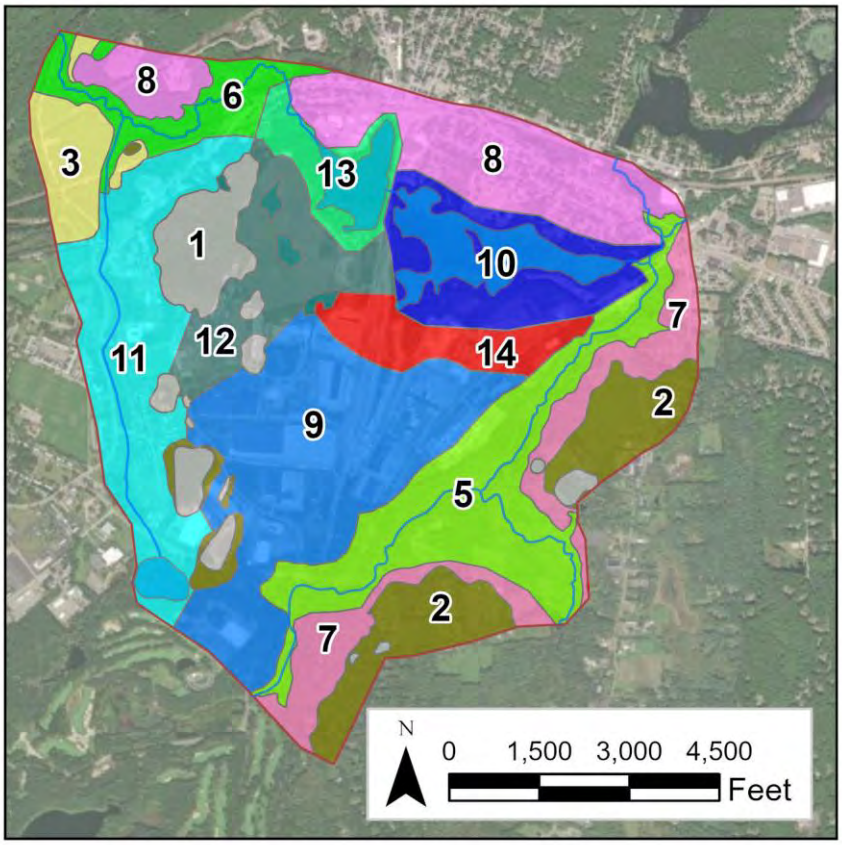



***Figure 5-5: Hydraulic Conductivity Zones***

The Project Team also used the hydraulic conductivity zones to assign specific storage, specific yield, and porosity throughout the model domain. Specific storage is the volume of water released from storage in a unit volume of aquifer given a unit decrease in hydraulic head (Freeze and Cherry, 1979). Specific yield is similar to specific storage but is the volume of water released per unit surface area of aquifer per unit decrease in the water table for an unconfined aquifer (Freeze and Cherry, 1979). Porosity is the ratio of the volume of voids per total volume for a unit volume of the aquifer material (Freeze and Cherry, 1979). Table 5-2 provides each of these values for the zones shown in Figure 5-5. The Project Team selected the values shown in Table 5-2 based on the surficial geology and professional judgement and experience.

***Table 5-2: Aquifer Properties: Specific Storage, Specific Yield, and Porosity***

| Zone | Geology | Specific Storage | Specific Yield | Porosity |
|---|---|---|---|---|
| | | 1/ft | -- | -- |
| 1 | bedrock | 0.00001 | 0.00 | 0.10 |
| 2 | till | 0.00002 | 0.30 | 0.35 |
| 3 | alluvium | 0.00002 | 0.25 | 0.35 |
| 4 | swamp deposits | 0.00040 | 0.20 | 0.45 |
| 5 | swamp deposits | 0.00005 | 0.30 | 0.35 |
| 6 | swamp deposits | 0.00005 | 0.30 | 0.35 |
| 7 | glacial deposits | 0.00005 | 0.30 | 0.40 |
| 8 | glacial deposits | 0.00005 | 0.30 | 0.40 |
| 9 | glacial deposits | 0.00002 | 0.25 | 0.35 |
| 10 | glacial deposits | 0.00002 | 0.25 | 0.35 |
| 11 | glacial deposits/fill | 0.00005 | 0.30 | 0.40 |
| 12 | glacial deposits | 0.00040 | 0.20 | 0.45 |
| 13 | swamp deposits | 0.00005 | 0.30 | 0.35 |
| 14 | glacial deposits | 0.00002 | 0.25 | 0.35 |

## 5.2 Groundwater Flow Model Calibration

### 5.2.1 Calibration Dataset

Prior to evaluating PFAS transport with the MODFLOW-USG model, the Project Team calibrated the steady-state groundwater flow model to a set of groundwater elevation measurements. In order to provide good spatial coverage throughout the model domain, the measurements come from two data sources: USACE - PFAS RI wells (collected in April 2020 and March 2020) and Shepley's Hill Landfill investigation wells (collected in March-April 2013-2014).

The steady-state calibration period is intended to represent March 2020. The Project Team determined that the inclusion of April 2020 measurements was appropriate because of the temporal proximity of the measurements (i.e., one month apart). We also determined that the inclusion of SHL investigation wells was appropriate given that they represented the same season of the year and given that the groundwater table reported in CDM (1993) was consistent with the observed water levels in the SIRI dataset. Figure 5-6 shows the location of each well used in the calibration dataset. Attachment 3 of this report provides relevant well information and the value used in model calibration as a table. Figure 5-6 includes six "artifical model wells" along brooks. These calibration targets are taken as the ground surface elevation based on the assumption that the ground surface elevation in those cells is representative of the water surface for the relevant brook.

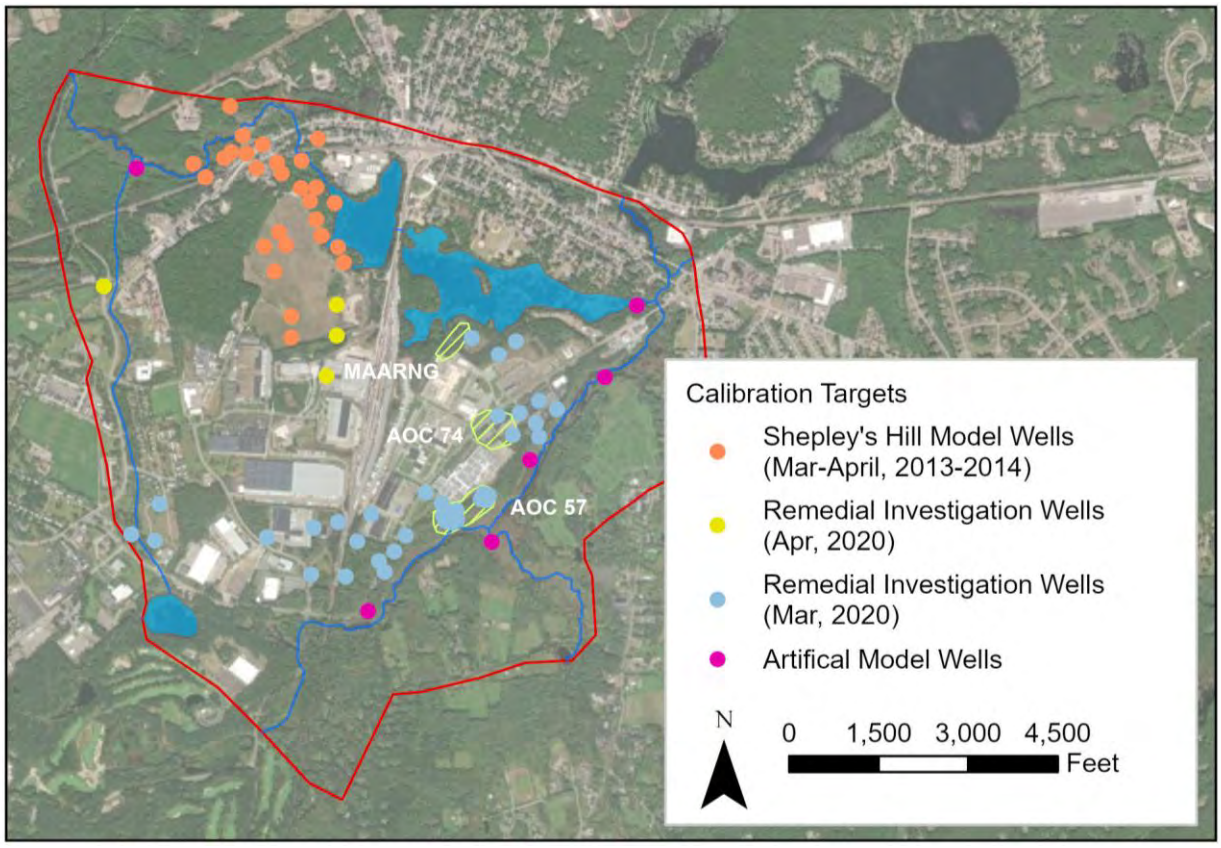



***Figure 5-6: Groundwater Surface Calibration Targets***

### 5.2.2 Calibration Parameters

The Project Team used recharge, evapotranspiration, hydraulic conductivity, and CLN FSKIN values to calibrate the steady-state model to observed groundwater elevations. These calibration parameters can be divided into two groups. The appropriate values for recharge and evapotranspiration apply across the entire model domain. We calibrated these model parameters manually (i.e., running the model one time, evaluating calibration performance, and adjusting the value). The appropriate hydraulic conductivity and FSKIN values were calibrated using PEST. PEST is a software package that automates calibration of a numerical model (PEST, 2024). The Project Team used the graphical user interface Groundwater Vistas (ESI, 2020) to develop the MODFLOW-USG model. PEST is integrated into Vistas. Given a set of calibration parameters and starting values along with calibration targets, PEST runs the MODFLOW-USG model many times progressively iterating the calibration parameters to optimize the agreement between modeled and observed values at each target. The inputs to PEST include an initial value and an allowable range. The initial values for each hydraulic conductivity zone and FSKIN (i.e., pond bottom and stream bed vertical hydraulic conductivity) were based on the final values from CDM (1993) and Geosyntec (2020). The allowable range for each value was established by applying log-based minimum and maximum scaling factor. The log-based scaling factor for horizontal hydraulic conducitivity was from $1x10^{-5}$ to $1x10^{4}$. The vertical hydraulic conductivity scaling factor was from $1x10^{-5}$ to $1x10^{2}$.

Figure 5-7 shows the final calibrated values for hydraulic conductivity.

Table 5-3 presents the final calibrated values for recharge and evapotranspiration, and Figure 5-8 shows the final calibrated values for CLN FSKIN. The final calibration values are reasonable. They are consistent with the geology. For example, Zone 1 represents bedrock outcrops. Zone 1 has the lowest horizontal hydraulic conductivity within the model. The hydraulic conductivity values are also consistent with prior modeling. For example, Zone 10 is the region that surrounds grove pond and has the highest hydraulic conductivity within the model.

PEST returns model parameter values (e.g., hydraulic conductivity) without an evaluation of appropriate significant figures. The values shown in Figure 5-7 and Figure 5-8 show these values with a maximum of three significant figures.

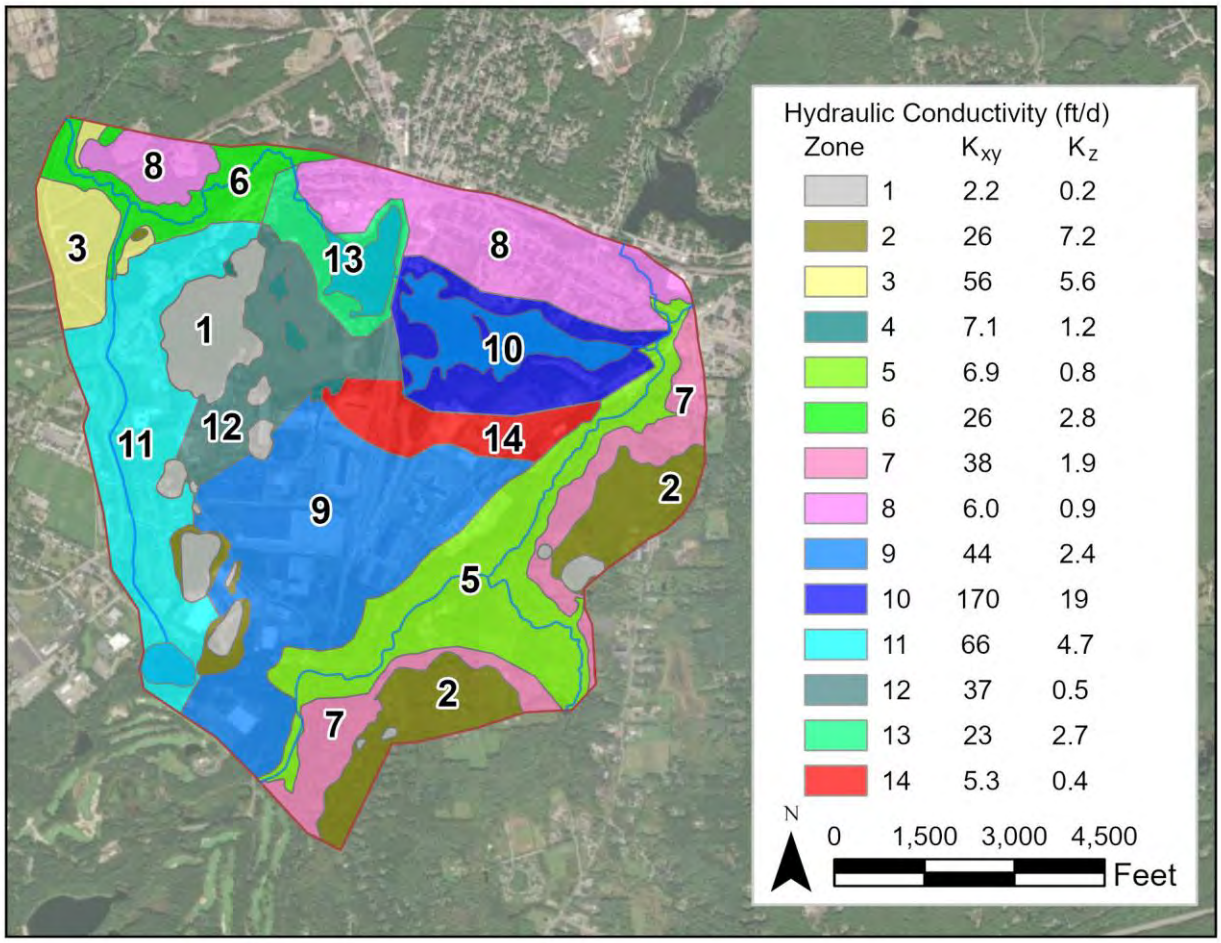



***Figure 5-7: Hydraulic Conductivity Calibrated Values***

***Table 5-3: Recharge and Evapotranspiration Calibrated Values***

| Calibration Parameter | ft/d* | in/yr |
|---|---|---|
| **Recharge** | | |
| Wetland | 0.0055 | 24.1 |
| Open Space | 0.0055 | 24.1 |
| Semi-Open Space | 0.0036 | 15.8 |
| Impervious | 0.0000 | 0.0 |
| Surface Water | 0.0000 | 0.0 |
| **Evapotranspiration** | | |
| Wetland/Open Space/Semi-OpenSpace** | 0.0040 | 17.5 |
| Impervious/Surface Water | 0.0000 | 0.0 |

* MODFLOW requires model inputs to be provided in consistent units. For model setup using English units, the appropriate units for precipitation and recharge are feet per day (ft/d).
** 17.5 in/yr is equivalent to 1.46 in/month, and within the range of values provided by NRCC.

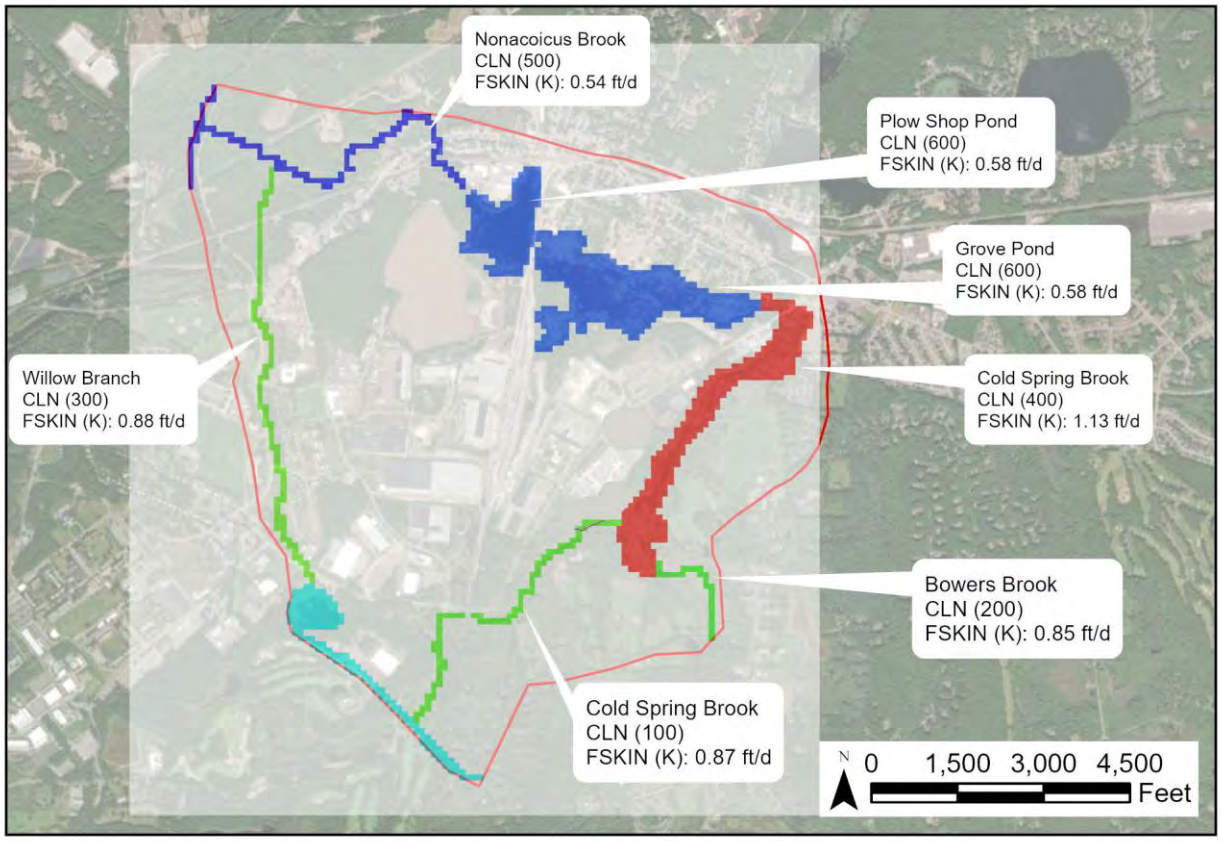



***Figure 5-8: CLN FSKIN Calibrated Values***

### 5.3 Groundwater Flow Model Calibration Performance

The Project Team evaluated the quality of the groundwater flow model calibration both quantitatively and qualitatively. The quantitative evaluation is based on how the modeled groundwater levels compare to the observed water levels at each target well. The qualitative evaluation is based on how well the modeled groundwater table captures important features of the aquifer (e.g., the interaction of Cold Spring Brook and the aquifer).

Figure 5-9 and Figure 5-10 present the calibrated model groundwater table. These figures show the groundwater elevation contours as blue lines. Each calibration target is shown as a colored circle where red dots indicate where the model overpredicts the groundwater elevation and green dots indicate where the model underpredicts the groundwater elevation. The size of the circle is an indication of the magnitude of the difference between modeled and observed.

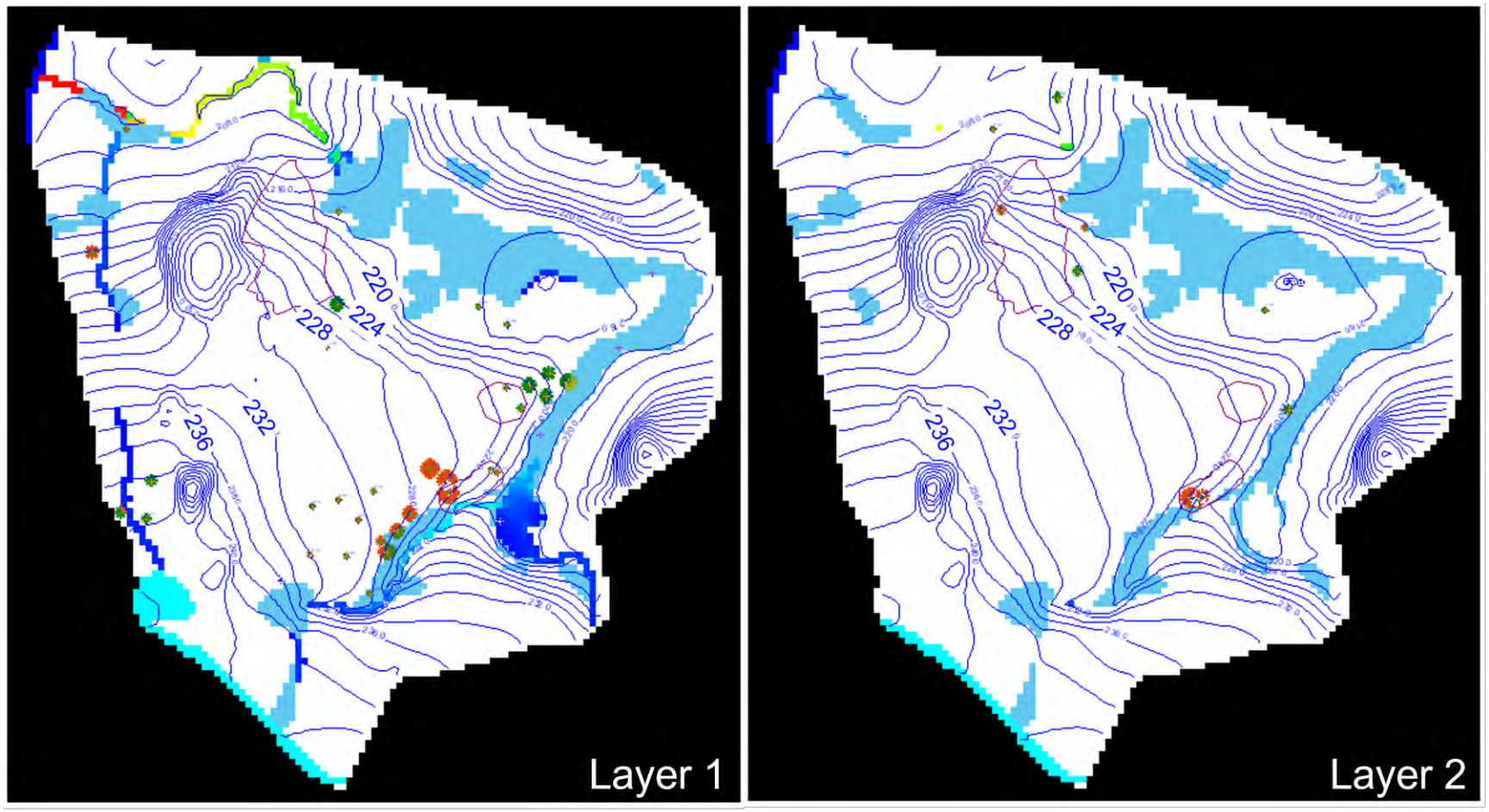



***Figure 5-9: Calibrated Groundwater Flow Model Groundwater Elevation (Layer 1 and Layer 2)***
elevation contours relative to feet NAVD88

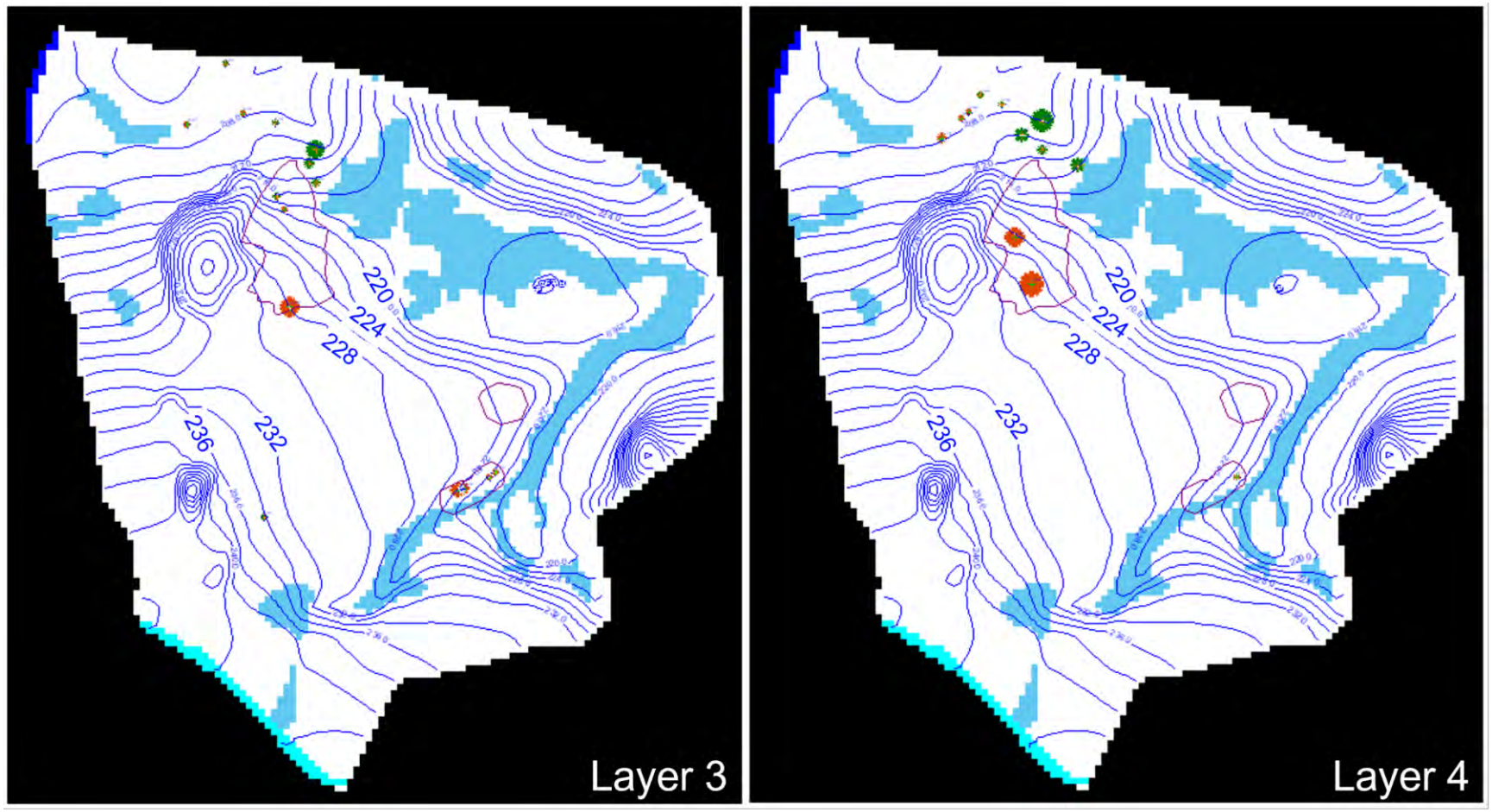



***Figure 5-10: Calibrated Groundwater Flow Model Groundwater Elevation (Layer 3 and Layer 4)***
elevation contours relative to feet NAVD88

### 5.3.1 Quantitative Evaluation of Groundwater Flow Model Calibration

The model results presented in these figures show a good statistical match between modeled and observed groundwater levels. The mean residual (i.e. the average difference between the modeled and observed groundwater levels) is -0.14 ft with a standard deviation of 1.93 ft. The residual sum of squares is 280. The model error relative to the range of observed groundwater levels shows a scaled residual standard deviation of 5.1%, a scaled absolute mean error of 4.1%, and a scaled root mean square error of 5.1%. The Project Team considers a good calibration to be when the scaled metrics are all less than 10%. The calibration shown in Figure 5-9 and Figure 5-10 meets that threshold.

Figure 5-11 plots the target residual values versus the observed groundwater elevation. The plot is also color-coded by model layer. There is no clear trend in residual as a function of observed groundwater elevation, nor is there any clear trend in residual as a function of model layer. Figure 5-12 plots the simulated groundwater elevations (head) versus the observed groundwater elevations (head), the plot is again color-coded by model layer. Figure 5-12 includes a black line representing a one-to-one or perfect correlation between the modeled and observed groundwater levels. The figure includes a linear regression line for the dataset as a red-dashed line. The regression line matches very closely to the one-to-one correlation line with a square of the Pearson Correlation Coefficient ($R^2$) of 0.95. This is further evidence that the calibration of the groundwater flow model is quantitatively good.

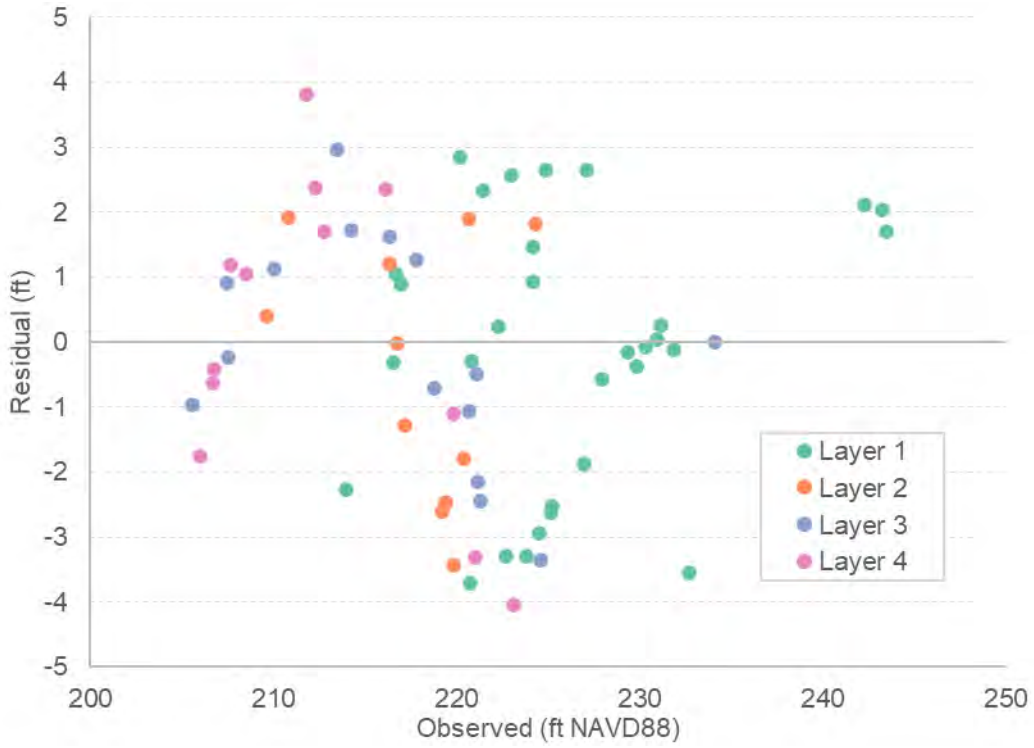



***Figure 5-11: Calibration Residual Values Versus Observed Groundwater Levels***

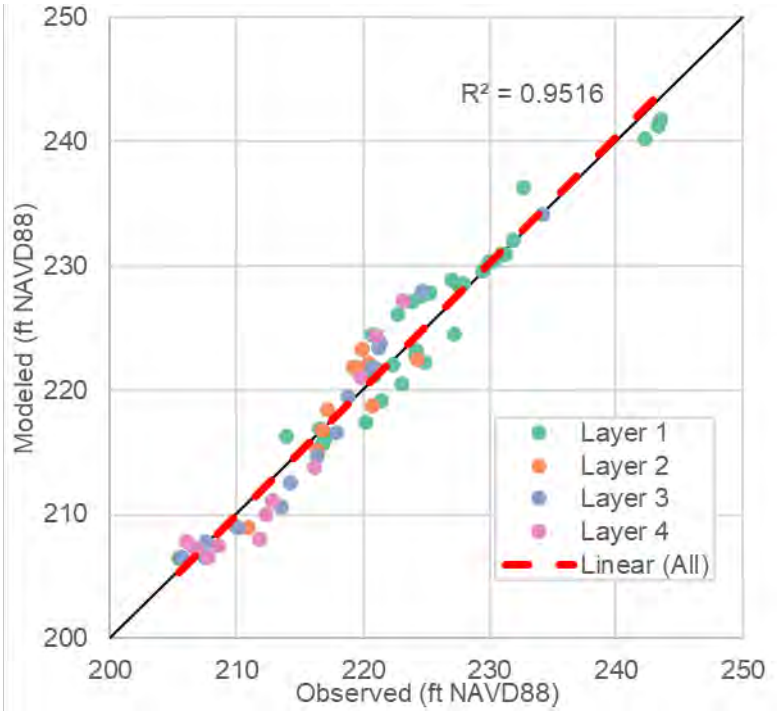



***Figure 5-12: Modeled Groundwater Levels Versus Observed Groundwater Levels***

### 5.3.2 Qualitative Evaluation of Groundwater Flow Model Calibration

In addition to the statistical performance of the model, the Project Team evaluated how well the model captured specific features that are relevant to the goal of evaluating PFAS transport to the Grove Pond wellfield. The Project Team evaluated whether the model appropriately simulated the forced infiltration of water from Grove Pond into the aquifer from pumping and the influence of Cold Spring Brook on the groundwater table. We also compared the model results to the groundwater flow modeling study that is currently being conducted for the entire Fort Devens.

#### 5.3.2.1 Infiltration at Grove Pond

CDM reported that the "…pumping of the Grove Pond wells causes a cone of depression around the wells and induced infiltration from Grove Pond" (CDM, 1993, pg. 4-2). The cone of depression around the wells is evident in Figure 5-9. The Project Team also verified that the net movement of water from Grove Pond is into the aquifer and into the wells. Figure 5-13 shows a screen capture from Vistas indicating the groundwater flux for the CLNs within the model. Positive values indicate flux into the aquifer and negative values indicate flux out of the aquifer. Groundwater flux in Grove Pond is positive and higher in the vicinity of the well locations, confirming that the infiltration of pond water is present in the model.

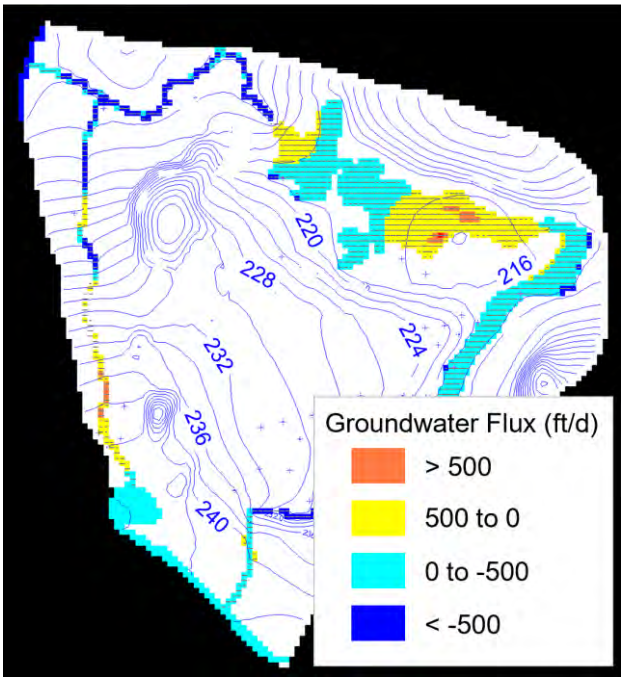



***Figure 5-13: Groundwater Head and Water Flux in Model CLNs***

#### 5.3.2.2 Cold Spring Brook

Both AOC 74 and AOC 57 are close to Cold Spring Brook, and the PFAS plumes from AOC 57 are migrating towards Cold Spring Brook. KGS (2020) delineated groundwater contours that show groundwater flow converges towards Cold Spring Brook indicating that the brook is fed by the aquifer. As a part of the qualitative evaluation of model performance, the Project Team confirmed that the same behavior is captured in the model. Figure 5-14 shows the groundwater elevation contours near Cold Spring Brook for both the model (upper) and the observed (lower). The modeled and observed conditions show good agreement based on visual inspection.

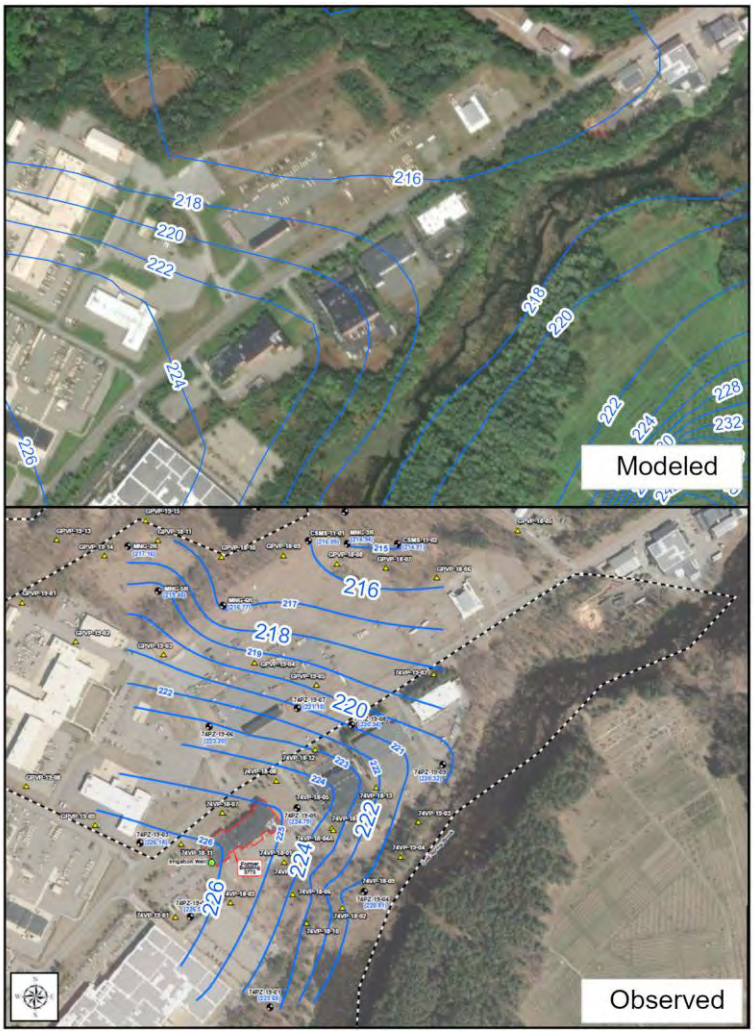



***Figure 5-14: Cold Spring Brook Groundwater Surface Contour Comparison***

#### 5.3.2.3 Comparison to Former Fort Devens Regional Groundwater Flow Model

As a part of the site wide investigation of PFAS at Fort Devens, the USACE commissioned the development of a regional groundwater model of Fort Devens. S.S. Papadopulos & Associates, Inc. (Papadopulos) completed the report entitled "Regional Groundwater Flow Model of the Former Fort Devens, Massachusetts" (Papadopulos, 2022) in November of 2022. The USACE provided a copy of the report to the Project Team in February of 2024. The scope of the modeling effort includes all of Fort Devens. The model has a much larger domain than the groundwater flow model focused on the Grove Pond wellfield. Papadopulos used the same modeling software (MODFLOW-USG) for many of the same reasons that the Project Team sites (e.g., incorporation of CLNs).

The Project Team used the Papadopulos report as another touchstone for qualitative assessment of our groundwater flow model's performance. Figure 5-15 shows an excerpt from Papadopulos (2022, Figure D.3). The figure shows groundwater contours from the regional model. The contours are at 10-ft intervals and do not have sufficient resolution to indicate the influence of the Grove Pond wellfield, but the contours do show the influence of Cold Spring Brook as a sink (i.e., withdrawing water from the aquifer) and the presence of groundwater mounding at the bedrock outcrops to the west of Grove Pond.

The two models cannot be compared in greater detail, but after reviewing Papadopulos (2022), the Project Team concluded that the results that are shown in that report support the conclusion that our groundwater flow model is well calibrated to groundwater levels and appropriately simulating groundwater flow within the model domain.

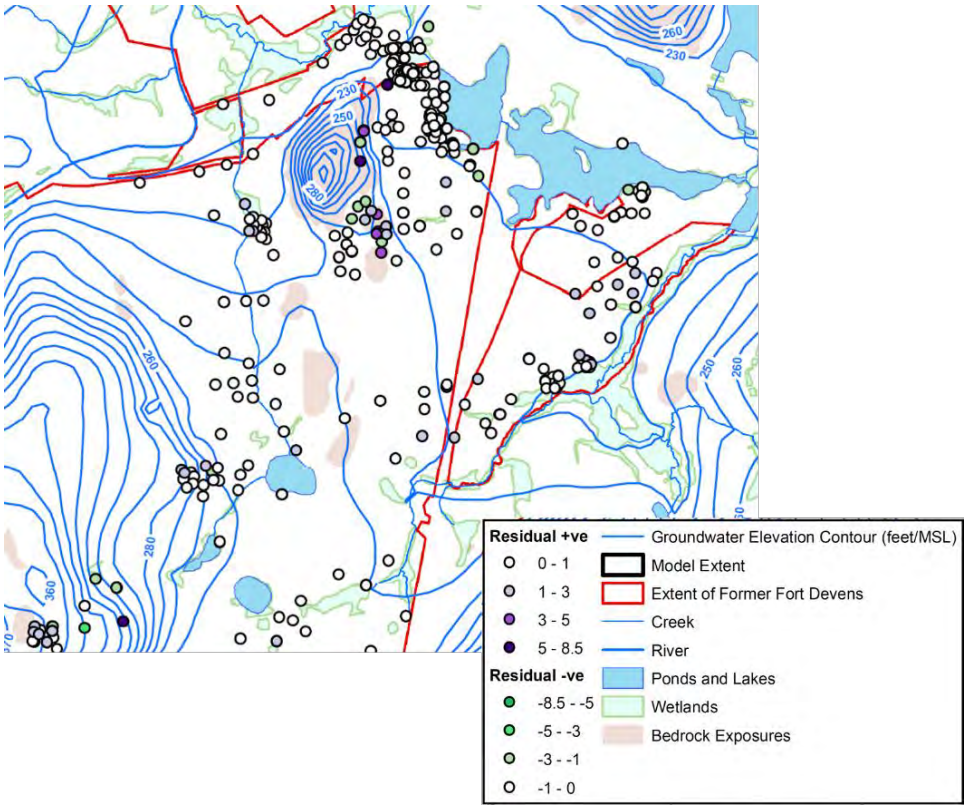



***Figure 5-15: Regional Groundwater Flow Model Results (Papadopulos, 2022)***

## 5.4 Summary of Groundwater Flow Modeling

The Project Team developed a steady-state groundwater flow model of the aquifer that feeds the Grove Pond wellfield. We calibrated the model to more than 70 groundwater elevation measurements, and we evaluated its performance both quantitatively and qualitatively. Based on that evaluation, the Project Team concluded that the model is appropriate for evaluating groundwater flow and transport of PFAS to the Grove Pond wellfield.

# 6.0 GROUNDWATER TRANSPORT MODELING

The steady-state groundwater flow model serves as the foundation for evaluating the transport of PFAS. To simulate transport, the Project Team made two changes to the groundwater flow model. We converted the model to transient by adding a dynamic boundary condition (i.e., Grove Pond wellfield pumping), and we added source terms for each of the PFAS compounds evaluated in the modeling.

## 6.1 Model Setup

### 6.1.1 Transient Boundary Conditions

The transient version of the model has 55 stress periods where each stress period represents a portion of the years 1960 through 2022. Section 5.1.3 and Section 5.1.4 discuss the boundary conditions, recharge, and evapotranspiration in the groundwater flow model. Each of these can be dynamic in the transient version of the model, but there is insufficient information to characterize these boundary conditions over the necessary time period. They were kept static in the transient model and as such represent long-term average conditions.

The rate and location of pumping at the Grove Pond wellfield is the most critical boundary condition for evaluating the migration of PFAS from source locations to the wells. The transient version of the model incorporates annual pumping rates at each Grove Pond well consistent with town records and records collected from the Massachusetts DEP. The town records do not provide individual well pumping rates. For the period from 1960 through 1985, the total pumping is divided equally between GP-01 and GP-02. Figure 6-1 presents the annual pumping rate at each well. Given the proximity of these two wells, this is an acceptable approximation.

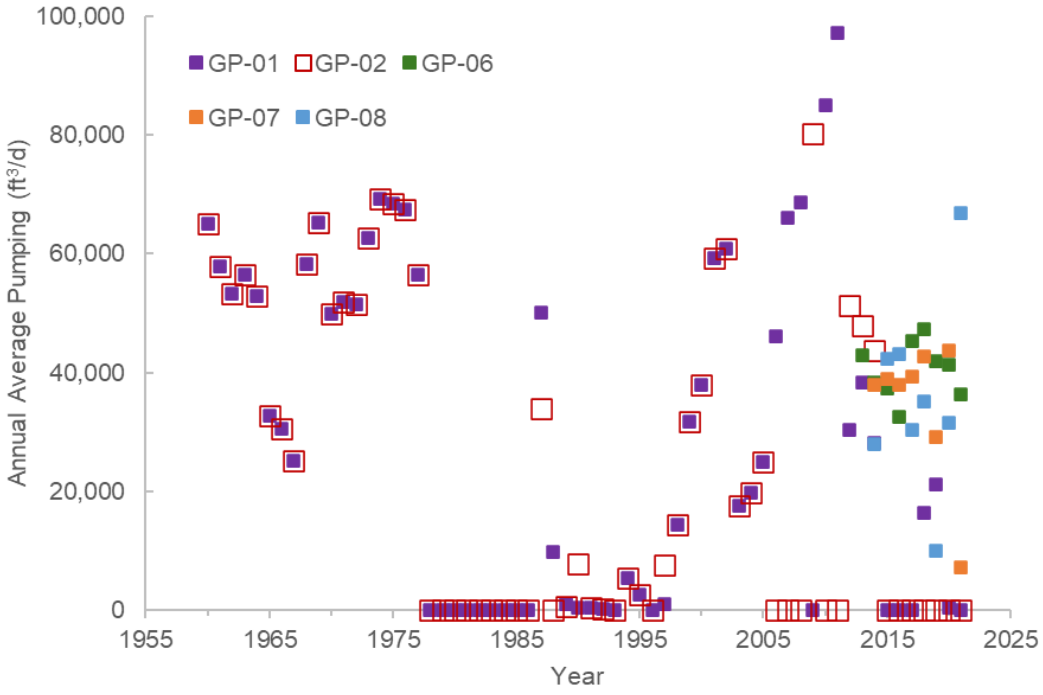



***Figure 6-1: Transient Model Pumping Rates for Grove Pond Wells***

### 6.1.2 Transport Boundary Conditions

The CSM includes three PFAS sources contributing PFAS to the Grove Pond wellfield. These sources are the MAARNG, AOC 74, and AOC 57. There is very limited information about the history of each source, but very good information about the dimensions of the PFAS plumes from each source as of the winter 2019-2020. The Project Team evaluated multiple options to incorporate PFAS sources into the model. We ultimately concluded that the most defensible approach was to include each source as a constant source beginning at the estimated time of initial release. We also identified the need to split the MAARNG into two distinct sources (i.e., MAARNG South (S) and MAARNG North (N)) based on groundwater sample results (see Section 4.2). Figure 6-2 shows the location of each source on the model grid.

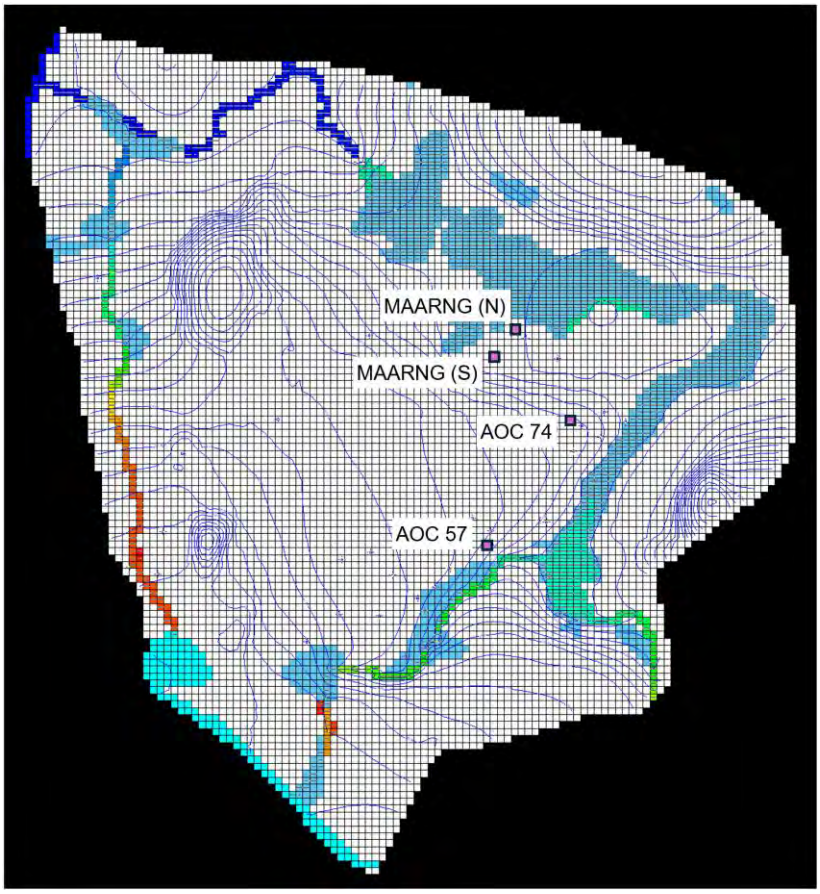



***Figure 6-2: Transport Model PFAS Source Terms***

The MAARNG sources are activated in the model beginning in the year 1960. AOC 57 is activated in the model in 1977, and AOC 74 is activated in the model in 1996. The Project Team used these years based on our best understanding of the site history related to PFAS releases at the site. The source concentrations were determined as a part of the confidence-building process.

Given that PFNA concentrations at the Grove Pond wellfield are consistently measured as non-detect and that there is no evidence of PFNA plume approaching the wellfield from any of the sources, the Project Team did not construct a transport model for PFNA.

## 6.2 Transport Model Confidence Building

The Project Team calibrated the groundwater flow model to observed groundwater elevations through both a quantitative assessment of model performance (i.e., comparison of modeled groundwater elevations to observed groundwater elevations) and a qualitative process (i.e., visual inspection and consistency with the CSM). The quantitative assessment provides the ability to calculate error statistics and, if desired, a quantitative assessment of the uncertainty associated with the groundwater flow model performance.

Unfortunately, the type of quantitative analysis completed for the groundwater flow model is not available for the groundwater transport model. There are fewer available data and limited or no information on past events and practices. In the place of quantitative analysis, we assessed the groundwater transport model through qualitative assessment and a process of confidence building as advanced by Hassan (2004).

The goal of this study is to estimate the PFAS concentrations in the Grove Pond wells from the year 2000 through the year 2022 before groundwater sampling for PFAS commenced. In principle, it makes sense to conduct a quantitative assessment of the transport model to determine the uncertainty associated with the transport model results. In practice, a quantitative assessment of transport model performance is not possible because the uncertainty associated with critical model inputs is unquantifiable. While there is clear evidence of PFAS releases to groundwater at the MAARNG, at AOC 57, and at AOC 74 from the SIRI dataset, there is very limited historical information about how the PFAS came to be in the groundwater. The Project Team identified six areas where the associated uncertainty of model inputs/assumptions is not quantifiable.

- Definitive information is not available about the time frame, frequency, or quantity of PFAS releases at AOC 74.
- There is no definitive information about the types of PFAS released at AOC 57.
- There is no information about whether PFAS was released at the MAARNG as a part of fire-fighting activities or from a related source (e.g., the material stored at the location of the fire).
- Only limited information is available to determine which Grove Pond wells were being pumped and with what intensity from the years 1960 through 1985.
- The historical usage of the Fort Devens wellfield is unknown.
- The specific transport mechanism that caused elevated concentrations at the MAARNG N is unknown.

The Project Team used a different approach to assessing the transport model performance. We describe this approach as confidence building, and it represents a qualitative assessment of model performance that does not misrepresent the accuracy of the model results.

Hassan (2004) describes confidence building as a “long-term, iterative process.” He states that confidence building “…cannot ensure acceptable prediction or quality of the model…” but that confidence building “…provides evidence that the model is valid for making decisions.” Hassan focuses on the application of groundwater models to remediation strategies and decision-making. The Project Team believes that the rationale and perspective that he describes is relevant to this study.

The Project Team engaged in an iterative process of adjusting the model inputs of source strength and retardation factors to ensure that the transport model provides an acceptable match between the model results and the observed PFAS plumes. We then evaluated those model results relative to the CSM transport mechanisms. After an evaluation of the consistency between model results and the CSM, we

returned to the transport model inputs of source strength and retardation factors to refine the transport model and improve the consistency with the CSM. We used this process to develop multiple lines of evidence demonstrating that the model results and the CSM are consistent and represent the best achievable estimate of PFAS concentrations at the Grove Pond wellfield given available information.

### 6.2.1 Transport Model Source Concentrations

Figure 6-1 shows the source concentrations used to produce the final model results. These concentrations are consistent with the observed concentrations from the SIRI dataset, but the values were adjusted as part of the confidence-building approach to improve the match between the observed PFAS contours and the modeled PFAS contours.

***Table 6-1: Transport Model PFAS Source Strength Concentrations***

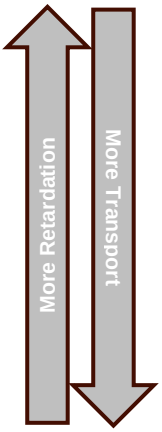
| | PFAS Concentrations (ng/L) | | | | |
|---|---|---|---|---|---|
| Model Layer | PFOS | PFOA | PFHpA | PFHxS | PFHxA |
| **MAARNG North** | | | | | |
| 1 | 300 | 200 | 500 | 50 | 100 |
| 2 | 500 | 100 | 300 | 200 | 500 |
| 3 | 900 | 100 | 0 | 100 | 100 |
| 4 | 400 | 100 | 100 | 100 | 0 |
| **MAARNG South** | | | | | |
| 1 | 0 | 0 | 0 | 0 | 0 |
| 2 | 50 | 200 | 400 | 0 | 200 |
| 3 | 0 | 0 | 0 | 0 | 0 |
| 4 | 0 | 0 | 0 | 0 | 0 |
| **AOC 74** | | | | | |
| 1 | 0 | 200 | 100 | 0 | 100 |
| 2 | 600 | 1,600 | 800 | 0 | 1,400 |
| 3 | 0 | 2,300 | 1,400 | 0 | 2,000 |
| 4 | 0 | 0 | 0 | 0 | 600 |
| **AOC 57** | | | | | |
| 1 | 1,100 | 1,800 | 1,600 | 1,100 | 1,300 |
| 2 | 1,100 | 3,900 | 800 | 4,100 | 1,500 |
| 3 | 0 | 100 | 100 | 0 | 100 |
| 4 | 0 | 0 | 0 | 0 | 0 |

### 6.2.2 Transport Model Retardation Factors

The CSM includes the assumption that PFAS transport will be heavily retarded by the partitioning of PFAS to soils (i.e., solid materials). For conventional pollutants, the degree of retardation is well understood with

laboratory testing in agreement with field observation. PFAS partitioning coefficients are PFAS compound-specific, and there is no consensus on the relationship between retardation and laboratory-derived organic carbon partitioning coefficients ($K_{OC}$) (ITRC, 2024a). ITRC (2024b) provides a table of reported log($K_{OC}$) values for various PFAS. The Project Team recognizes that there is no consensus on "correct" values for PFAS but sees the ITRC data table as a summary of the best available information. We converted the low and high log($K_{OC}$) values from the ITRC data table into retardation factors ($K_d$) values using a fraction organic carbon[1] ($f_{OC}$) value of 0.001 to establish a basis for the retardation factor in the transport model. Table 6-2 provides the log($K_{OC}$) values from ITRC, the calculated retardation factor range, and the final retardation factor used in the transport model. We used the retardation factor range as a starting point but did not considered it to be fixed given the state of research and knowledge with respect to PFAS transport in the environment. Higher retardation leads to less transport (see arrows to left of Table 6-2). The PFAS are organized in the table from most retarded to least retarded.

***Table 6-2: Transport Model Retardation Factors***




| PFAS | Low log($K_{OC}$) | High log($K_{OC}$) | Low $K_d$ | High $K_d$ | Model $K_d$ |
|---|---|---|---|---|---|
| PFOS | 2.27 | 5.6 | 0.02 | 52 | 0.0242 |
| PFOA | 1.9 | 5.0 | 0.01 | 13 | 0.0103 |
| PFHpA | 1.36 | 4.5 | 0.003 | 4.1 | 0.003 |
| PFHxS | 1.15 | 4.5 | 0.002 | 4.0 | 0.0018 |
| PFHxA | 0.9 | 4.2 | 0.001 | 2.1 | 0.001 |

### 6.2.3 Transport Model Dispersivity

Dispersivity is a model parameter that accounts for the chemical process of diffusion and the physical process of dispersion. These two processes result in the spreading of a plume both longitudinally and laterally as a plume migrates through the aquifer. The Project Team used work by Gelhar et al. (1992) as a guide for determining a reasonable range for longitudinal dispersivity. The US EPA has developed an online tool for calculating an approximate lower and upper limit for dispersivity (US EPA, 2024b) based on Gelhar et al. (1992). The Project Team used a plume length of 700 ft to establish a dispersivity range from 1.3 ft to 3,800 ft. Preliminary testing led us to select the dispersivity value of 30 ft for use in the transport model.

[1] The Project Team did not find any measurements of $f_{oc}$ in the available datasets. In the absence of site-specific measurements, the Project Team relied on available literature to determine an appropriate range. CDM (1993) characterized the aquifer geology as glacial terrace deposits composed of sand, pebbles, and gravel. Wiedemer (1999, pg. 147) provides an $f_{oc}$ range of 0.00029 to 0.073 for glacial fine to coarse sand and a value of 0.00125 for glacial medium sand to gravel. US EPA (2000) notes that a value of 0.001 is often used when the actual value is unknown. An $f_{oc}$ value equal to 0.001 aligns well with literature values for similar geology and with an EPA recommendation.

### 6.3 Transport Model Results

During the confidence-building process we adjusted source concentrations, retardation factors, and dispersivity. This yielded a set of model results that compare well to the observed PFAS plumes in the vicinity of the Grove Pond wellfield. Figure 6-3 through Figure 6-7 compare the PFAS iso-concentration contours generated from the SIRI dataset with the modeled PFAS contours from the transport model. The figures show the model results from layer 2 of the model. This layer generally corresponds to the upper portion of the aquifer and the groundwater table. Attachment 4 shows the same presentation for all layers of the model.

The model results approximately match the observed PFAS concentrations in groundwater for the winter 2019-2020. These results are a snapshot of the PFAS plumes and their migration towards the Grove Pond wellfield. The snapshot provides compelling evidence that the CSM is sound. The following lines of evidence suggest that the model results sufficiently represent current conditions, and that the groundwater model is an appropriate tool for estimating past PFAS concentrations at the PWS wells despite large uncertainties in the source terms.

1. Each PFAS source shows the highest groundwater concentrations in the immediate vicinity of the release of PFAS. The center of mass of each PFAS plume is very close to the release location. This suggests that the PFAS are substantially retarded. It also supports the modeling decision to set each source as a constant source within the transport model.

2. The final retardation factors used in the model are on the very low end of the range of retardation suggested by the ITRC summary dataset (ITRC, 2024b). The leading edge of the PFAS plumes align well with the observed contours. More retardation would either result in a poor match between modeled and observed iso-concentration contours or require an even earlier release of PFAS. The age of the primary source (i.e., 1960 release in the MAARNG) relative to the earliest extensive use of PFAS (i.e., 1950s (ITRC, 2024c)) suggest an earlier release is not likely and potentially not possible. This is particularly true for PFOS.

3. The predicted concentrations at the Grove Pond wells are the correct order of magnitude for each PFAS compound at each well. This supports the combination of source strength and retardation factors used in the transport model.

4. The plumes from the MAARNG and from AOC 74 have merged for both PFHpA and PFHxA. That behavior is captured in the model results. This supports both the CSM timeline of releases and the selection of retardation factors.

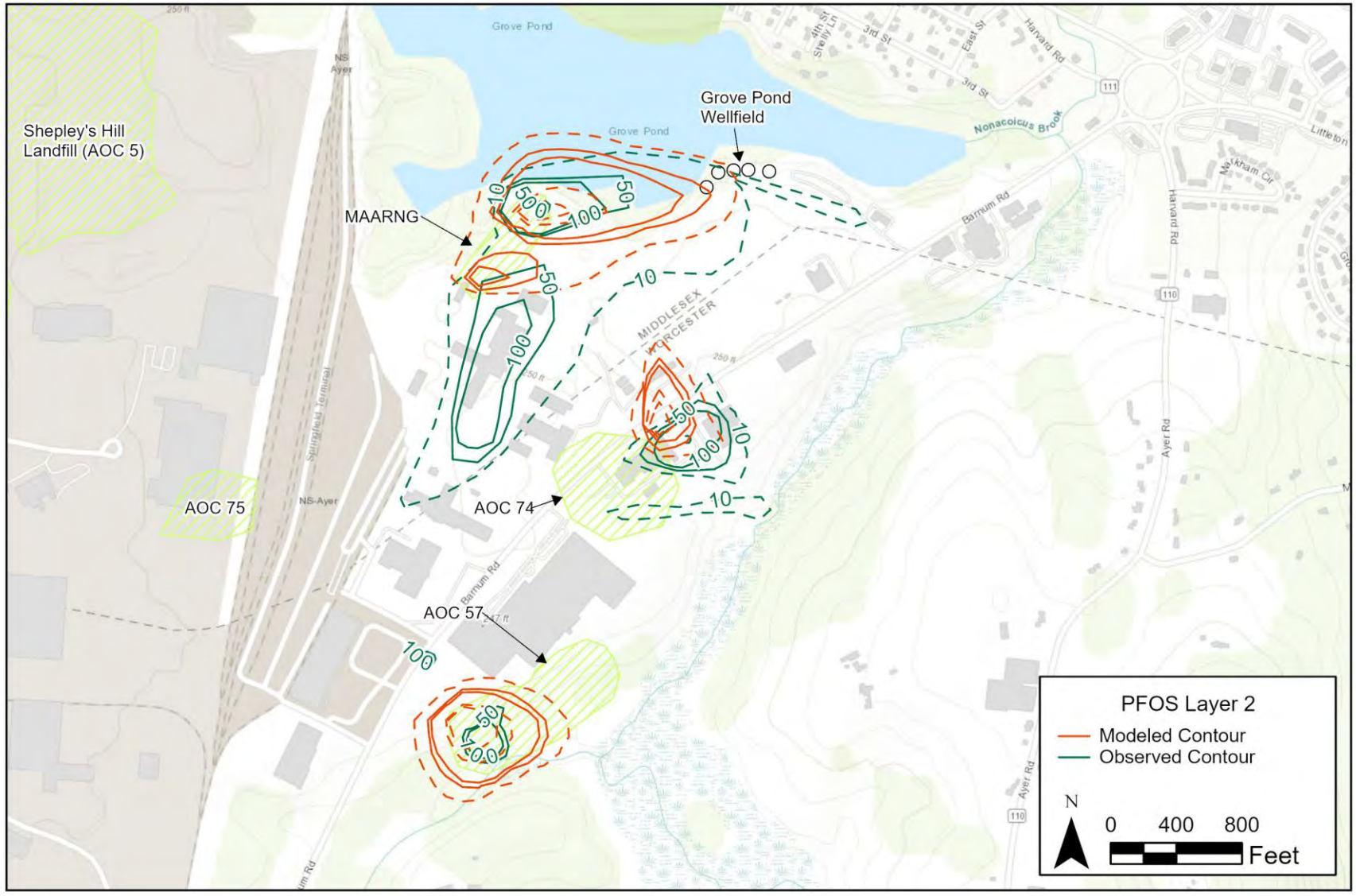



***Figure 6-3: Modeled and Observed Iso-Concentration Contours of PFOS in Groundwater***

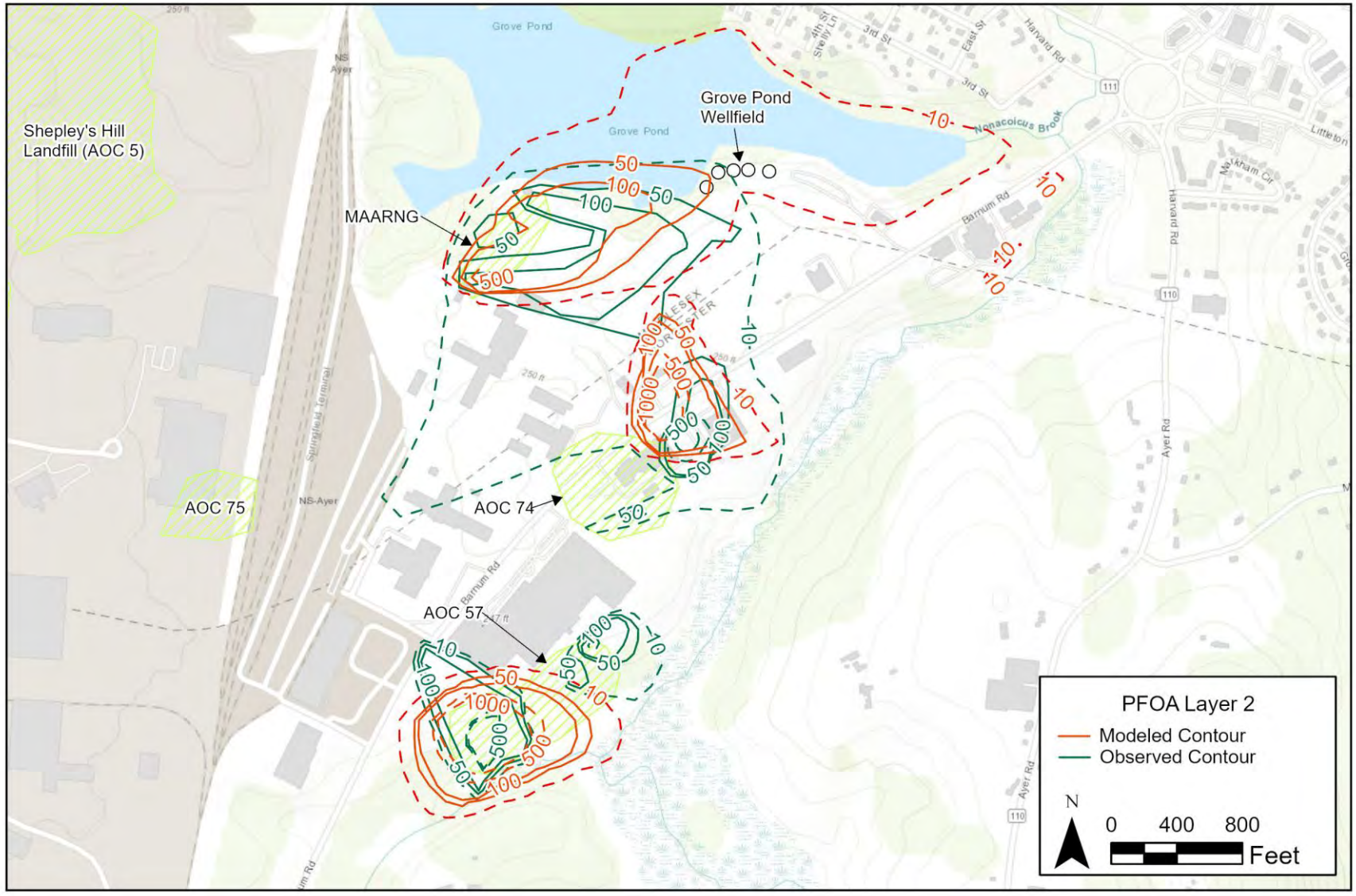



***Figure 6-4: Modeled and Observed Iso-Concentration Contours of PFOA in Groundwater***

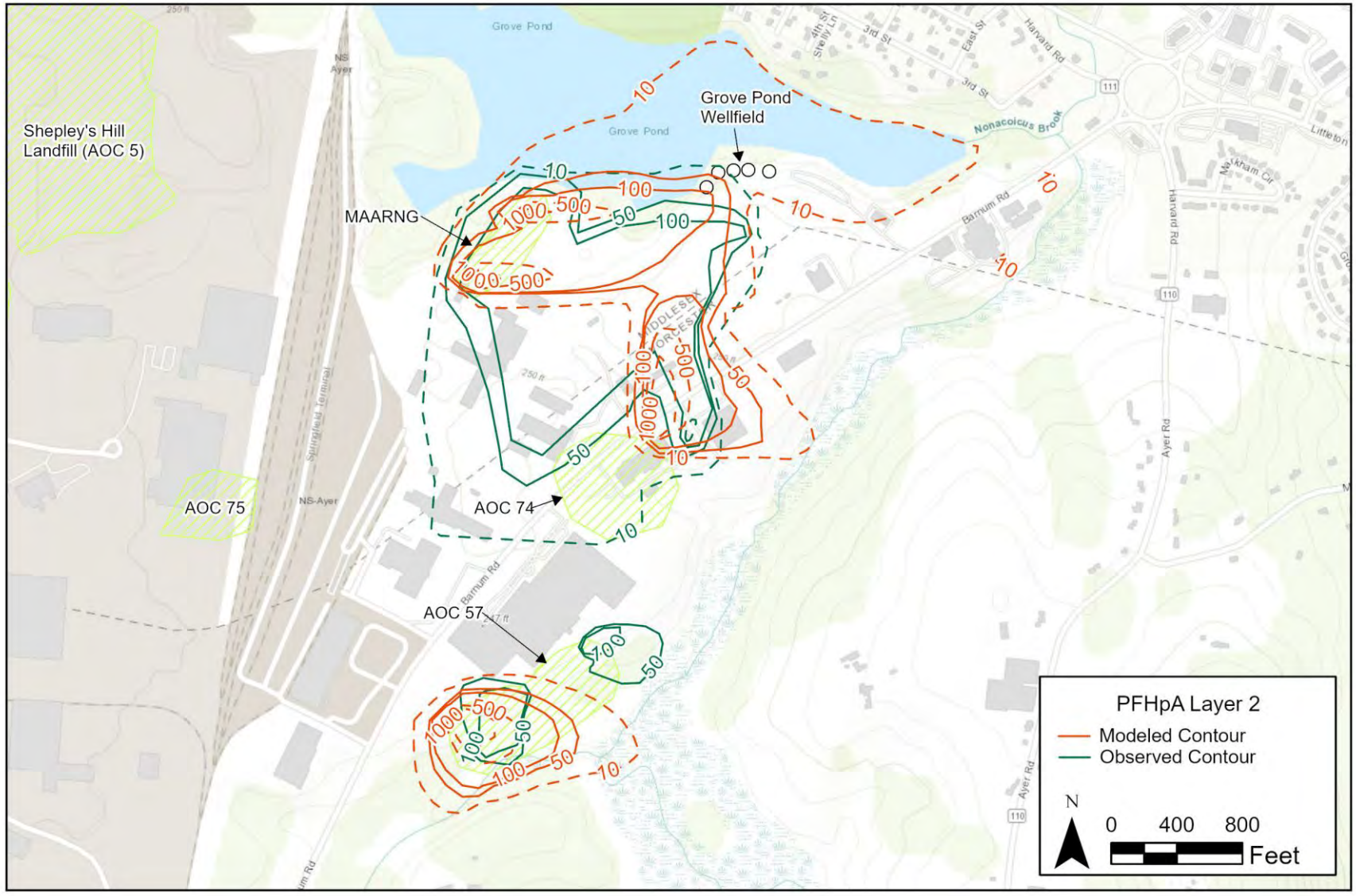



***Figure 6-5: Modeled and Observed Iso-Concentration Contours of PFHpA in Groundwater***

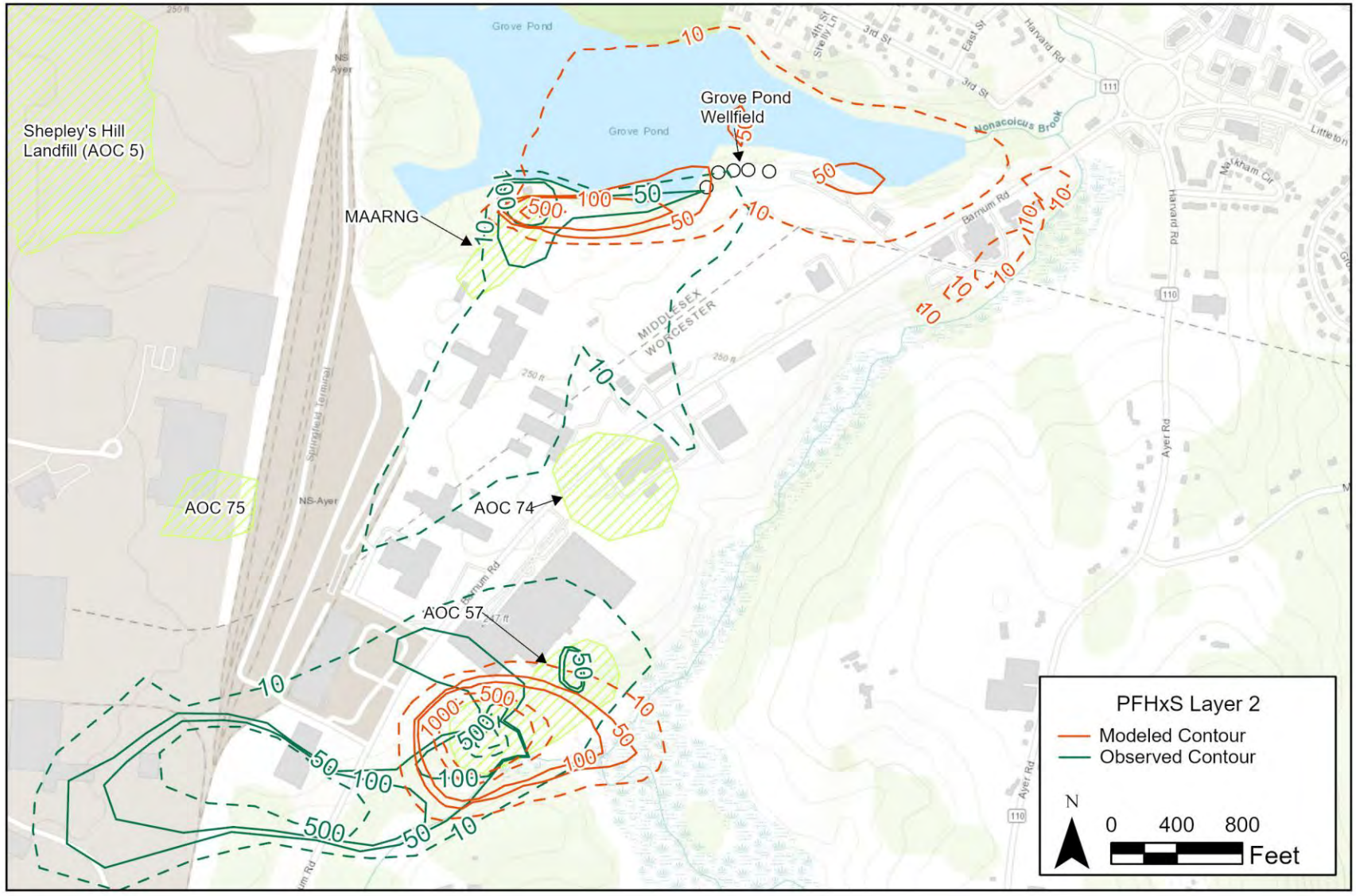



***Figure 6-6: Modeled and Observed Iso-Concentration Contours of PFHxS in Groundwater***

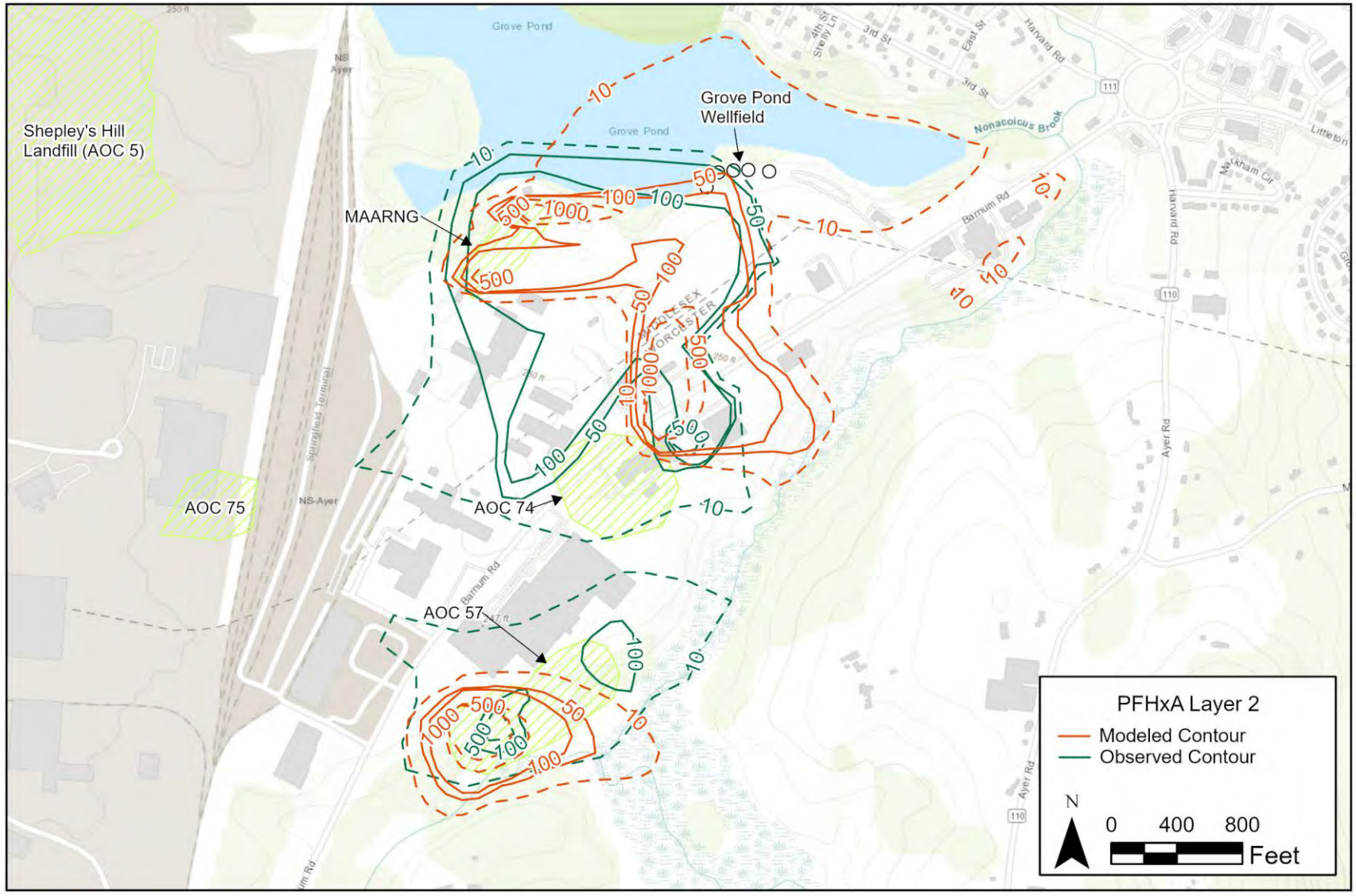



***Figure 6-7: Modeled and Observed Iso-Concentration Contours of PFHxA in Groundwater***

## 6.4 Sensitivity Analysis

The Project Team evaluated the sensitivity of PFAS concentrations at the wells to the PFAS source concentrations. The final model configuration resulted in PFAS concentrations that are at the lower end of observed concentrations at the wells. In lieu of presenting modeling results for a specified change in source concentrations, we conducted additional modeling to determine what scaling factor would be necessary for the model results to represent the upper end of observed concentrations at the wells. The result of that investigation is that by scaling the source terms in the transport model by a factor of four (a.k.a., 4x), the model estimates well concentrations that are approximately equivalent to the upper bound of the observed concentrations at the Grove Pond wells. Figure 6-8 through Figure 6-12 present the model results from the final modeling results and the scaled source model results at GP-08. The same graph for all wells is included with this report as Attachment 4.

Figure 6-8 through Figure 6-12 also show a “recommended” time series that is discussed in Section 7.0 of this report.

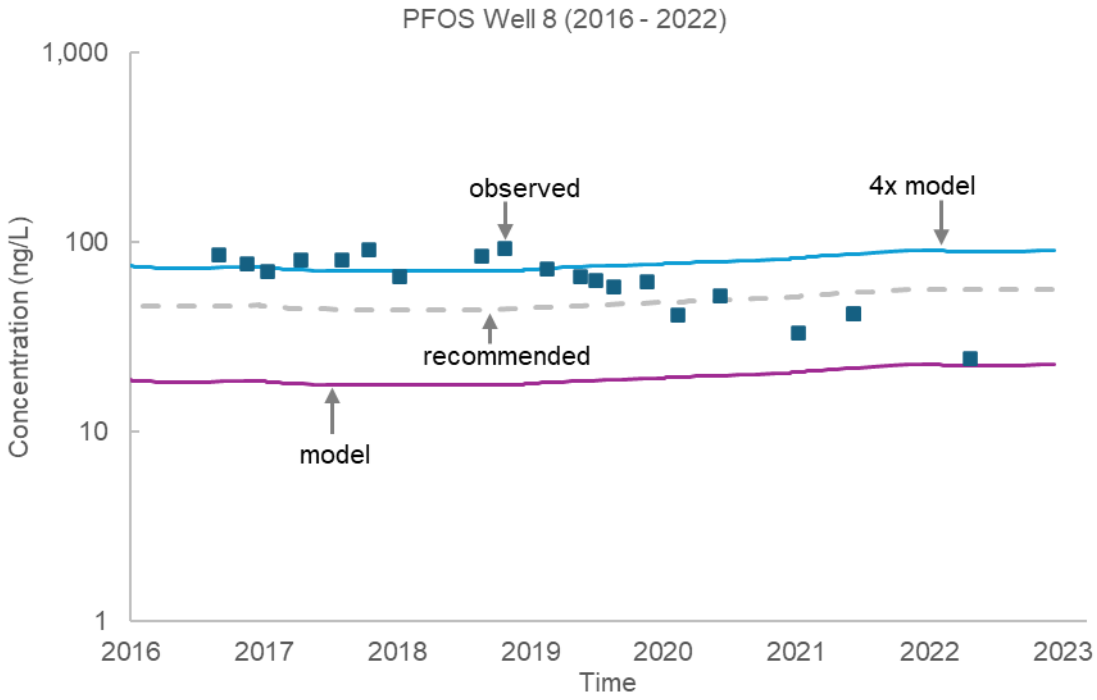



***Figure 6-8: Modeled and Observed PFOS Concentrations at GP-08 (2016-2022)***

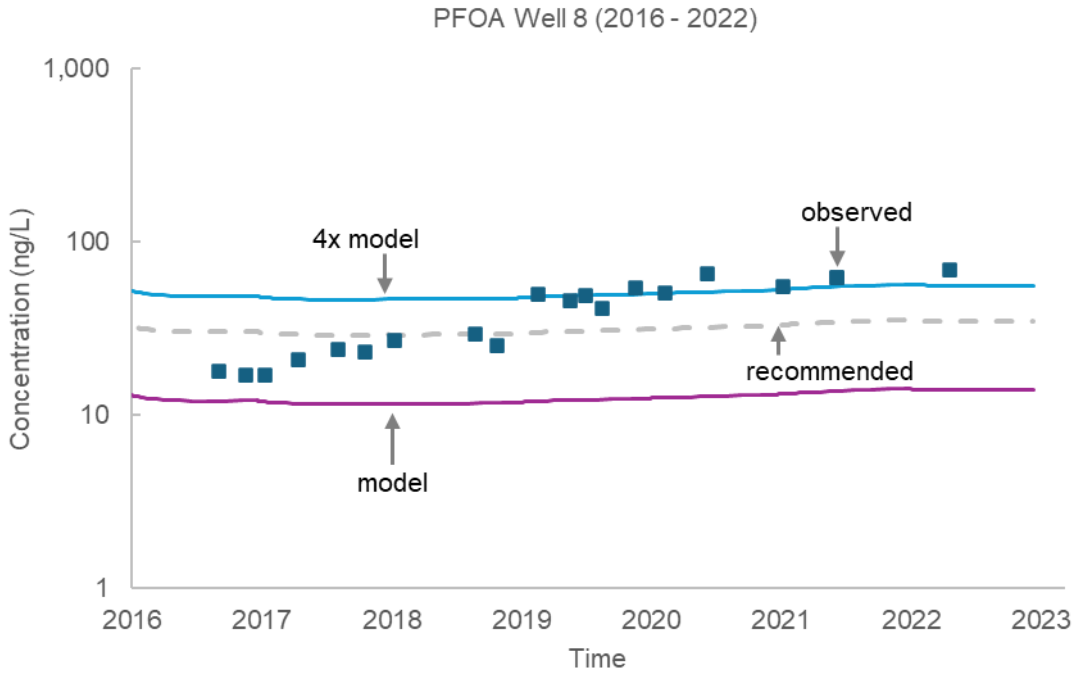



***Figure 6-9: Modeled and Observed PFOA Concentrations at GP-08 (2016-2022)***

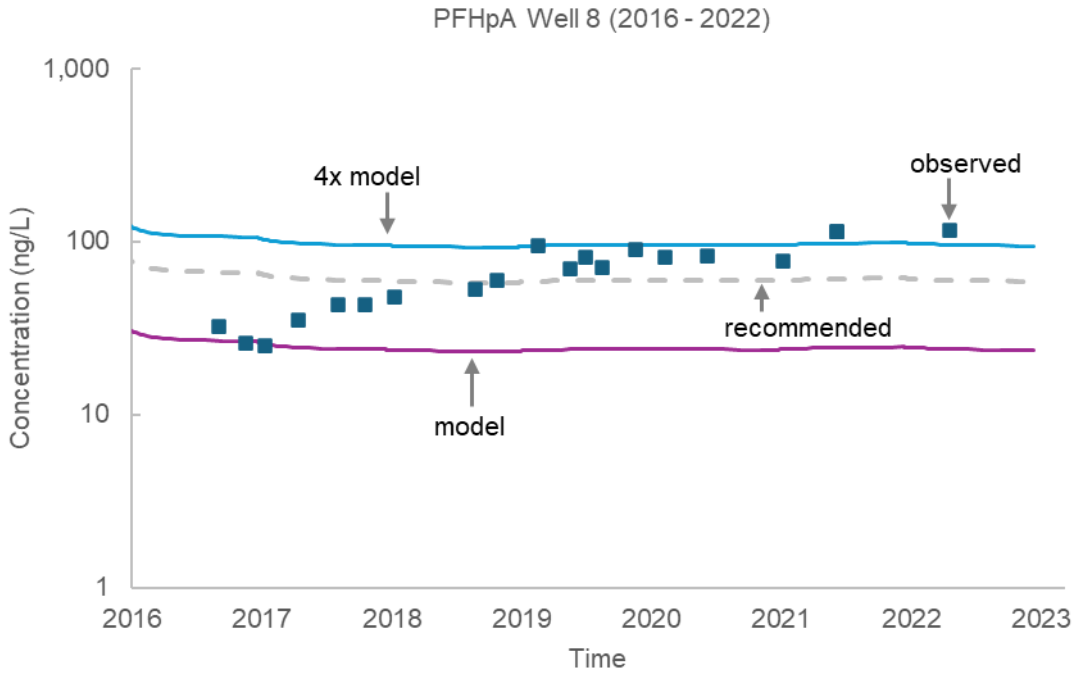



***Figure 6-10: Modeled and Observed PFHpA Concentrations at GP-08 (2016-2022)***

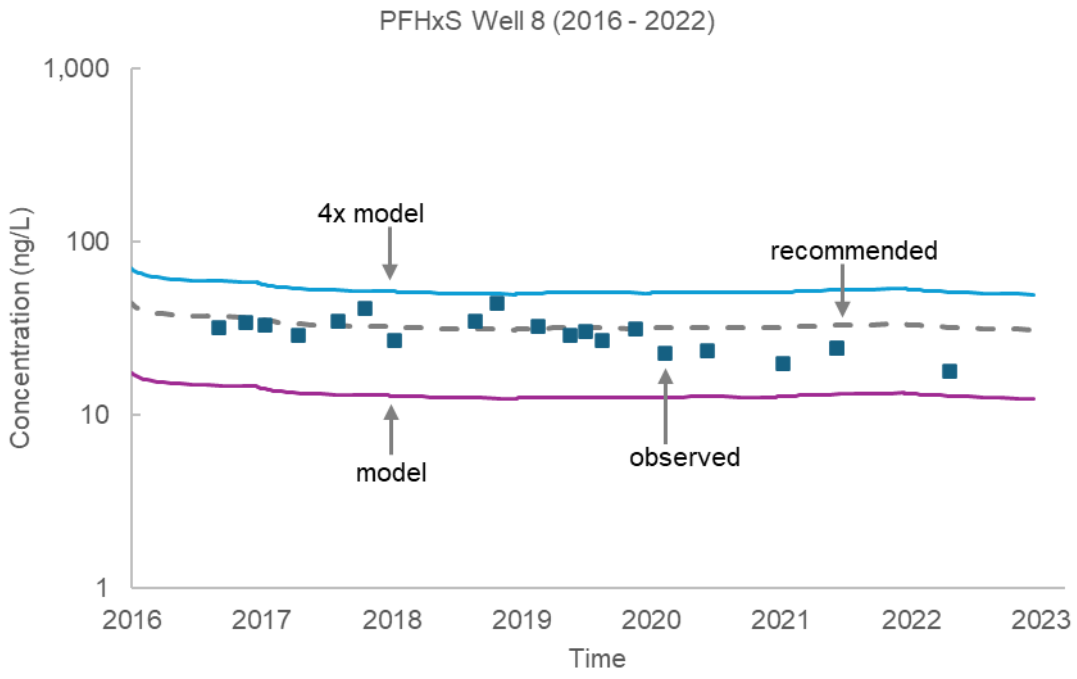



***Figure 6-11: Modeled and Observed PFHxS Concentrations at GP-08 (2016-2022)***

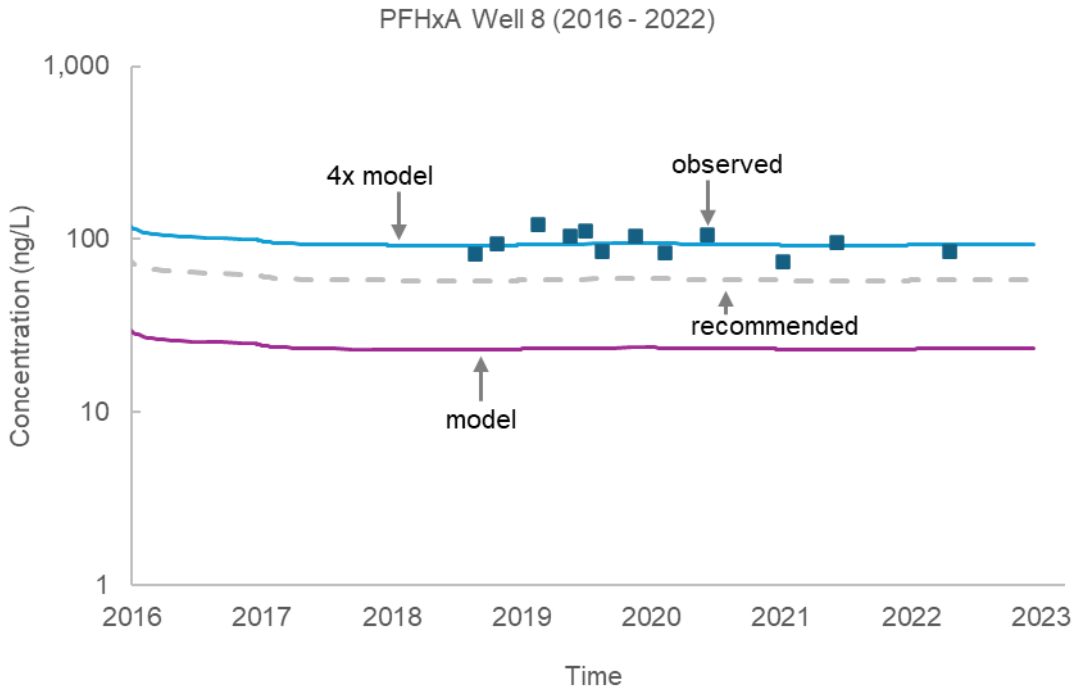



***Figure 6-12: Modeled and Observed PFHxA Concentrations at GP-08 (2016-2022)***

## 7.0 ESTIMATE OF PFAS CONCENTRATIONS AT GROVE POND WELLS

Implementation of the CSM through the transport model provides a set of time series estimates of PFAS concentrations at each well in the Grove Pond wellfield. The Project Team has used the transport model to make two sets of estimates that capture both the lower bound and upper bound of observed concentrations at the Grove Pond wellfield. These estimates are based on and consistent with the CSM for the site. The Project Team took steps to build confidence in the estimates and believes that they are an appropriate application of the available information to estimate PFAS concentrations at the Grove Pond wellfield in the years 2000 through 2022.

These bounding estimates represent appropriate upper and lower limits of PFAS at the Grove Pond wellfield, and the Project Team believes that these limits should be carried forward in the additional analysis that is part of ATSDR PFAS MSS. There is no "correct" estimate within the upper and lower limits, but the Project Team understands the need for a single time series of PFAS at the wells. We recommend that the average of the upper and lower limits be used as that single time series.

Figure 7-1 shows the bounding estimates and the recommended estimate (i.e., average) of PFAS concentration for PFOS, PFOA, PFHpA, PFHxS, and PFHxA at GP-08. GP-08 is the well that is closest to the primary source of PFAS and has the highest concentrations of each PFAS. In considering the estimates shown in Figure 7-1, it is important to remember that GP-08 did not start pumping until approximately 2014. That fact is highlighted in the figure by the dashed lines used until that year. Prior to 2014, pumping at GP-01 and GP-02 are estimated to have had lower PFAS concentrations given that they are farther away from the primary source of PFAS. Figure 7-2 shows the bounding estimates and recommended estimate of PFAS concentrations at GP-01. Wells GP-02, GP-06, and GP-07 have estimated concentrations that are between GP-08 and GP-01. Attachment 6 of this report includes a data table that provides upper, lower, and recommended estimated concentrations for all five wells and all five PFAS. Additional insights with respect to an individual well/PFAS can be drawn from that set of tables.

The estimated PFAS concentrations at the Grove Pond wellfield are an estimate of the PFAS concentrations entering the Ayer drinking water supply system. The transport modeling indicates that the PFAS plumes were migrating towards the wells throughout 2000-2022. PFAS concentrations at the Grove Pond wellfield were slowly and steadily increasing until 2013 when wells GP-06, GP-07, and GP-08 were developed. Each of those wells are located west of GP-01 and GP-02, closer to the primary PFAS source, and at locations with elevated PFAS concentrations relative to wells GP-01 and GP-02. Prior to 2013 estimated PFAS concentrations from the Grove Pond wellfield range from approximately 1 to 40 ng/L depending on the specific PFAS compound. After 2013, estimated PFAS concentrations at the Grove Pond wellfield range from 4 to 125 ng/L depending on the specific PFAS compound.

The Project Team did not develop a transport model for PFNA because there is no evidence of a groundwater plume migrating toward the Grove Pond wellfield. PFNA is part of the study goals. The Project Team calculated the minimum, maximum, and average[2] PFNA concentration for each well at the Grove

[2] The calculated average is based on both detect and non-detect sample results. The Project Team elected to assign a concentration of half the detection limit for all non-detect sample results. All qualified (e.g., J-qualified) sample results were assigned the qualified concentration. Not all of the public water supply (PWS) sample results include a lab-specified detection limit. If no detection limit was available for a non-detect value, the Project Team assigned a concentration of half of the reporting limit. If a non-detect sample result included neither a detection limit nor a reporting limit, the Project Team excluded the non-detect from calculation.

Pond wellfield. The estimated concentration for PFNA from 2000 through 2022 should be considered constant. Table 7-1 presents these calculated values for each well.

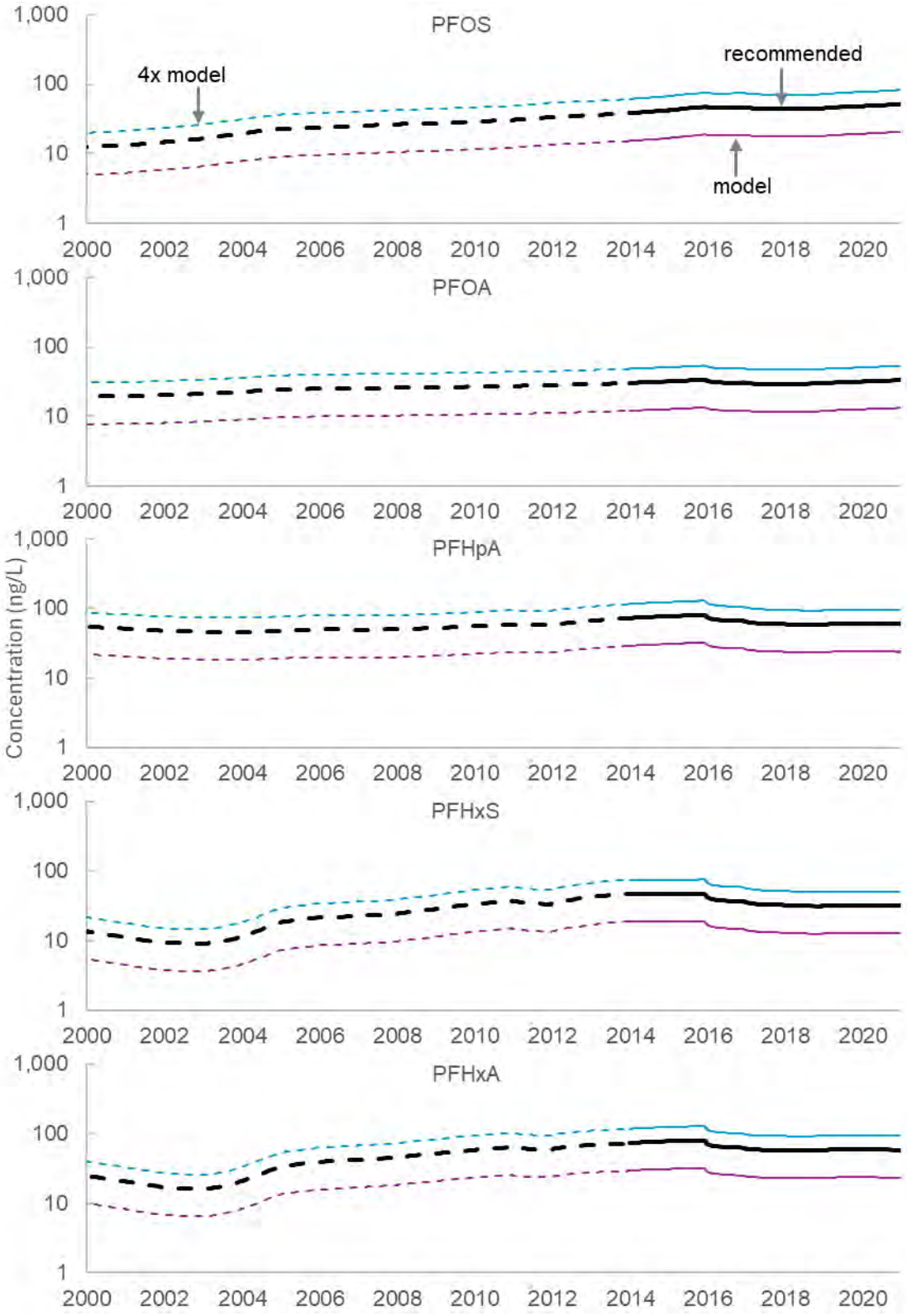



***Figure 7-1: Estimated PFAS Concentrations at GP-08 (2000-2022)***

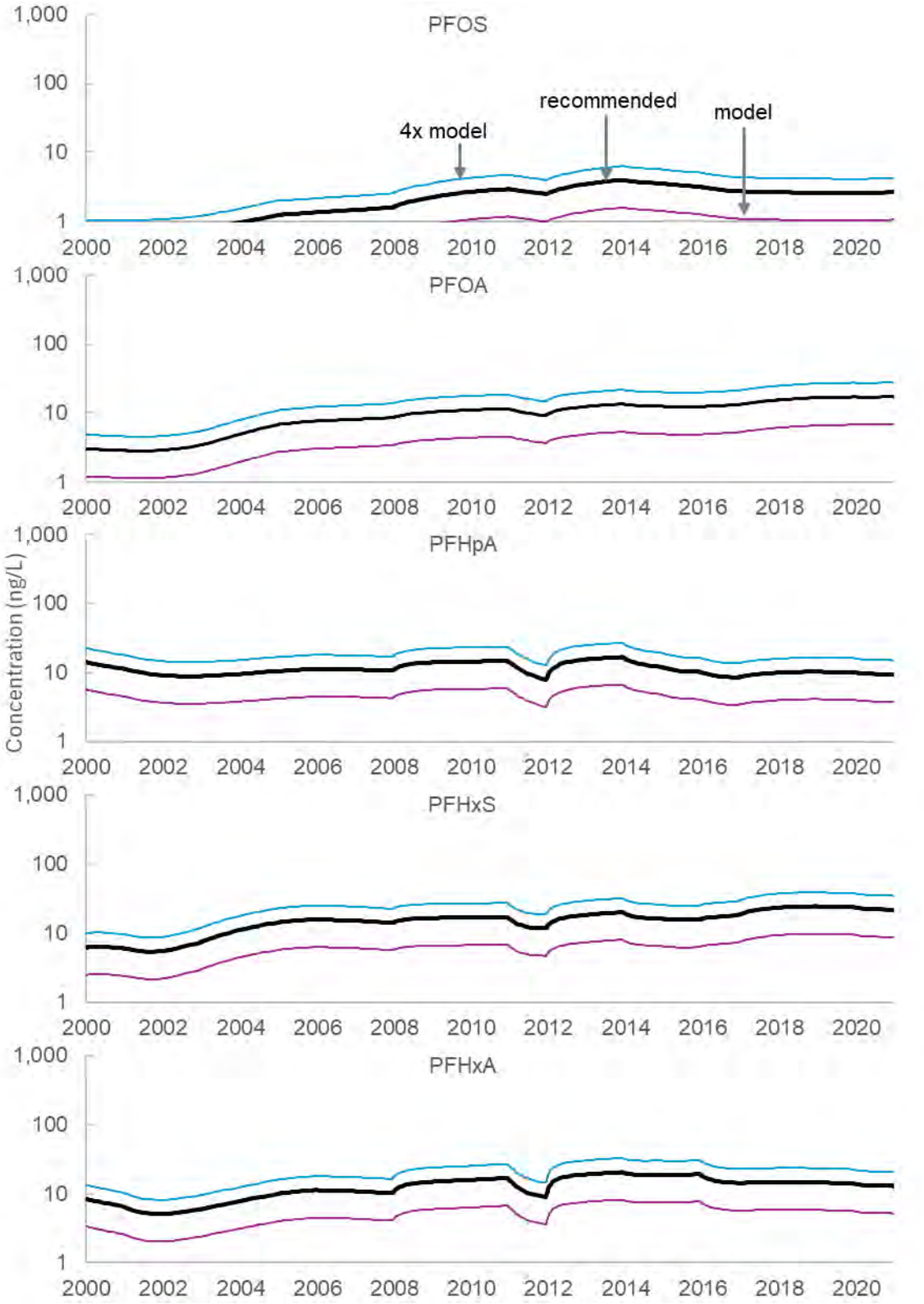



***Figure 7-2: Estimated PFAS Concentrations at GP-01 (2000-2022)***

***Table 7-1: Average PFNA Concentration at Grove Pond Wellfield***

| | Count of Samples | | | Concentration (ng/L) | | |
|---|---|---|---|---|---|---|
| Well | Total | ND | ND No DL/RL | Minimum | Maximum | Average |
| GP-01 | 13 | 7 | 2 | 0.7 | 3.3 | 1.1 |
| GP-06 | 21 | 17 | 8 | 0.3 | 1.0 | 0.8 |
| GP-07 | 21 | 17 | 8 | 0.3 | 1.0 | 0.7 |
| GP-08 | 20 | 12 | 9 | 0.9 | 2.1 | 1.7 |

## 8.0 REFERENCES

ATSDR (Agency for Toxic Substances and Disease Registry), 2024. Pease Study Report. United State Department of Health and Human Services, Agency for Toxic Substances and Disease Registry, Office of Community Health Hazard Assessment. Atlanta, GA. January 12, 2024.

Ayer (Town of Ayer), 2025. Town of Ayer, PFAS Drinking Water. Retrieved 14 March 2025 from: https://www.ayer.ma.us/water-department/pages/pfas-drinking-water.

CDM (Camp Dresser & McKee, Inc.), 1993. Town of Ayer, Massachusetts Grove Pond Wells Hydrogeologic Investigation and Zone II Aquifer Mapping. Camp Dresser & McKee, Inc. Cambridge, MA. January 1993.

EEA (Executive Office of Energy & Environmental Affairs), 2022. Energy & Environmental Affairs, Data Portal, Search for Drinking Water. Retrieved 22 September 2022 from: https://eeaonline.eea.state.ma.us/Portal/#!/search/drinking-water

ESI (Environmental Simulations, Inc.), 2020. Guide to Using Groundwater Vistas, Version 8. Environmental Solutions Inc. Leesport, Pennsylvania.

Freeze, R. Allen and Cherry, John A., 1979. Groundwater. Prentice Hall. Englewood Cliffs, New Jersey. 1979.

Gelhar, Lynn W., Welty, Claire, and Rehfeldt, Kenneth R., 1992. A Critical Review of Data on Field-Scale Dispersion in Aquifers. Water Resources Research, Vol. 28, No. 7. Pages 1955-1974. July 1992.

Geosyntec, 2020. Final, Shepley's Hill Landfill, Groundwater Flow Model Revision Report, Former Fort Devens Army Installation, Devens Massachusetts. Geosyntec Consultants. Acton, MA. July 2020.

Hassan, A. E., 2004. Validation of Numerical Ground Water Models Used to Guide Decision Making. Ground Water. Vol. 42, No. 2, Pg. 277-290. March-April 2004.

ITRC (Interstate Technology Regulatory Council), 2024a. PFAS – Per- and Polyfluoroalkyl Substances, 5 Environmental Fate and Transport Processes. Interstate Technology Regulatory Council. Retrieved 16 May 2024 from: https://pfas-1.itrcweb.org/5-environmental-fate-and-transport-processes/.

ITRC (Interstate Technology Regulatory Council), 2024b. PFAS – Per- and Polyfluoroalkyl Substances, Data Tables, Section 4: Physical and Chemical Properties Table 4-1 Excel File. Interstate Technology Regulatory Council. Retrieved 4 January 2024 from: https://pfas-1.itrcweb.org/wp-content/uploads/2022/01/PhysChemProp_Table_July2023-FINAL.xlsx.

ITRC (Interstate Technology Regulatory Council), 2024c. PFAS – Per- and Polyfluoroalkyl Substances, 2 PFAS Chemistry and Naming Conventions, History and Use of PFAS, and Sources of PFAS Releases to the Environment. Retrieved 29 October 2024 from: https://pfas-1.itrcweb.org/2-pfas-chemistry-and-naming-conventions-history-and-use-of-pfas-and-sources-of-pfas-releases-to-the-environment-overview/.

ITRC (Interstate Technology Regulatory Council), 2025a. Per- and Polyfluoroalkyl Substances, 3 Firefighting Foams. Interstate Technology Regulatory Council. Available from: https://pfas-1.itrcweb.org/3-firefighting-foams/#3_1. Accessed March 13, 2025.

ITRC (Interstate Technology Regulatory Council), 2025b. Per- and Polyfluoroalkyl Substances, 2 PFAS Chemistry and Naming Conventions, History and Use of PFAS, and Sources of PFAS Releases to the Environment. Interstate Technology Regulatory Council. Available from: https://pfas-1.itrcweb.org/2-pfas-chemistry-and-naming-conventions-history-and-use-of-pfas-and-sources-of-pfas-releases-to-the-environment-overview/. Accessed March 13, 2025.

KGS (KOMAN Government Services), 2017. FINAL, Base-Wide Preliminary Assessment for Evaluation of Perfluoroalkyl Substances, Former Fort Devens Army Installation, Devens, MA. KOMAN Government Solutions, LLC. Marlborough, MA. September 2017.

KGS, 2020. Area 1 Preliminary Site Characterization Summary, Per- and Polyfluoroalkyl Substances (PFAS) Remedial Investigation, Former Fort Devens Army Installation, Devens, MA. KOMAN Government Solutions, LLC. Marlborough, MA. June 2020.

MassDEP (Massachusetts Department of Environmental Protection), 2024. Energy & Environmental Affairs, Well Database. Commonwealth of Massachusetts, Executive Office of Energy & Environmental Affairs. Accessed October 3 2024. Available from: https://www.mass.gov/info-details/well-database.

MassGIS, 2024a. MassGIS Data: USGS 1:24,000 Surficial Geology, July 2022. Commonwealth of Massachusetts Executive Office of Technology Services and Security. Accessed October 3, 2024. Available from: https://www.mass.gov/info-details/massgis-data-usgs-124000-surficial-geology.

MassGIS, 2024b. MassGIS Data: 2016 Land Cover/Land Use, May 2019. Commonwealth of Massachusetts Executive Office of Technology Services and Security. Accessed October 10, 2024. Available from: https://www.mass.gov/info-details/massgis-data-2016-land-coverland-use.

Mercadante, A.M., Colman, J.A., Buursink, M.L., 1999. USGS Water-Resources Investigations Report 99-4241, Map Showing Morphometry, Bathymetry, and Soft-Sediment Thickness of Plow Shop Pond and Grove Pond Ayer, Massachusetts. Department of the Interior, U.S. Geological Survey. 1999.

NOAA (National Oceanic and Atmospheric Administration), 2023. Daily Summaries Station Details (Ayer 0.1 SW, MA US). National Oceanic and Atmospheric Administration, National Center for Environmental Information. Accessed September 9, 2023. Available from: https://www.ncdc.noaa.gov/cdo-web/datasets/GHCND/stations/GHCND:US1MAMD0025/detail .

NRCC (Northeast Regional Climate Center), 2024. Northeast Regional Climate Center, Potential Evapotranspiration (PET) Estimates (inches). Cornell University, Northeast Regional Climate Center. Accessed October 10, 2024. Available from: https://www.nrcc.cornell.edu/wxstation/pet/pet.html.

Panday, Sorab, Langevin, C.D., Niswonger, R.G., Ibaraki, Motomu, and Hughes, J.D., 2013. MODFLOW–USG version 1: An unstructured grid version of MODFLOW for simulating groundwater flow and

tightly coupled processes using a control volume finite-difference formulation. United States Geological Survey Techniques and Methods, 6-A45. Reston, Virginia. 2013.

Papadopulos (S.S. Papadopulos & Associates, Inc.), 2022. Regional Groundwater Flow Model of the Former Fort Devens, Massachusetts. S.S. Papadopulos & Associates, Inc. Rockville, Maryland. November 22, 2022.

Tata & Howard, 1999. Conceptual Zone II Delineation for the Spectacle Pond Wells, Ayer Massachusetts. Tata & Howard, Inc. Westborough, MA. March 1999.

US EPA (United States Environmental Protection Agency), 2000. BIOCHLOR, Natural Attenuation Decision Support System, User's Manual, Version 1.0 EPA/600/R-00/008. United States Environmental Protection Agency. Washington D.C. January 2000.

US EPA (United States Environmental Protection Agency), 2024a. PFAS Master List of PFAS Substances (RETIRED). United States Environmental Protection Agency. Retrieved 16 May 2024 from: https://comptox.epa.gov/dashboard/chemical-lists/PFASMASTER.

USGS (United States Geological Survey), 2024. MODFLOW and Related Programs. U.S. Department of the Interior, U.S. Geological Survey. Accessed: October 9, 2024. Available from: https://www.usgs.gov/mission-areas/water-resources/science/modflow-and-related-programs.

Wiedemer, T.H., Rifai, H.S., Newell, C.J., and Wilson, J.T., 1999. Natural Attenuation of Fuels and Chlorinated Solvents in the Subsurface. John Wiley & Sons, Inc. New York. 1999.

.

**Attachment 1: Excerpt from The Public Spirit**
**September 15, 1960**



The Public Spirit

Ayer, Massachusetts — Thursday, September 15, 1960

## Devens Warehouse Destroyed By Fire

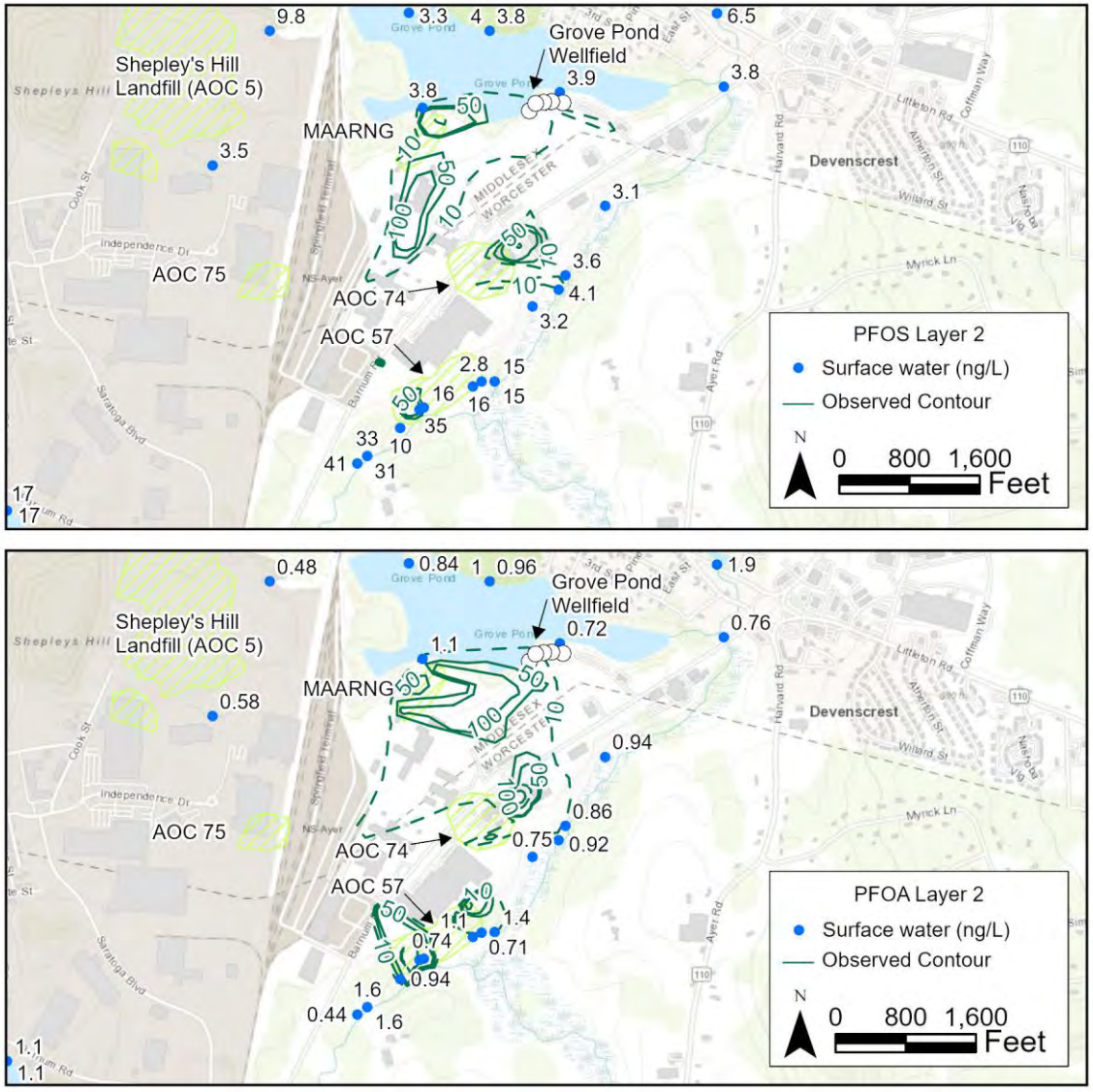
AYER—Fire destroyed a huge warehouse near the northeast gate of Fort Devens last week Thursday afternoon causing a loss of several htousands of dollars and requiring the help of firefighters from this town and Shirley.

The 90 by 200 foot building in the ordnance depot section was completely enveloped in flames when the post fire department arrived at 4:45 p. m. in response to an alarm. Dense clouds of smoke could be seen for miles in all directions and the initial columns of smoke that rose from the area led people in the middle of town to believe that the fire was at the tannery.

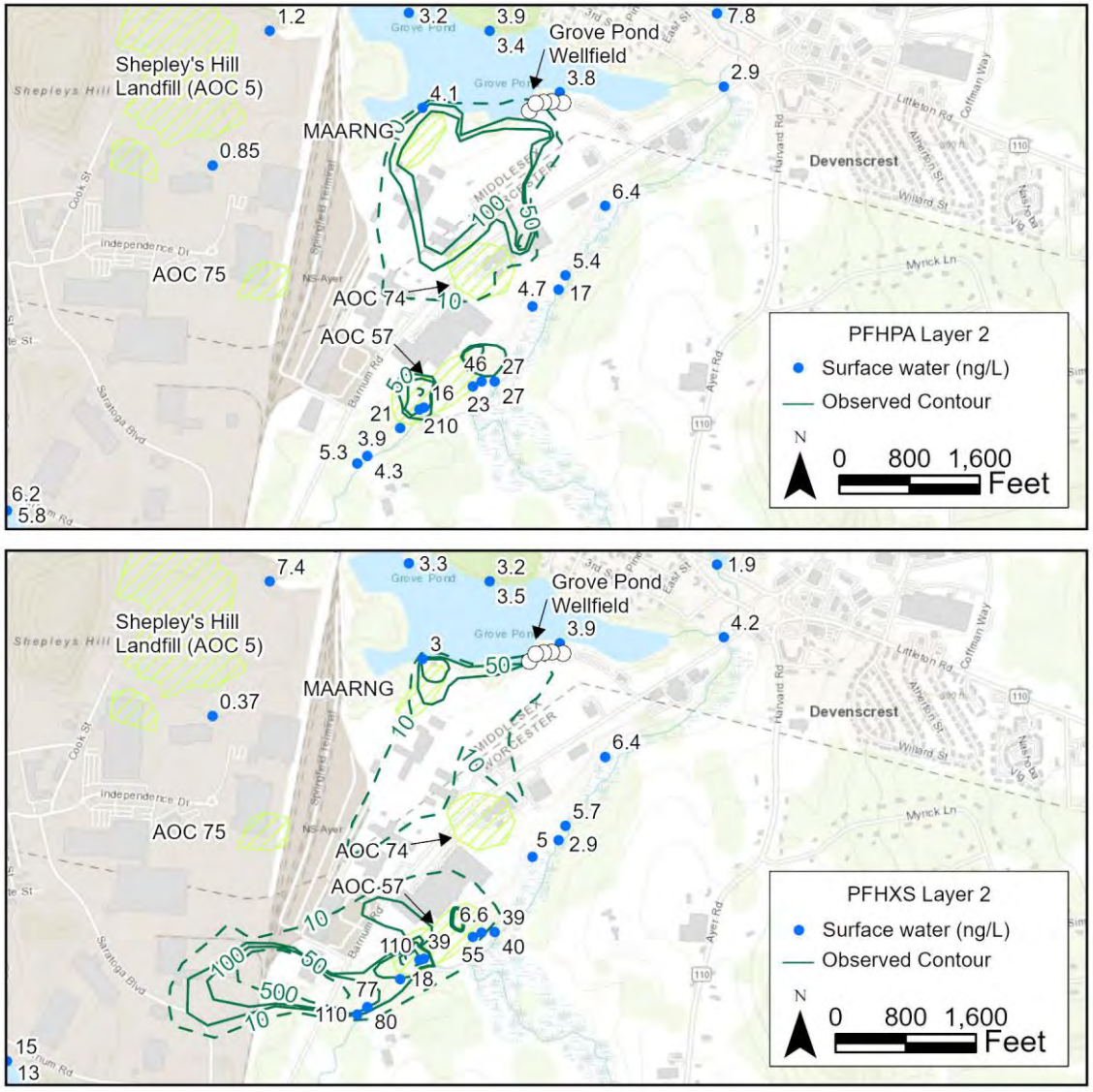
Ayer and Shirley firefighters remained at the scene of the fire for more than three hours pouring water on the burning ruins. Equipment and parts for tanks and military vehicles owned and stored in the warehouse by the Massachusetts National Guard were destroyed and the building was a total loss.

The cause of the fire is under investigation.

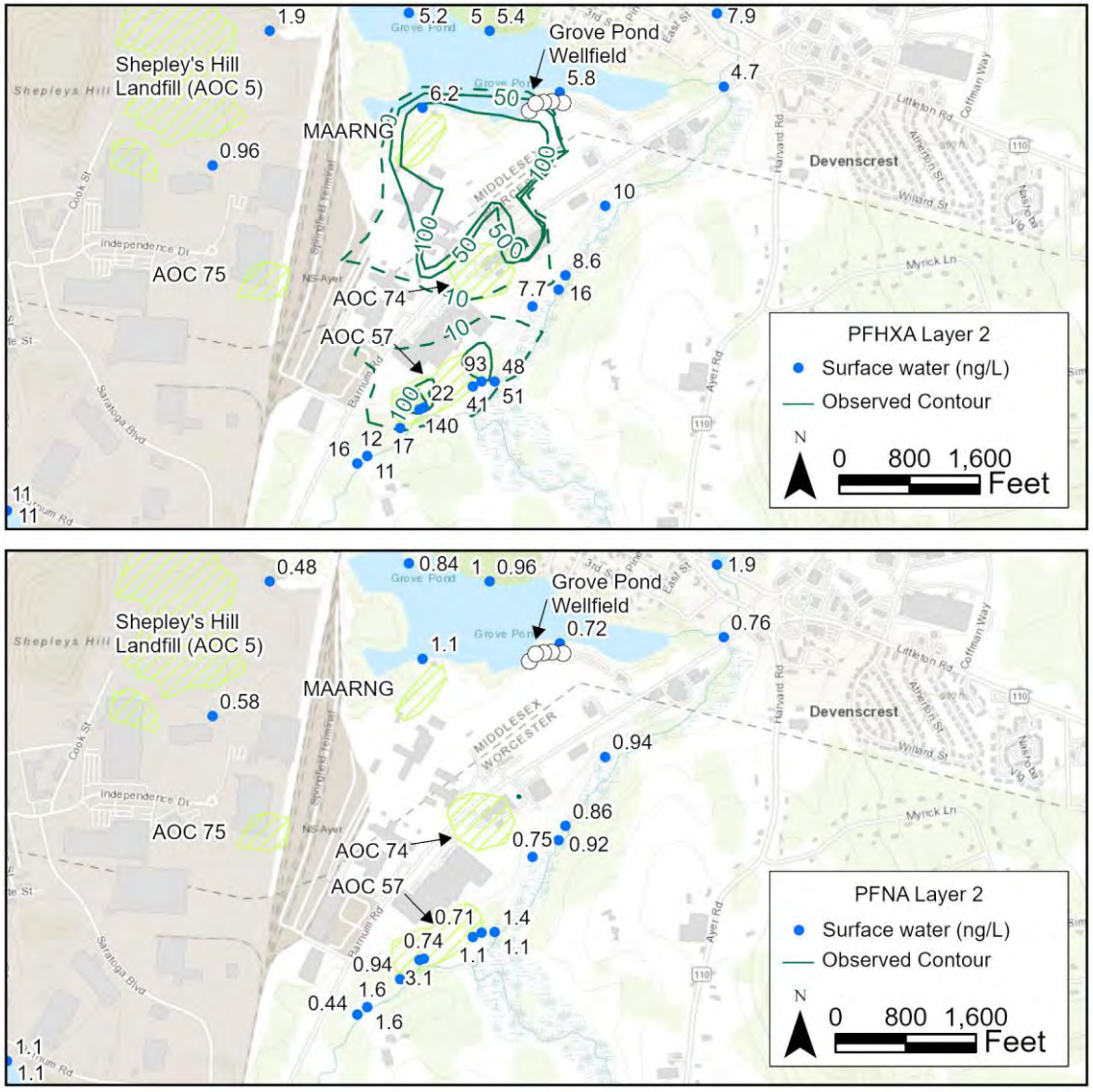
**Attachment 2: PFAS Concentration Sample Results in Surface Water with Plume Contour Delineation**




***Iso-concentration Contours of PFAS in Groundwater with Surface Water Concentrations (PFOS,PFOA)***




***Iso-concentration Contours of PFAS in Groundwater with Surface Water Concentrations (PFHpA, PFHxS)***



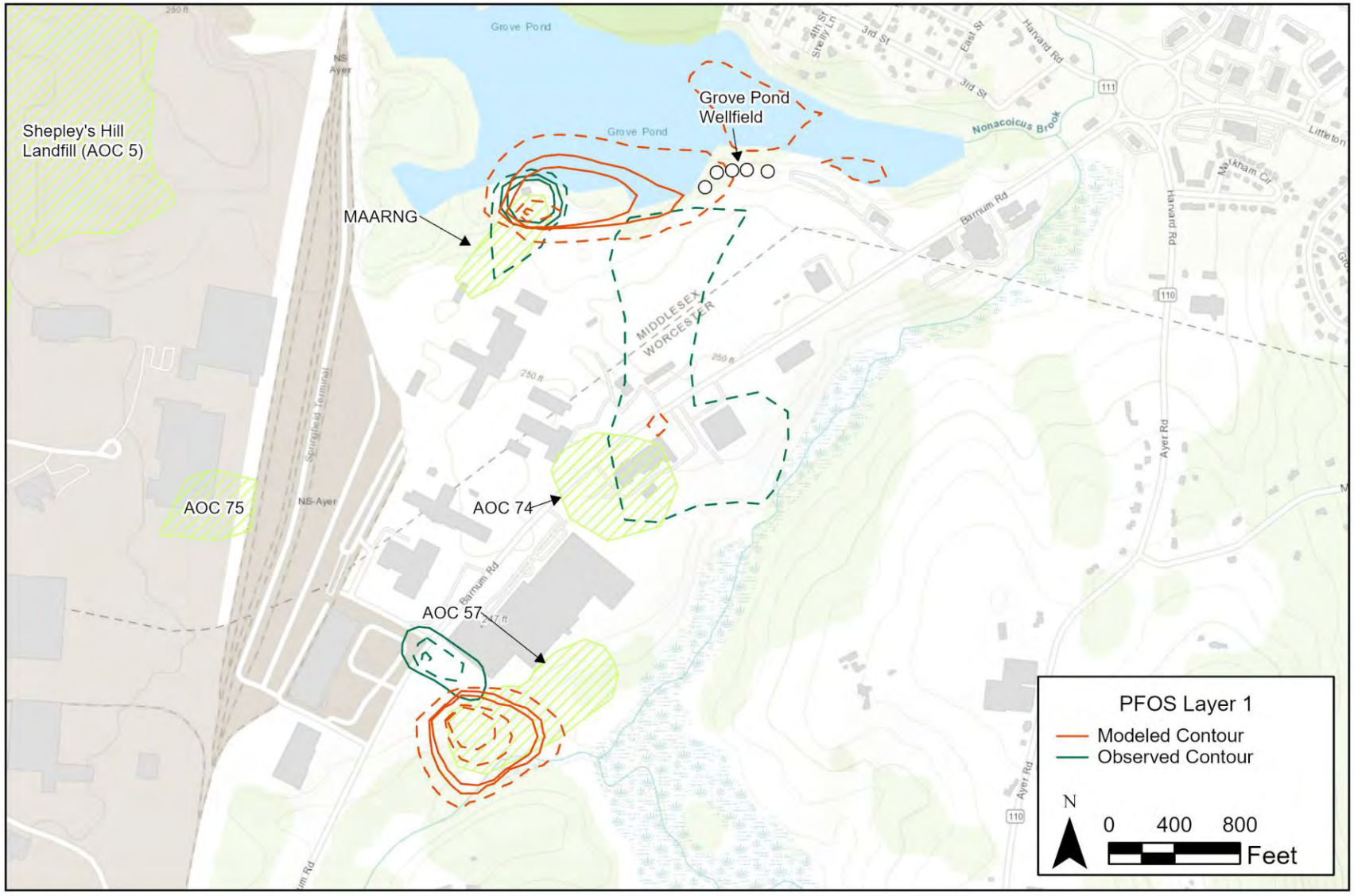

***Iso-concentration Contours of PFAS in Groundwater with Surface Water Concentrations (PFHxA, PFNA)***

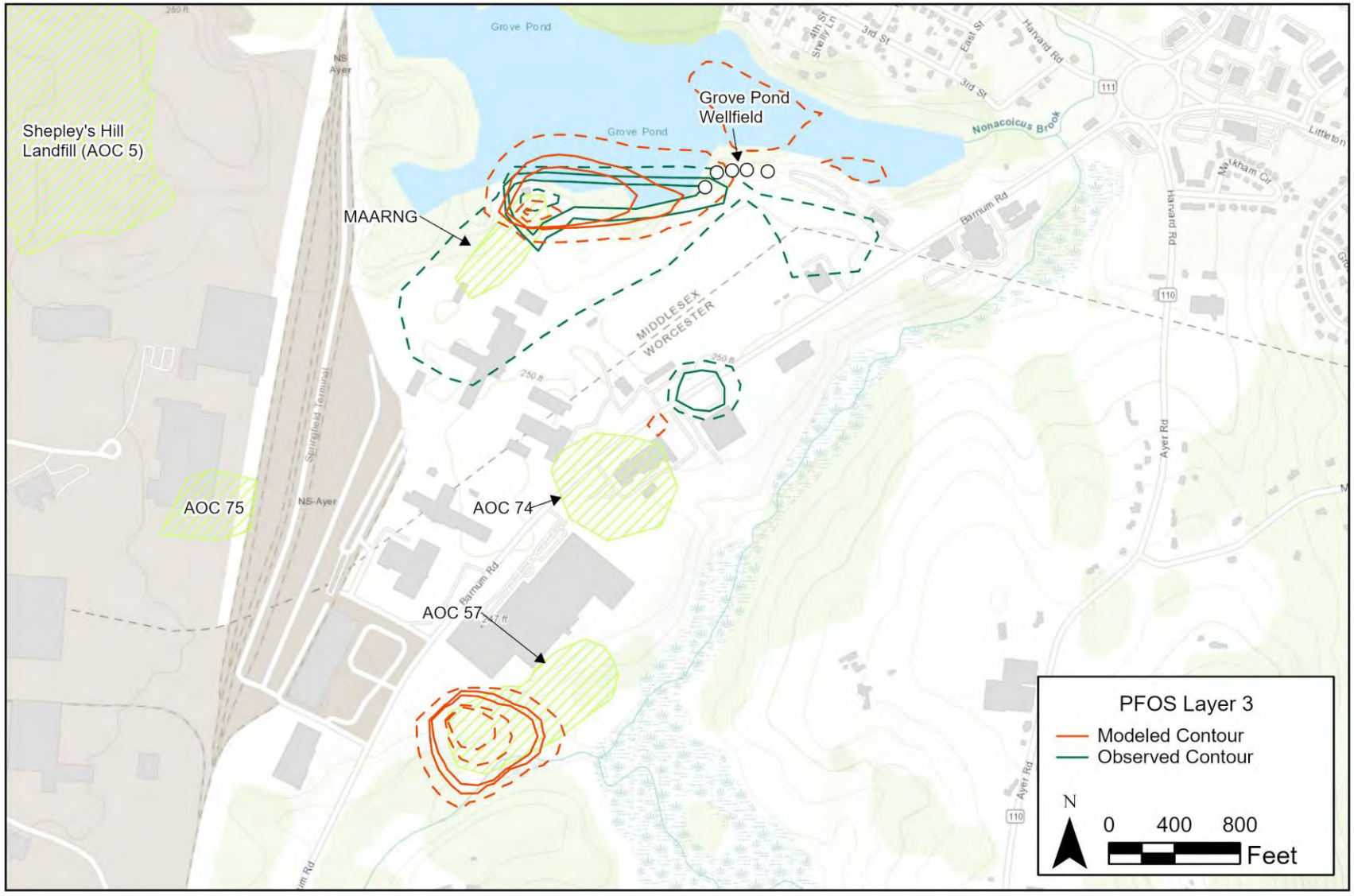
# Attachment 3: Hydrogeologic Calibration Targets

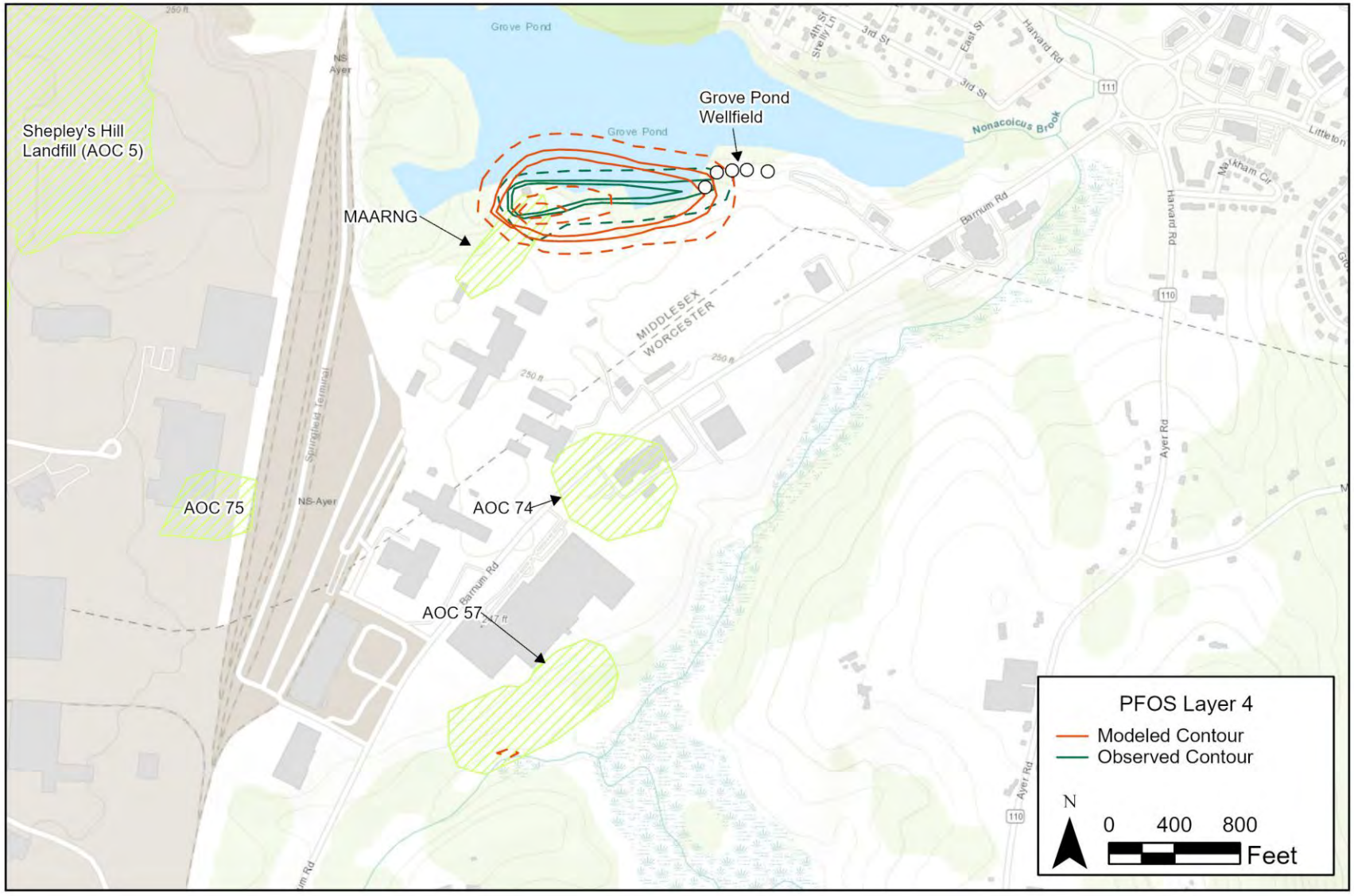
| | | MA State Plane (ft) | | Elevation NAVD88 (ft) | | |
|---|---|---|---|---|---|---|
| Group | Location Name | X | Y | Top Screen | Bot Screen | GW Surface |
| SHL 2013-2014 | N1-P123 | 630,723 | 3,027,868 | 162.8 | 157.8 | 216.2 |
| SHL 2013-2014 | N3-P2 | 630,778 | 3,027,130 | 214.7 | 209.7 | 216.6 |
| SHL 2013-2014 | N7-P2 | 629,991 | 3,025,618 | 224.5 | 219.5 | 224.6 |
| SHL 2013-2014 | SHL-10 | 630,877 | 3,026,868 | 225.1 | 210.1 | 217.2 |
| SHL 2013-2014 | SHL-11 | 630,496 | 3,027,316 | 222.4 | 207.4 | 216.8 |
| SHL 2013-2014 | SHL-8S | 630,407 | 3,028,127 | 166.5 | 165.3 | 213.5 |
| SHL 2013-2014 | SHM-05-39AB | 629,761 | 3,028,544 | 184.8 | 182.8 | 210.1 |
| SHL 2013-2014 | SHM-07-03 | 629,411 | 3,028,445 | 203.0 | 193.0 | 209.7 |
| SHL 2013-2014 | SHM-10-01 | 628,868 | 3,028,617 | 146.1 | 136.1 | 206.7 |
| SHL 2013-2014 | SHM-10-04 | 628,959 | 3,029,485 | 154.7 | 144.7 | 207.5 |
| SHL 2013-2014 | SHM-10-05A | 630,442 | 3,028,943 | 185.2 | 175.2 | 210.9 |
| SHL 2013-2014 | SHM-10-06A | 630,301 | 3,027,896 | 169.0 | 159.0 | 214.3 |
| SHL 2013-2014 | SHM-10-08 | 628,352 | 3,028,526 | 165.7 | 155.7 | 205.6 |
| SHL 2013-2014 | SHM-10-11 | 629,991 | 3,025,972 | 210.9 | 200.9 | 223.1 |
| SHL 2013-2014 | SHM-10-12 | 629,717 | 3,026,719 | 207.0 | 197.0 | 221.1 |
| SHL 2013-2014 | SHM-10-13 | 629,906 | 3,027,157 | 181.4 | 171.4 | 218.8 |
| SHL 2013-2014 | SHM-10-14 | 629,785 | 3,027,373 | 174.8 | 154.8 | 217.9 |
| SHL 2013-2014 | SHM-10-16 | 629,834 | 3,028,355 | 141.7 | 131.7 | 212.3 |
| SHL 2013-2014 | SHM-11-06 | 630,411 | 3,027,590 | 208.3 | 198.3 | 216.3 |
| SHL 2013-2014 | SHM-13-01 | 628,557 | 3,028,295 | 166.8 | 156.8 | 206.0 |
| SHL 2013-2014 | SHM-13-02 | 628,981 | 3,028,714 | 156.9 | 146.9 | 206.8 |
| SHL 2013-2014 | SHM-13-03 | 629,173 | 3,028,991 | 167.8 | 157.8 | 207.7 |
| SHL 2013-2014 | SHM-13-06 | 629,245 | 3,028,695 | 188.2 | 178.2 | 207.5 |
| SHL 2013-2014 | SHM-13-08 | 629,515 | 3,028,838 | 173.2 | 163.2 | 208.6 |
| SHL 2013-2014 | SHM-96-5B | 630,158 | 3,028,113 | 137.4 | 127.4 | 212.8 |
| SHL 2013-2014 | SHM-99-32X | 630,169 | 3,028,575 | 147.1 | 137.1 | 211.8 |
| SHL 2013-2014 | SHP-99-29X | 629,539 | 3,027,143 | 222.4 | 212.4 | 220.4 |
| RI MARCH 2020 | 5702MW-19-01A - W | 632,240 | 3,023,026 | 227.7 | 217.7 | 223.8 |
| RI MARCH 2020 | 5702MW-20-01A - W | 632,765 | 3,022,576 | 189.6 | 179.6 | 219.4 |
| RI MARCH 2020 | 5702MW-20-02A - W | 632,508 | 3,022,840 | 211.7 | 201.7 | 222.7 |
| RI MARCH 2020 | 5702MW-20-03A - W | 632,530 | 3,022,636 | 208.8 | 198.8 | 220.7 |
| RI MARCH 2020 | 5702MW-20-04A - W | 632,758 | 3,022,724 | 162.7 | 152.7 | 221.2 |
| RI MARCH 2020 | 5702MW-20-05A - W | 632,579 | 3,022,546 | 193.3 | 183.3 | 219.9 |
| RI MARCH 2020 | 5702MW-20-06A - W | 632,671 | 3,022,689 | 164.1 | 154.1 | 221.3 |
| RI MARCH 2020 | 5702MW-20-07A - W | 632,695 | 3,022,515 | 189.4 | 179.4 | 219.2 |
| RI MARCH 2020 | 5703MW-20-01A - W | 633,310 | 3,022,964 | 223.2 | 213.2 | 220.8 |
| RI MARCH 2020 | 5703MW-20-02A - W | 633,214 | 3,022,995 | 223.5 | 213.5 | 222.3 |
| RI MARCH 2020 | 5703MW-20-03A - W | 633,169 | 3,022,909 | 172.9 | 162.9 | 220.7 |
| RI MARCH 2020 | 5703MW-20-04A - W | 633,266 | 3,022,990 | 169.2 | 159.2 | 221.1 |
| RI MARCH 2020 | 5703PZ-19-01 - W | 633,267 | 3,022,897 | 157.7 | 152.7 | 219.8 |
| RI MARCH 2020 | 74MW-19-04A - A | 634,137 | 3,023,949 | 204.1 | 194.1 | 220.7 |
| RI MARCH 2020 | 74PZ-19-05 - W | 633,822 | 3,024,351 | 223.2 | 213.2 | 224.9 |
| RI MARCH 2020 | 74PZ-20-01 - W | 634,447 | 3,024,411 | 218.4 | 208.4 | 220.2 |
| RI MARCH 2020 | 74PZ-20-02 - W | 633,699 | 3,023,988 | 217.6 | 207.6 | 224.2 |
| RI MARCH 2020 | 74PZ-20-03 - W | 634,139 | 3,024,551 | 227.0 | 217.0 | 221.5 |

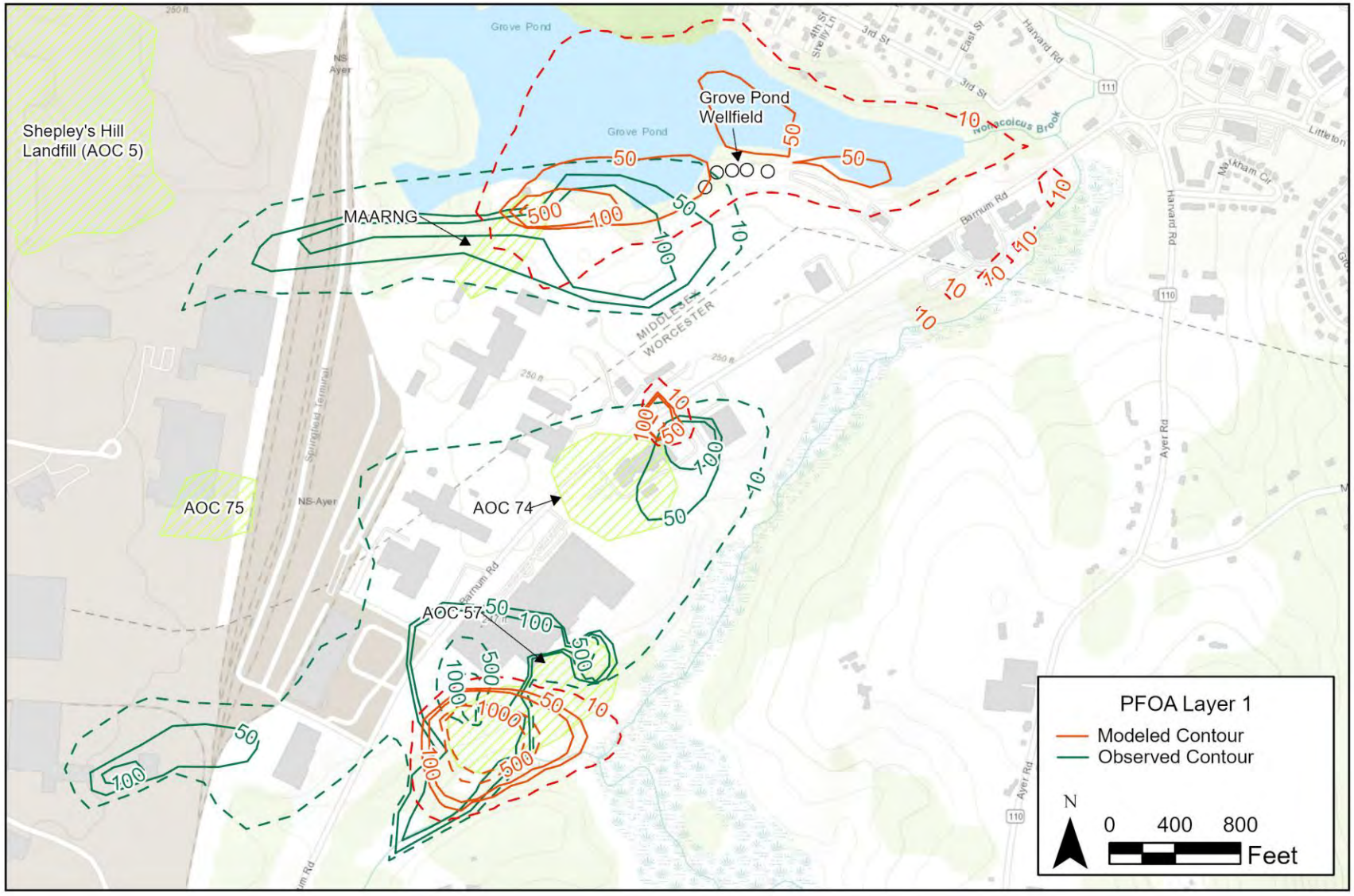
| | | MA State Plane (ft) | | Elevation NAVD88 (ft) | | |
|---|---|---|---|---|---|---|
| Group | Location Name | X | Y | Top Screen | Bot Screen | GW Surface |
| RI MARCH 2020 | 74PZ-20-04 - W | 633,457 | 3,024,309 | 225.5 | 215.5 | 224.2 |
| RI MARCH 2020 | 74PZ-20-05 - W | 634,093 | 3,024,184 | 224.4 | 214.4 | 223.0 |
| RI MARCH 2020 | 75MW-19-02A - W | 630,775 | 3,022,533 | 210.3 | 200.3 | 230.4 |
| RI MARCH 2020 | 75MW-19-04A - W | 631,715 | 3,022,035 | 208.1 | 198.1 | 225.1 |
| RI MARCH 2020 | 75PZ-19-02 - W | 630,327 | 3,021,645 | 233.0 | 223.0 | 231.9 |
| RI MARCH 2020 | 75PZ-19-04 - W | 629,581 | 3,022,270 | 225.4 | 215.4 | 234.2 |
| RI MARCH 2020 | 75PZ-20-01 - W | 631,916 | 3,022,301 | 224.9 | 214.9 | 225.3 |
| RI MARCH 2020 | 75PZ-20-02 - W | 631,328 | 3,022,659 | 231.4 | 221.4 | 229.4 |
| RI MARCH 2020 | 75PZ-20-03 - W | 631,092 | 3,022,209 | 229.5 | 219.5 | 229.9 |
| RI MARCH 2020 | 75PZ-20-04 - W | 630,904 | 3,021,622 | 232.3 | 222.3 | 230.9 |
| RI MARCH 2020 | 75PZ-20-06 - W | 630,364 | 3,022,431 | 233.4 | 223.4 | 231.2 |
| RI MARCH 2020 | 75PZ-20-07 - W | 631,558 | 3,021,697 | 224.3 | 214.3 | 224.5 |
| RI MARCH 2020 | 76PZ-19-04 - W | 627,714 | 3,022,222 | 244.6 | 234.6 | 243.5 |
| RI MARCH 2020 | 76PZ-19-13 - W | 627,787 | 3,022,831 | 237.0 | 227.0 | 242.3 |
| RI MARCH 2020 | 76PZ-19-15 - W | 627,309 | 3,022,325 | 242.0 | 232.0 | 243.3 |
| RI MARCH 2020 | GPMW-19-01A - W | 633,761 | 3,025,550 | 206.1 | 196.1 | 216.3 |
| RI MARCH 2020 | MNG-2R - ? | 633,011 | 3,025,607 | 219.5 | 209.5 | 217.0 |
| RI MARCH 2020 | MNG-6R - ? | 633,467 | 3,025,321 | 219.7 | 209.7 | 216.7 |
| RI MARCH 2020 | MW75-UNKNOWN - W | 631,457 | 3,021,873 | 226.2 | 216.2 | 227.0 |
| RI APRIL 2020 | 32PZ-19-01 - W | 630,757 | 3,025,651 | 228.4 | 218.4 | 227.2 |
| RI APRIL 2020 | 32PZ-19-02 - W | 630,586 | 3,024,969 | 228.3 | 218.3 | 227.9 |
| RI APRIL 2020 | 76PZ-19-09 - W | 626,849 | 3,026,475 | 210.8 | 200.8 | 214.0 |
| RI APRIL 2020 | SHM-95-27X | 630,753 | 3,026,165 | 204.8 | 194.8 | 224.3 |
| ARTIFICIAL | FC1 | 633,351 | 3,022,191 | NA | NA | 220.7 |
| ARTIFICIAL | FC2 | 635,786 | 3,026,156 | NA | NA | 220.4 |
| ARTIFICIAL | FC3 | 635,250 | 3,024,955 | NA | NA | 219.5 |
| ARTIFICIAL | FC4 | 633,994 | 3,023,569 | NA | NA | 224.8 |
| ARTIFICIAL | FC5 | 627,397 | 3,028,447 | NA | NA | 205.4 |
| ARTIFICIAL | FC6 | 631,278 | 3,021,038 | NA | NA | 227.6 |

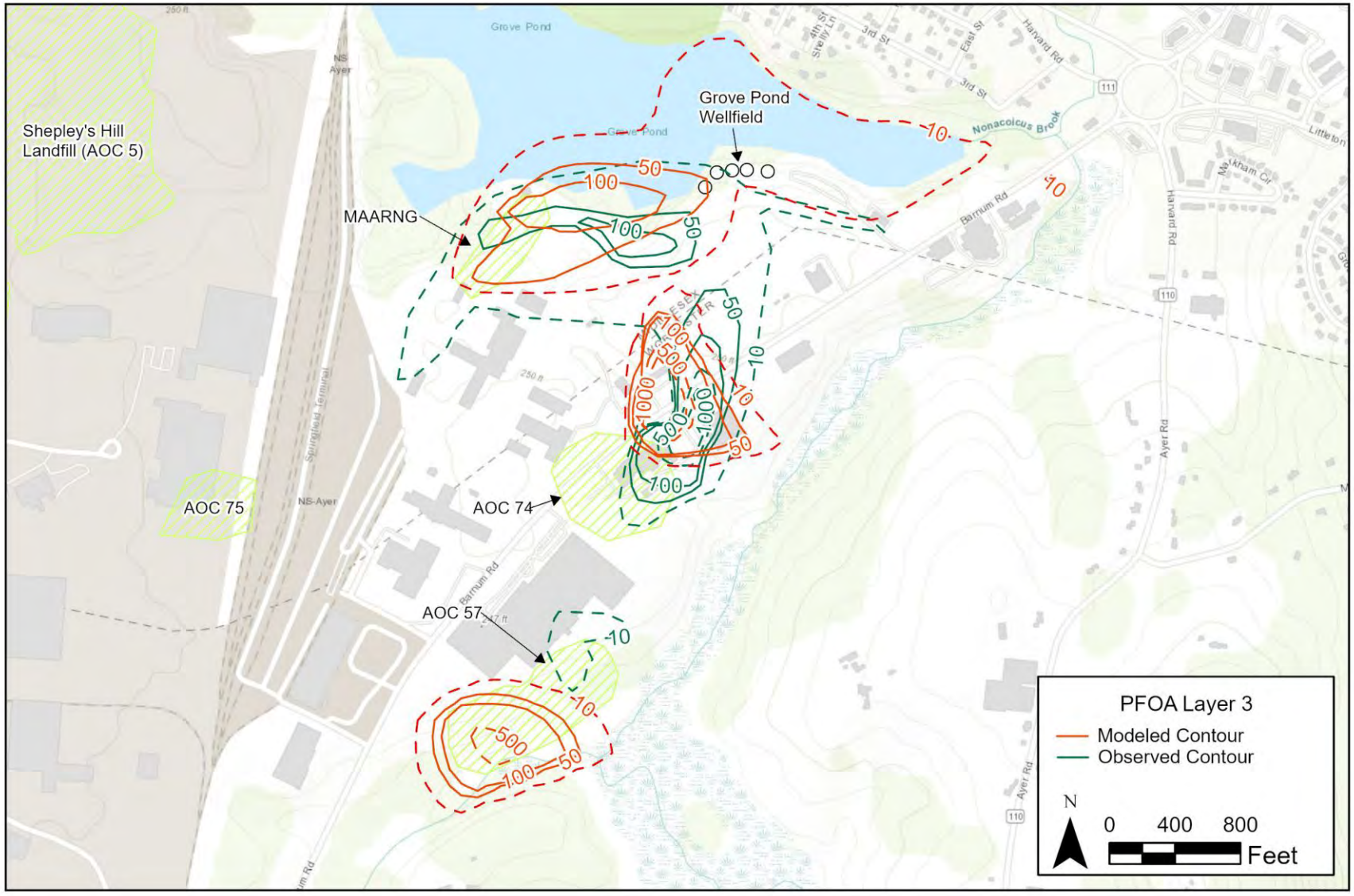
**Attachment 4: Observed and Modeled PFAS Contours for Model Layers 1, 3, and 4**

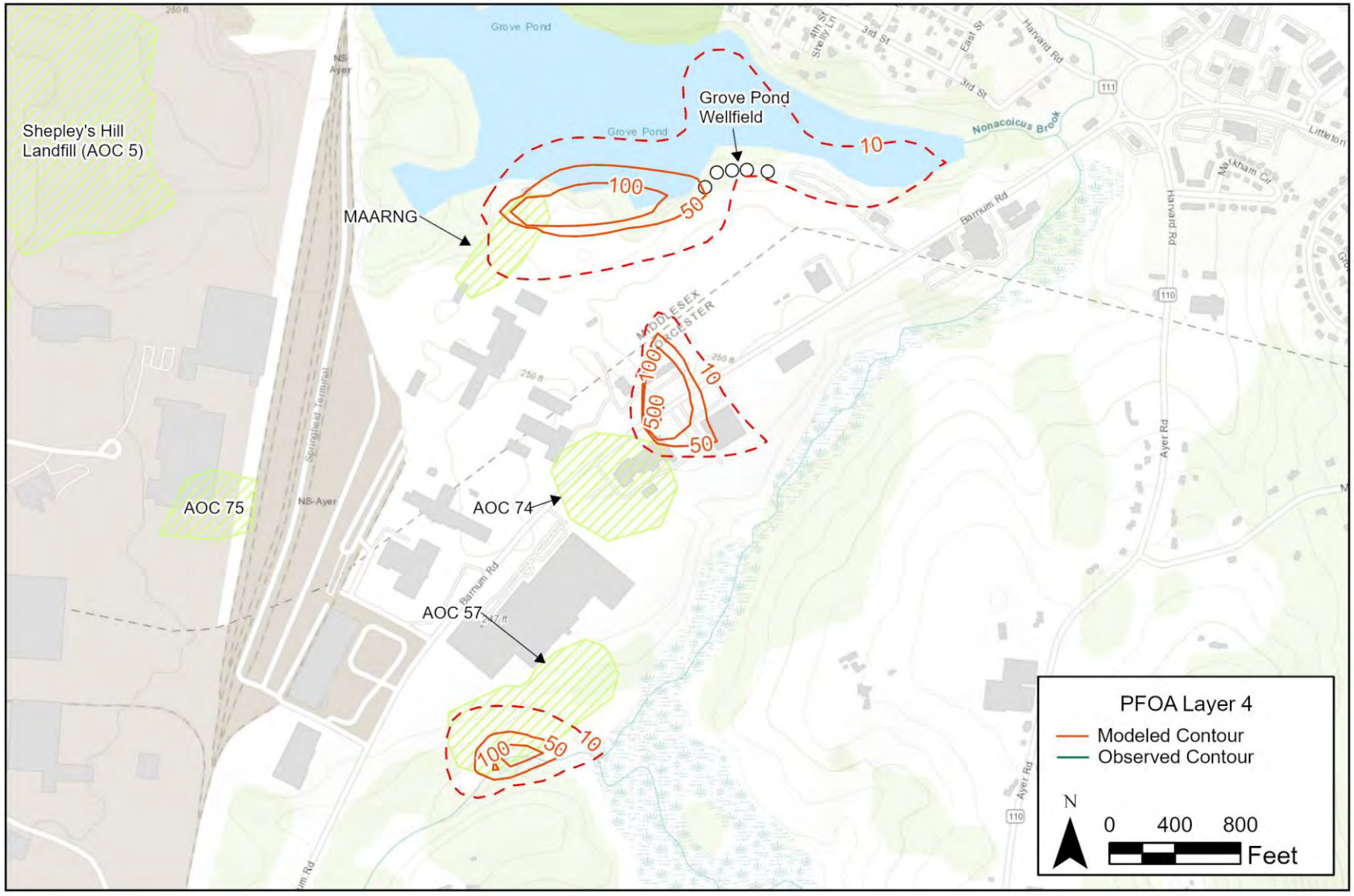

Grove Pond
Grove Pond Wellfield
Shepley's Hill Landfill (AOC 5)
MAARNG
AOC 75
AOC 74
AOC 57
NS-Ayer
Barnum Rd
Ayer Rd
Harvard Rd
Nonacoicus Brook
MIDDLESEX WORCESTER
PFOS Layer 1
Modeled Contour
Observed Contour
N
0 400 800
Feet

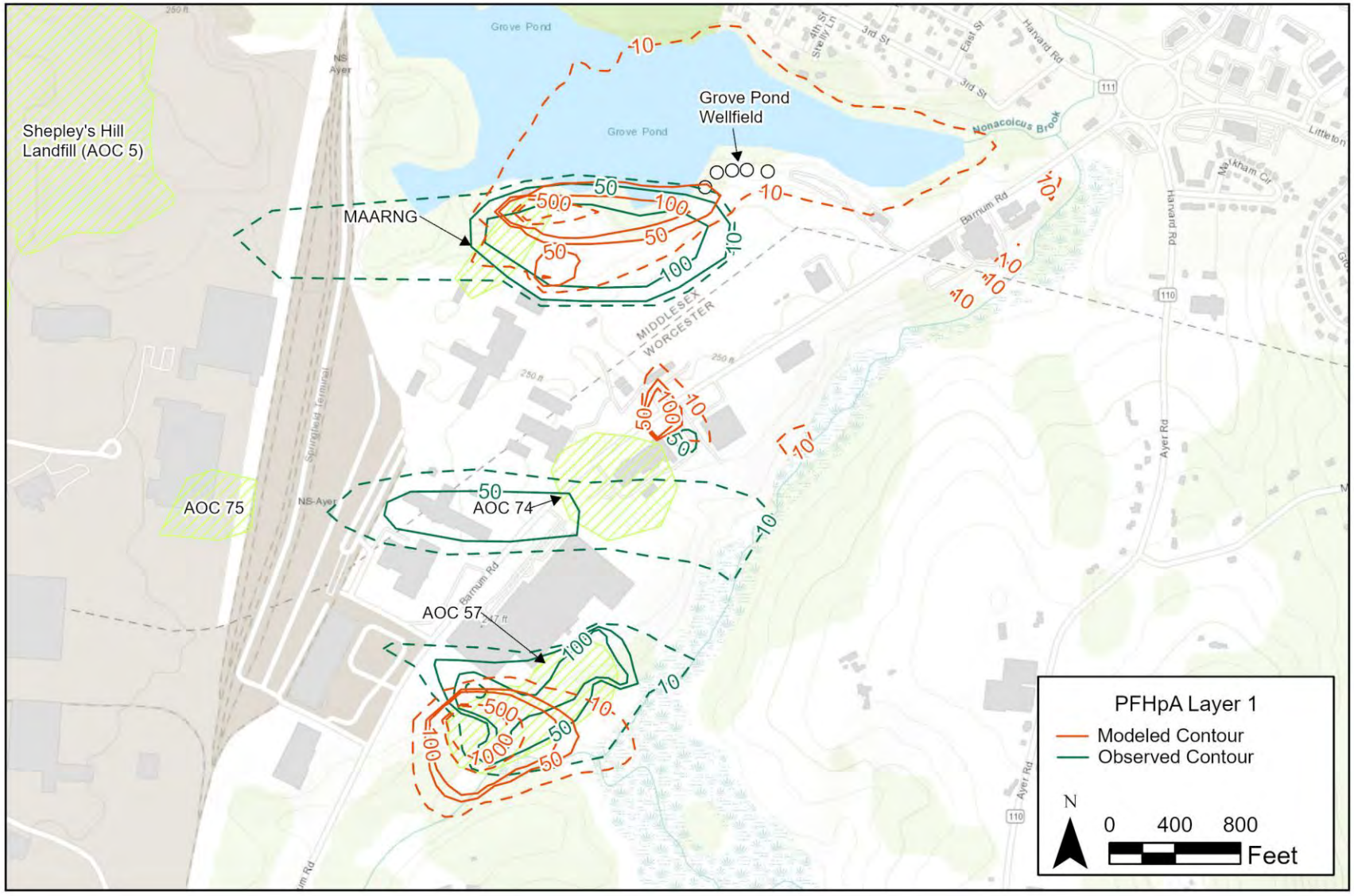

Grove Pond
Grove Pond Wellfield
Shepley's Hill Landfill (AOC 5)
MAARNG
AOC 75
AOC 74
AOC 57
MIDDLESEX WORCESTER
Barnum Rd
Ayer Rd
Harvard Rd
Nonacoicus Brook
NS-Ayer
Springfield Terminal
PFOS Layer 3
Modeled Contour
Observed Contour
N
0 400 800
Feet

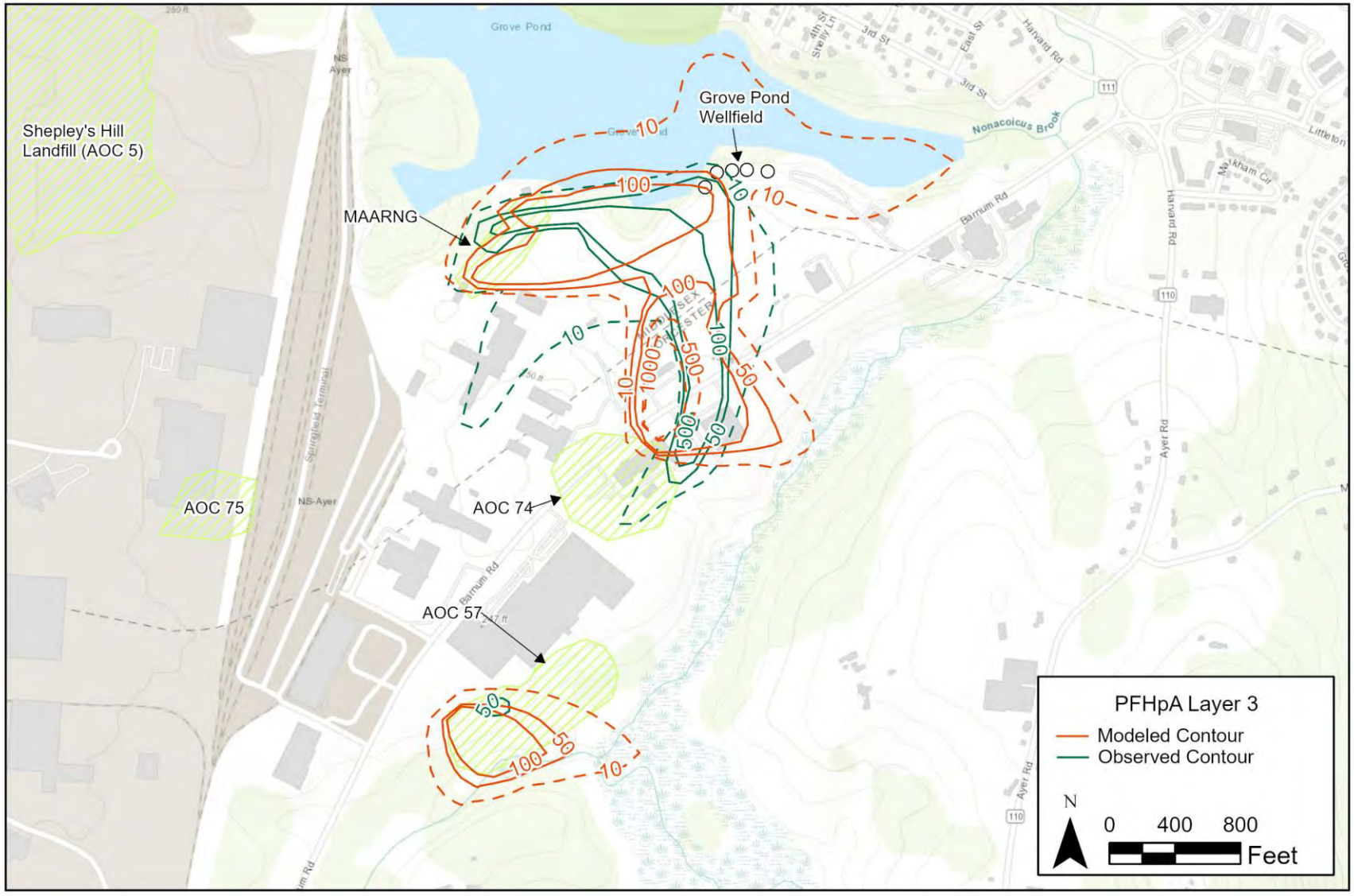

Grove Pond
Grove Pond Wellfield
Shepley's Hill Landfill (AOC 5)
MAARNG
AOC 75
AOC 74
AOC 57
MIDDLESEX
WORCESTER
Barnum Rd
Ayer Rd
Harvard Rd
Nonacoicus Brook
NS-Ayer
Springfield Terminal
PFOS Layer 4
Modeled Contour
Observed Contour
N
0
400
800
Feet

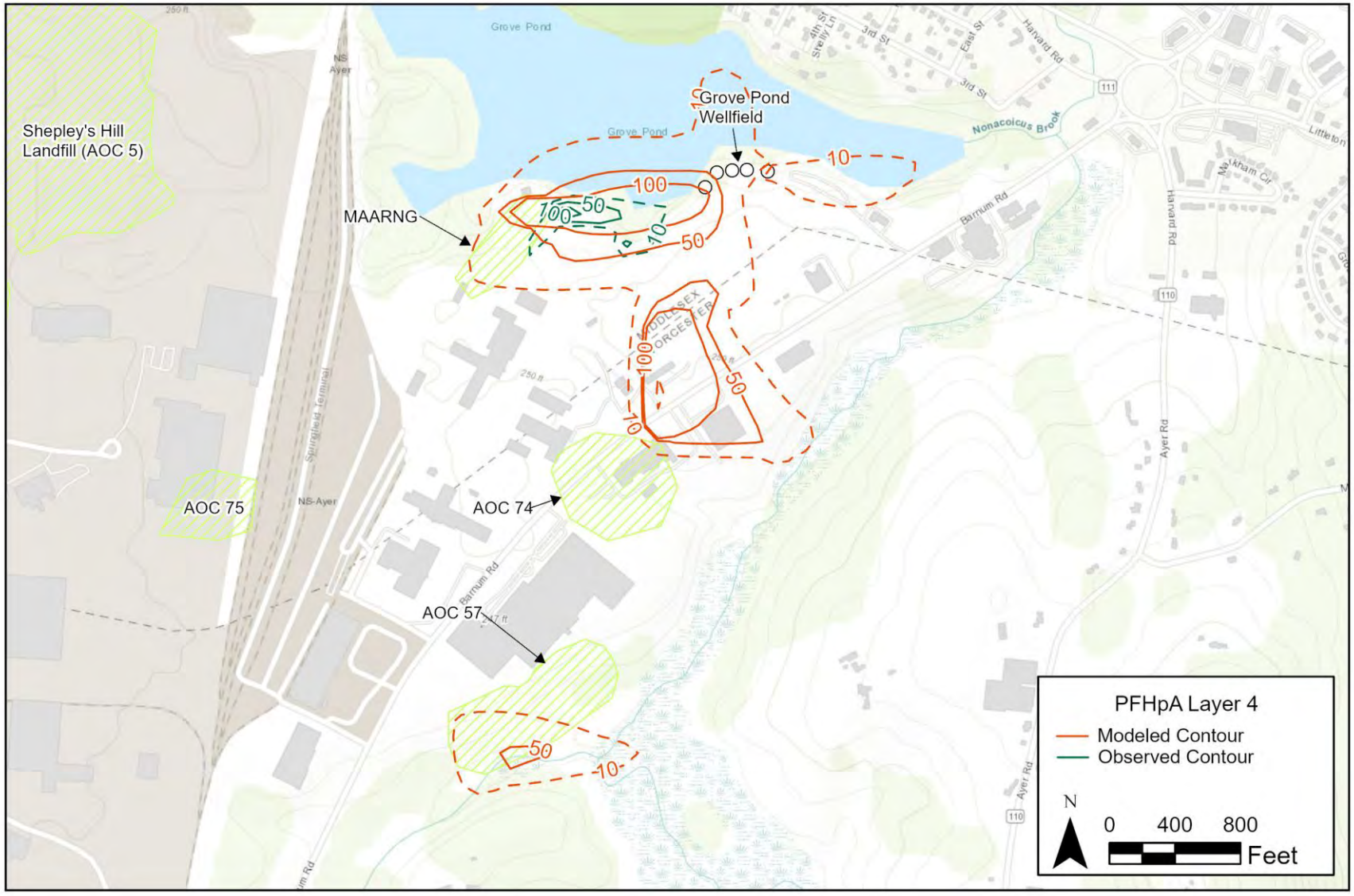

Grove Pond
Grove Pond Wellfield
Shepley's Hill Landfill (AOC 5)
MAARNG
AOC 75
AOC 74
AOC 57
NS-Ayer
Springfield Terminal
MIDDLESEX WORCESTER
Barnum Rd
Ayer Rd
Harvard Rd
PFOA Layer 1
Modeled Contour
Observed Contour
N
0 400 800
Feet

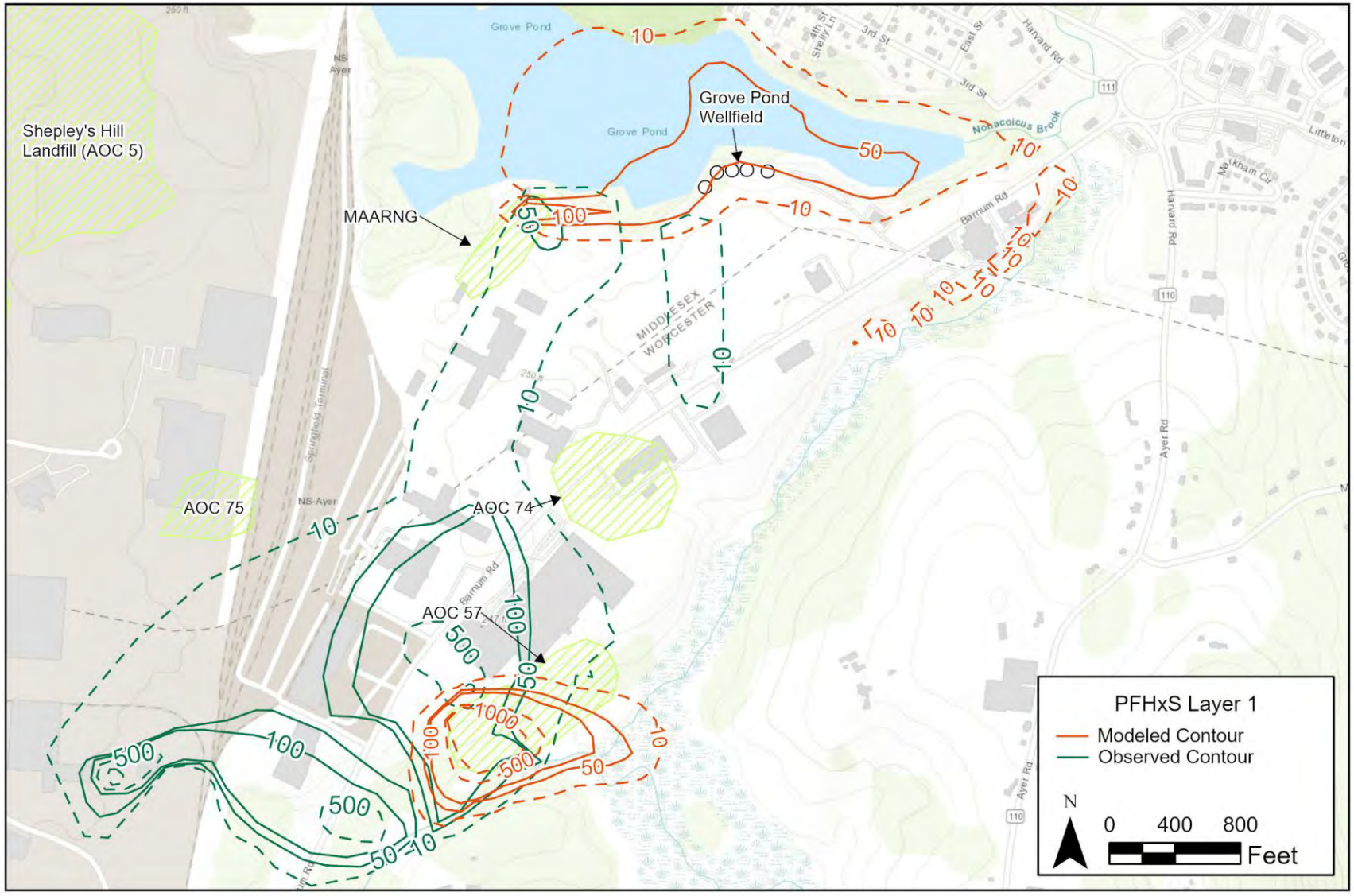

Grove Pond
Grove Pond Wellfield
Shepley's Hill Landfill (AOC 5)
MAARNG
AOC 75
AOC 74
AOC 57
NS-Ayer
Barnum Rd
Nonacoicus Brook
Ayer Rd
Harvard Rd
PFOA Layer 3
Modeled Contour
Observed Contour
N
0 400 800
Feet

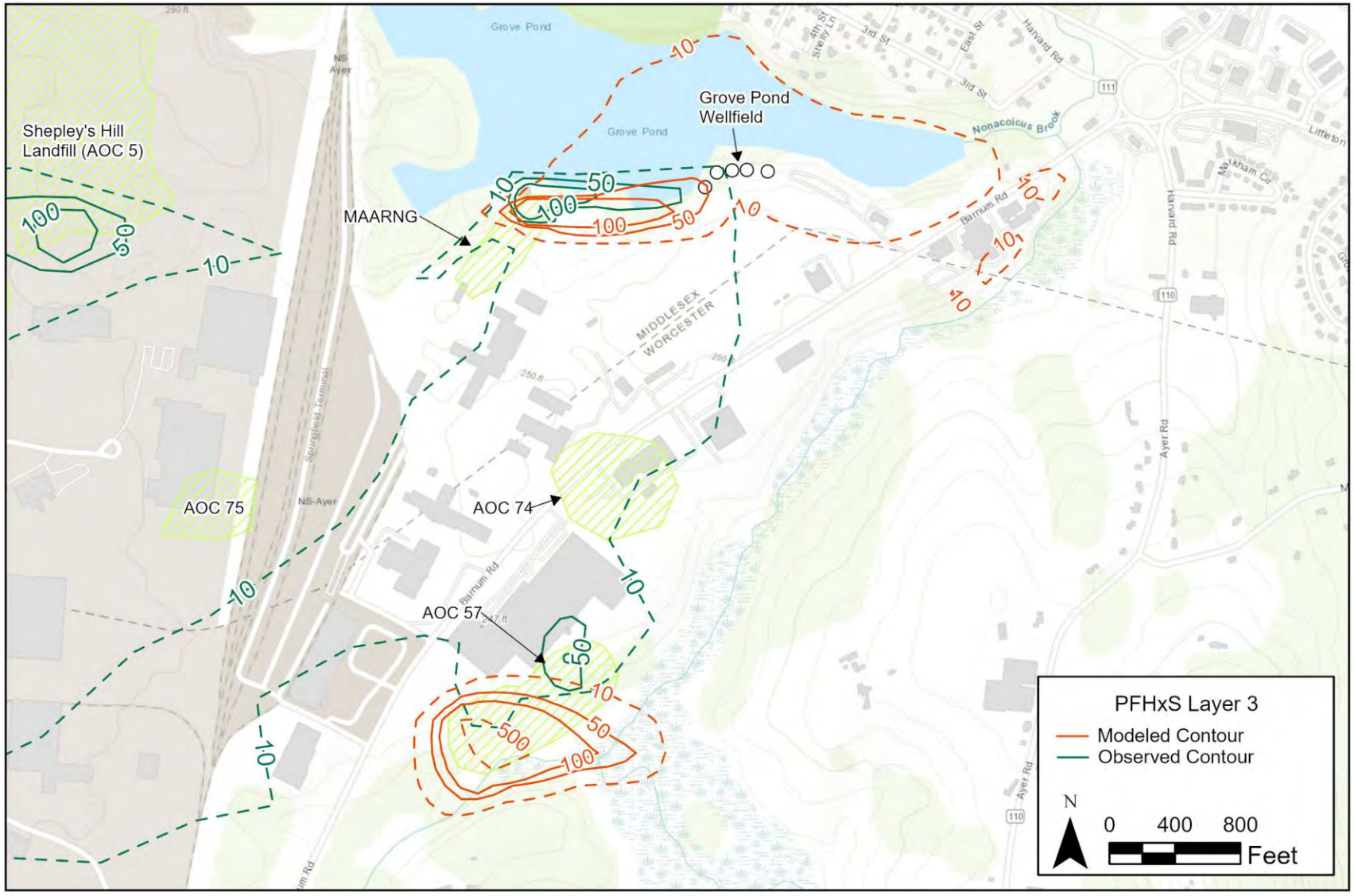

Grove Pond
Grove Pond Wellfield
Shepley's Hill Landfill (AOC 5)
MAARNG
AOC 75
AOC 74
AOC 57
NS-Ayer
Springfield Terminal
Barnum Rd
Ayer Rd
Harvard Rd
Nonacoicus Brook
MIDDLESEX
WORCESTER
100
50
10
PFOA Layer 4
Modeled Contour
Observed Contour
N
0
400
800
Feet

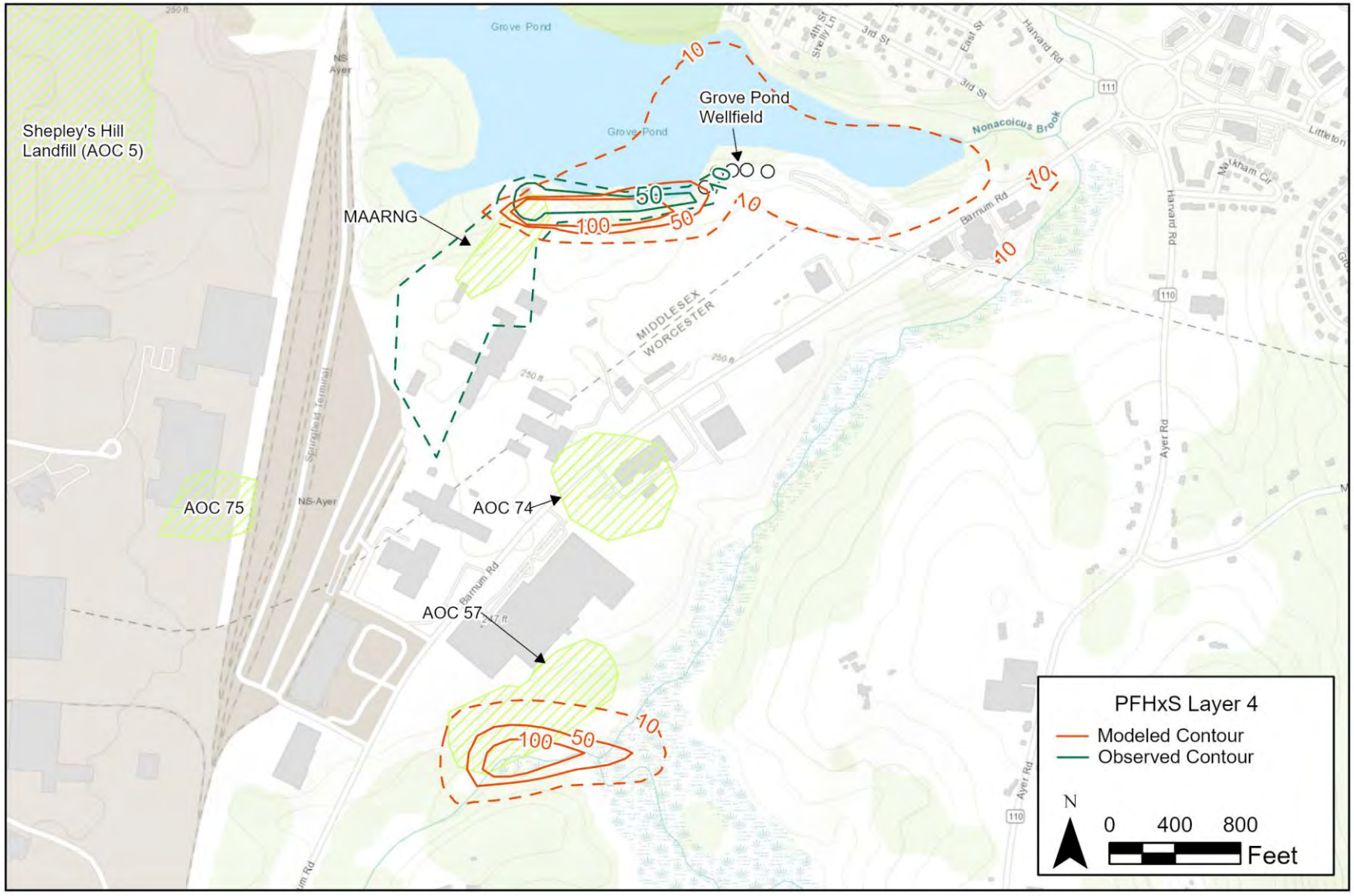

Grove Pond
Grove Pond Wellfield
Shepley's Hill Landfill (AOC 5)
MAARNG
AOC 75
AOC 74
AOC 57
MIDDLESEX
WORCESTER
Nonacoicus Brook
Barnum Rd
Harvard Rd
Ayer Rd
Springfield Terminal
NS-Ayer
PFHpA Layer 1
Modeled Contour
Observed Contour
N
0 400 800
Feet

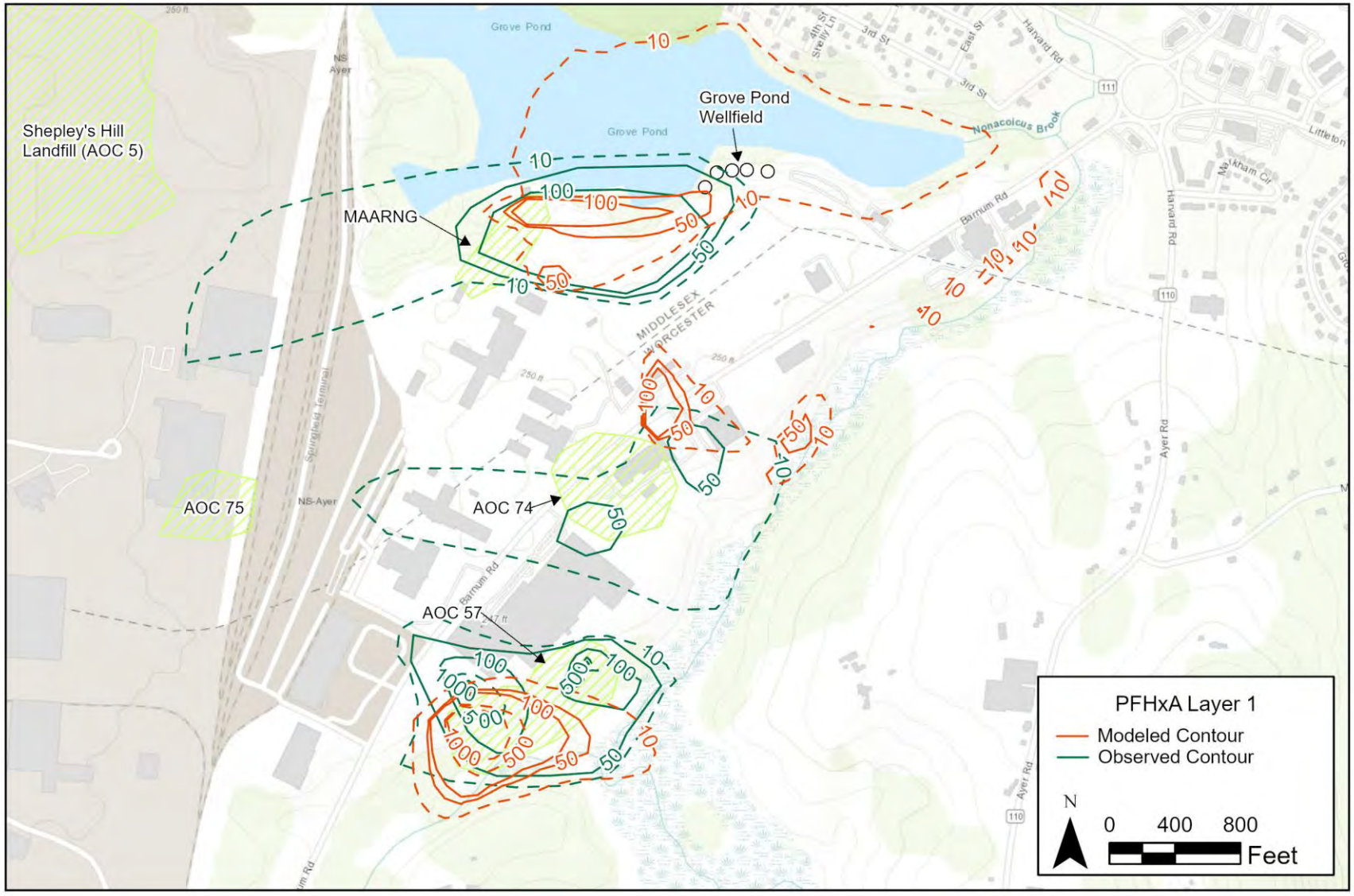

Grove Pond
Grove Pond Wellfield
Shepley's Hill Landfill (AOC 5)
MAARNG
AOC 75
AOC 74
AOC 57
NS-Ayer
Springfield Terminal
Barnum Rd
Nonacoicus Brook
Harvard Rd
Ayer Rd
PFHpA Layer 3
Modeled Contour
Observed Contour
N
0 400 800
Feet

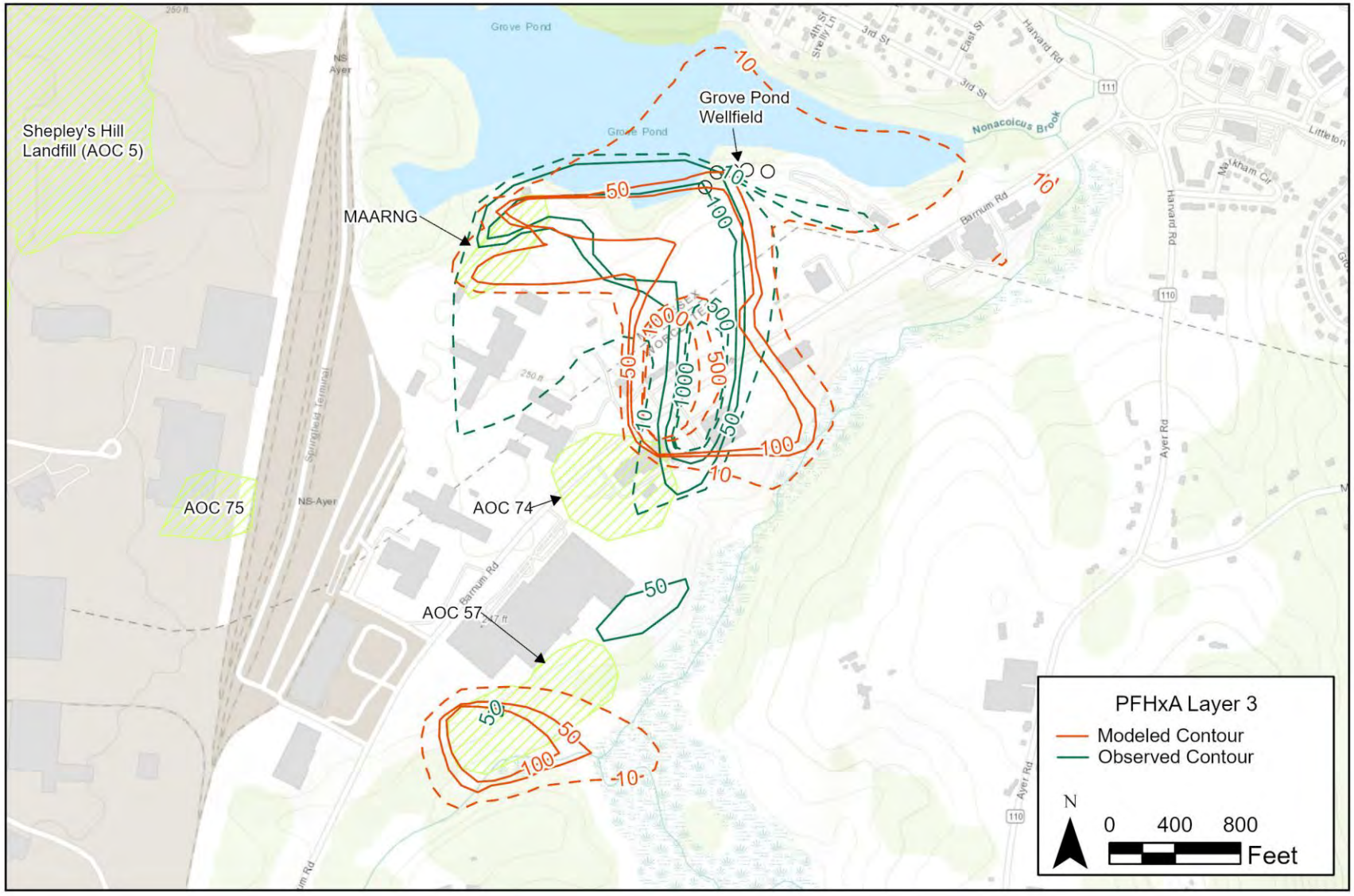

Grove Pond
Grove Pond Wellfield
Shepley's Hill Landfill (AOC 5)
MAARNG
AOC 75
AOC 74
AOC 57
NS-Ayer
Springfield Terminal
Barnum Rd
Nonacoicus Brook
Harvard Rd
Ayer Rd
100
50
10
PFHpA Layer 4
Modeled Contour
Observed Contour
N
0
400
800
Feet

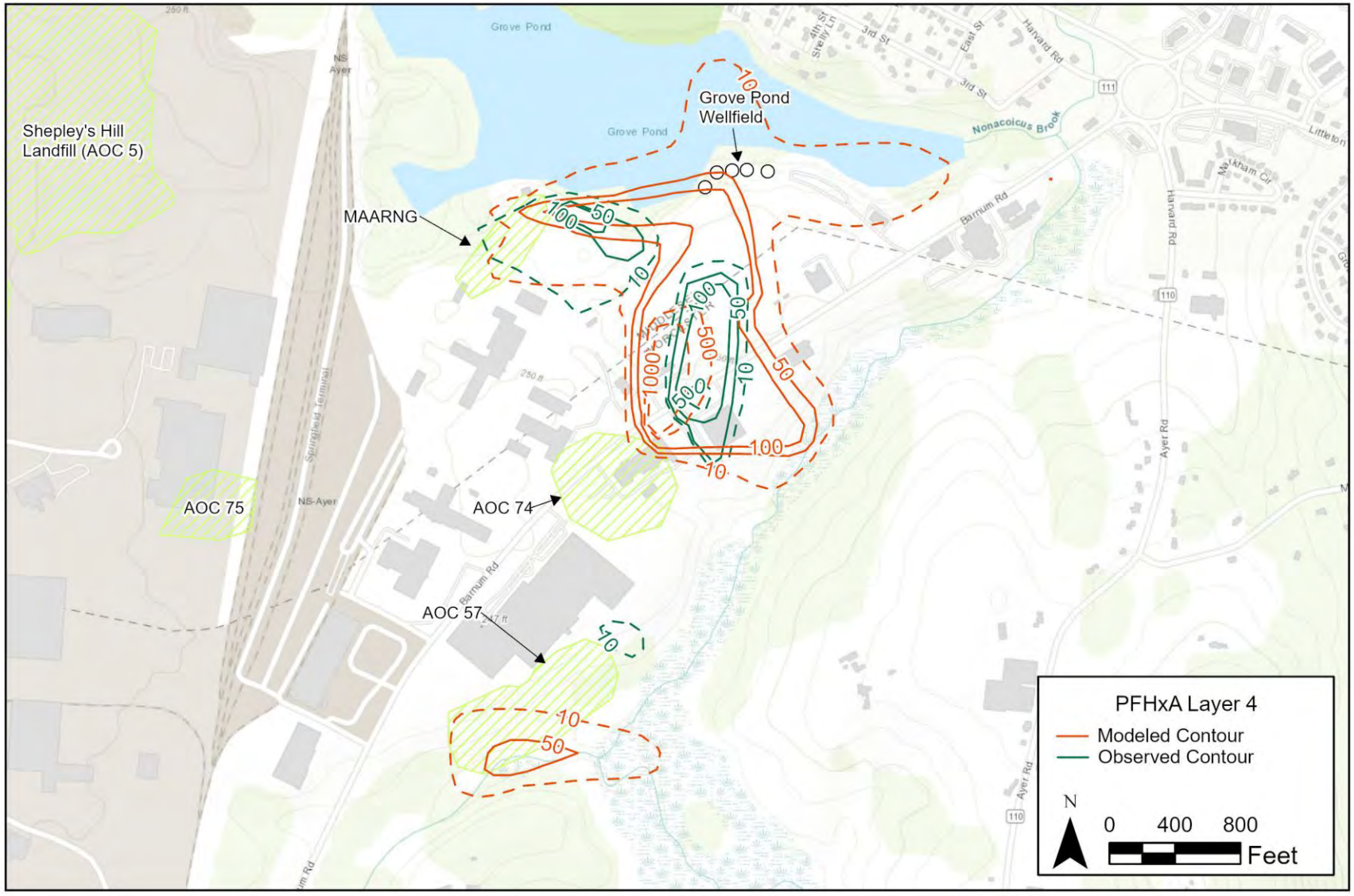

Grove Pond
Grove Pond Wellfield
Shepley's Hill Landfill (AOC 5)
MAARNG
AOC 75
AOC 74
AOC 57
NS-Ayer
Springfield Terminal
Barnum Rd
Ayer Rd
Harvard Rd
Nonacoicus Brook
MIDDLESEX WORCESTER
PFHxS Layer 1
Modeled Contour
Observed Contour
N
0 400 800
Feet


Grove Pond
Grove Pond Wellfield
Shepley's Hill Landfill (AOC 5)
MAARNG
AOC 75
AOC 74
AOC 57
NS-Ayer
Springfield Terminal
Barnum Rd
Ayer Rd
Harvard Rd
Nonacoicus Brook
MIDDLESEX WORCESTER
PFHxS Layer 3
Modeled Contour
Observed Contour
N
0 400 800
Feet

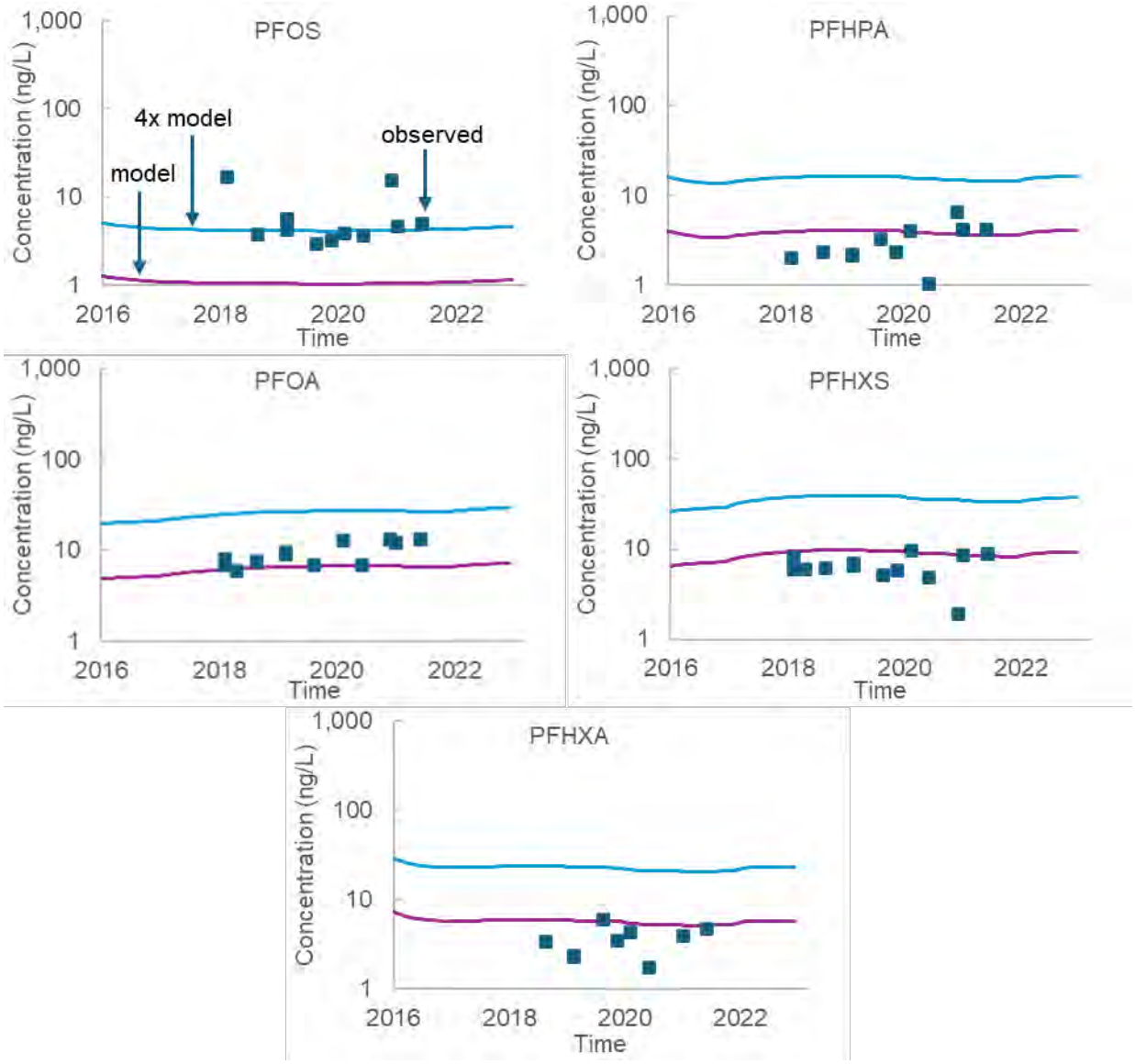

Grove Pond
Grove Pond Wellfield
Shepley's Hill Landfill (AOC 5)
MAARNG
AOC 75
AOC 74
AOC 57
NS-Ayer
Springfield Terminal
MIDDLESEX WORCESTER
Barnum Rd
Ayer Rd
Harvard Rd
Nonacoicus Brook
10
50
100
PFHxS Layer 4
Modeled Contour
Observed Contour
N
0
400
800
Feet


Grove Pond
Grove Pond Wellfield
Shepley's Hill Landfill (AOC 5)
MAARNG
AOC 75
AOC 74
AOC 57
NS-Ayer
Springfield Terminal
Barnum Rd
Nonacoicus Brook
Harvard Rd
Ayer Rd
MIDDLESEX
WORCESTER
PFHxA Layer 1
Modeled Contour
Observed Contour
N
0
400
800
Feet

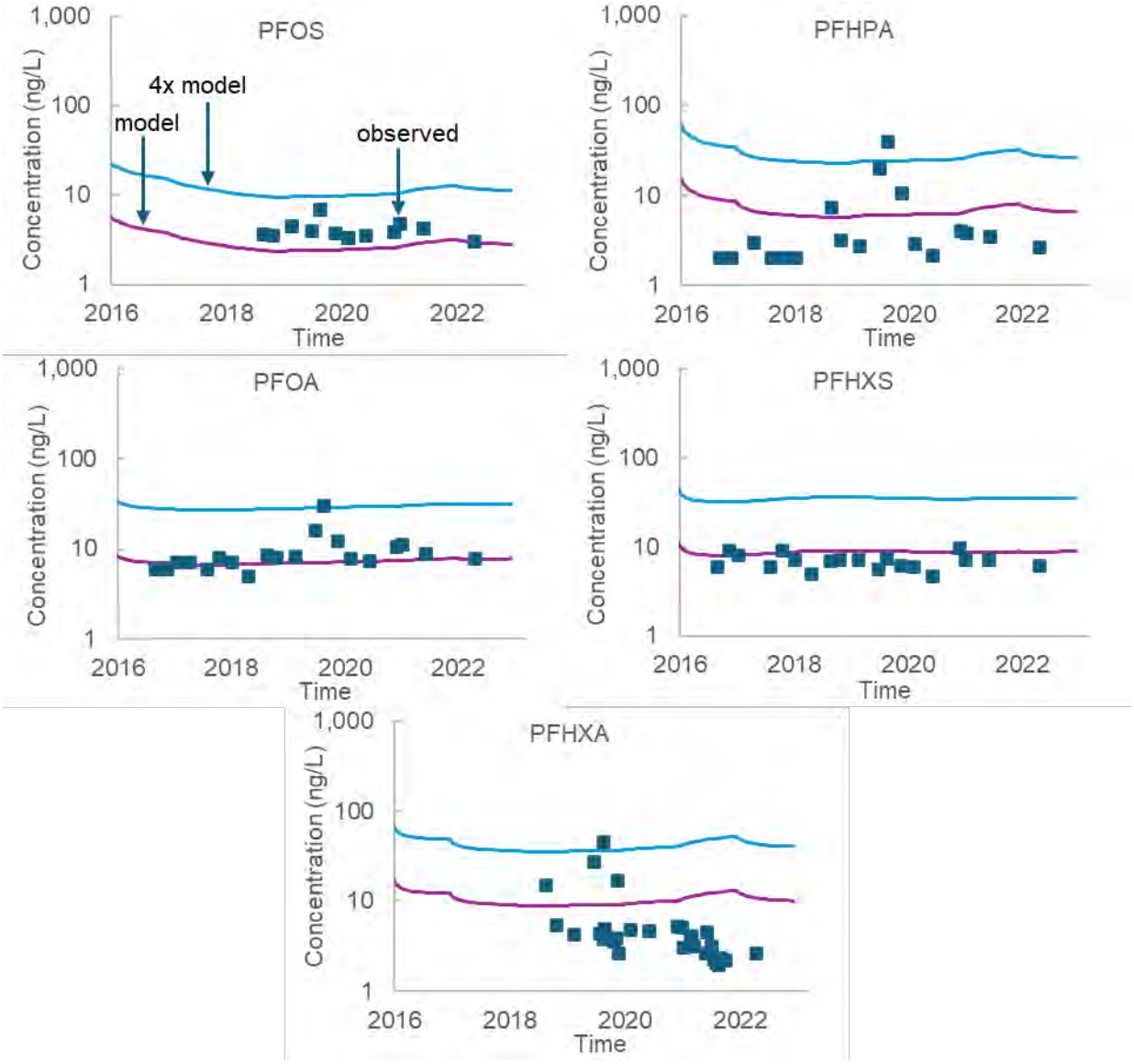

Shepley's Hill
Landfill (AOC 5)
Grove Pond
Grove Pond
Wellfield
MAARNG
AOC 75
AOC 74
AOC 57
NS-Ayer
Springfield Terminal
Barnum Rd
Nonacoicus Brook
Harvard Rd
Ayer Rd
PFHxA Layer 3
Modeled Contour
Observed Contour
N
0
400
800
Feet


Grove Pond
Grove Pond Wellfield
Shepley's Hill Landfill (AOC 5)
MAARNG
AOC 75
AOC 74
AOC 57
NS-Ayer
Springfield Terminal
Barnum Rd
Nonacoicus Brook
Harvard Rd
Ayer Rd
PFHxA Layer 4
Modeled Contour
Observed Contour
N
0
400
800
Feet

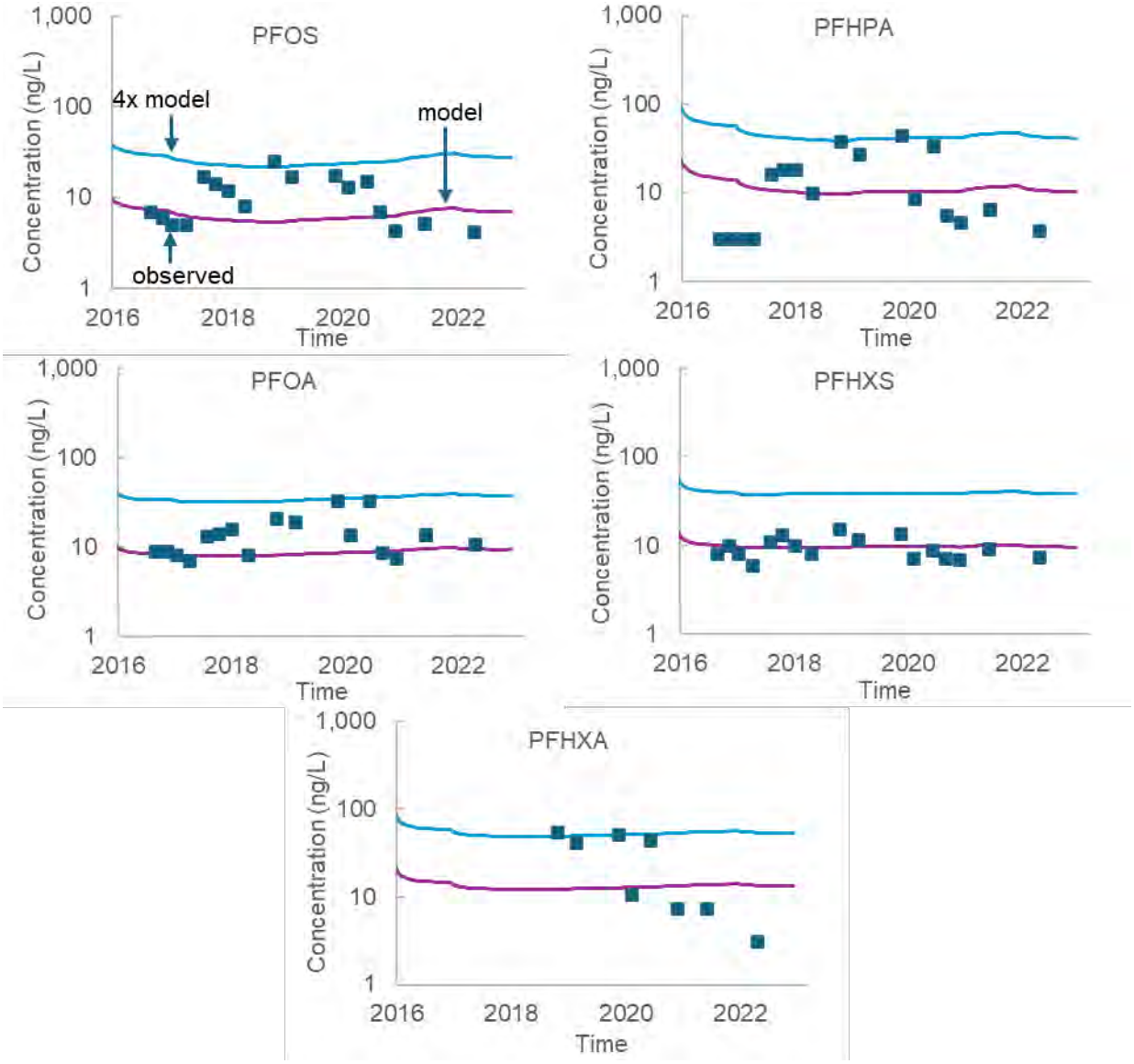
# Attachment 5: Observed and Modeled PFAS Concentrations at Grove Pond Wellfield Wells




***Modeled and Observed PFAS Concentrations at GP-01 (2016-2022)***




***Modeled and Observed PFAS Concentrations at GP-06 (2016-2022)***




***Modeled and Observed PFAS Concentrations at GP-07 (2016-2022)***

# Attachment 6: Estimated PFAS Concentrations at Grove Pond Wellfield

***Table 1: Grove Pond Well 1 Lower Estimate of PFAS Concentrations***

*Annual PFAS Concentration (ng/L)*

| *Year** | *PFOS* | *PFOA* | *PFHXS* | *PFHXA* | *PFHPA* |
|---|---|---|---|---|---|
| 1999 | 0.3 | 1.1 | 2.4 | 2.6 | 4.5 |
| 2000 | 0.3 | 1.2 | 2.2 | 2.0 | 3.6 |
| 2001 | 0.3 | 1.4 | 3.0 | 2.4 | 3.5 |
| 2002 | 0.3 | 1.9 | 4.4 | 3.1 | 3.8 |
| 2003 | 0.4 | 2.7 | 5.7 | 4.0 | 4.2 |
| 2004 | 0.5 | 3.0 | 6.3 | 4.5 | 4.5 |
| 2005 | 0.5 | 3.2 | 6.1 | 4.3 | 4.4 |
| 2006 | 0.6 | 3.4 | 5.7 | 4.3 | 4.4 |
| 2007 | 0.6 | 4.1 | 6.6 | 5.9 | 5.6 |
| 2008 | 0.9 | 4.4 | 6.7 | 6.3 | 5.7 |
| 2009 | 1.1 | 4.5 | 6.6 | 6.5 | 5.7 |
| 2010 | 1.2 | 3.8 | 5.0 | 4.2 | 3.4 |
| 2011 | 1.0 | 4.9 | 7.3 | 7.6 | 6.2 |
| 2012 | 1.4 | 5.3 | 7.8 | 8.0 | 6.5 |
| 2013 | 1.6 | 5.0 | 6.5 | 7.5 | 4.8 |
| 2014 | 1.4 | 4.9 | 6.4 | 7.5 | 4.0 |
| 2015 | 1.3 | 5.2 | 7.4 | 5.7 | 3.4 |
| 2016 | 1.1 | 6.1 | 9.3 | 5.9 | 4.0 |
| 2017 | 1.1 | 6.6 | 9.8 | 5.8 | 4.1 |
| 2018 | 1.0 | 6.8 | 9.4 | 5.6 | 4.0 |
| 2019 | 1.0 | 6.8 | 8.7 | 5.2 | 3.7 |
| 2020 | 1.1 | 6.7 | 8.4 | 5.4 | 3.7 |
| 2021 | 1.1 | 7.2 | 9.3 | 5.7 | 4.1 |
| 2022 | 1.1 | 7.3 | 9.3 | 5.7 | 4.1 |

** Estimated concentrations shown in this table are model outputs reported within the last five days of each calendar year (e.g., 1999 is the model result on 12/31/1999).*

***Table 2: Grove Pond Well 2 Lower Estimate of PFAS Concentrations***

| | *Annual PFAS Concentration (ng/L)* | | | | |
|---|---|---|---|---|---|
| *Year** | *PFOS* | *PFOA* | *PFHXS* | *PFHXA* | *PFHPA* |
| 1999 | 0.8 | 2.6 | 3.5 | 6.1 | 11.5 |
| 2000 | 0.8 | 2.6 | 3.3 | 5.2 | 10.3 |
| 2001 | 0.9 | 2.6 | 3.1 | 4.3 | 9.0 |
| 2002 | 1.0 | 2.8 | 3.7 | 4.2 | 8.4 |
| 2003 | 1.3 | 3.5 | 4.9 | 4.9 | 8.2 |
| 2004 | 1.5 | 4.2 | 6.4 | 6.5 | 8.3 |
| 2005 | 1.6 | 4.5 | 7.1 | 7.4 | 8.6 |
| 2006 | 1.7 | 4.7 | 6.9 | 7.6 | 8.6 |
| 2007 | 1.9 | 5.0 | 6.9 | 8.0 | 8.6 |
| 2008 | 2.0 | 5.3 | 8.7 | 10.0 | 9.5 |
| 2009 | 2.0 | 5.4 | 9.1 | 10.5 | 9.6 |
| 2010 | 2.1 | 5.6 | 8.6 | 10.7 | 9.7 |
| 2011 | 2.3 | 5.1 | 6.3 | 8.6 | 7.3 |
| 2012 | 2.6 | 6.1 | 9.5 | 11.4 | 10.4 |
| 2013 | 2.7 | 6.5 | 10.0 | 12.0 | 10.9 |
| 2014 | 3.3 | 6.6 | 8.6 | 14.1 | 11.0 |
| 2015 | 3.6 | 6.5 | 7.6 | 13.9 | 9.6 |
| 2016 | 2.3 | 5.5 | 6.7 | 9.2 | 4.8 |
| 2017 | 1.7 | 6.0 | 8.4 | 7.1 | 4.2 |
| 2018 | 1.5 | 6.3 | 8.7 | 6.7 | 4.2 |
| 2019 | 1.3 | 6.3 | 8.4 | 6.7 | 4.1 |
| 2020 | 1.3 | 6.2 | 7.6 | 7.4 | 4.0 |
| 2021 | 1.4 | 6.2 | 7.5 | 9.5 | 4.9 |
| 2022 | 1.4 | 6.8 | 8.4 | 7.4 | 4.5 |

** Estimated concentrations shown in this table are model outputs reported within the last five days of each calendar year (e.g., 1999 is the model result on 12/31/1999).*

***Table 3: Grove Pond Well 6 Lower Estimate of PFAS Concentrations***

| | *Annual PFAS Concentration (ng/L)* | | | | |
|---|---|---|---|---|---|
| *Year** | *PFOS* | *PFOA* | *PFHXS* | *PFHXA* | *PFHPA* |
| 1999 | 1.3 | 3.7 | 4.3 | 7.6 | 15.0 |
| 2000 | 1.4 | 3.8 | 4.1 | 6.5 | 13.6 |
| 2001 | 1.5 | 4.1 | 4.5 | 6.2 | 12.6 |
| 2002 | 1.7 | 4.7 | 5.7 | 7.0 | 11.9 |
| 2003 | 2.1 | 5.4 | 7.5 | 9.3 | 11.8 |
| 2004 | 2.5 | 5.7 | 8.2 | 10.4 | 12.1 |
| 2005 | 2.6 | 5.9 | 8.3 | 11.1 | 12.2 |
| 2006 | 2.8 | 6.1 | 8.5 | 12.0 | 12.3 |
| 2007 | 3.0 | 6.1 | 10.0 | 13.2 | 12.4 |
| 2008 | 2.9 | 6.2 | 10.6 | 13.8 | 12.5 |
| 2009 | 2.8 | 6.4 | 10.7 | 14.6 | 13.0 |
| 2010 | 2.9 | 6.6 | 8.7 | 14.1 | 12.7 |
| 2011 | 3.7 | 7.0 | 11.3 | 14.5 | 13.8 |
| 2012 | 3.7 | 7.3 | 11.7 | 14.5 | 14.1 |
| 2013 | 3.7 | 8.1 | 11.5 | 18.3 | 16.7 |
| 2014 | 4.8 | 8.3 | 10.4 | 16.9 | 15.4 |
| 2015 | 5.6 | 6.8 | 8.0 | 11.6 | 8.2 |
| 2016 | 3.7 | 6.7 | 8.7 | 9.1 | 6.0 |
| 2017 | 2.7 | 6.9 | 9.0 | 8.8 | 5.8 |
| 2018 | 2.4 | 7.1 | 8.8 | 9.2 | 6.1 |
| 2019 | 2.4 | 7.4 | 8.6 | 10.3 | 6.5 |
| 2020 | 2.6 | 7.8 | 8.7 | 12.5 | 7.8 |
| 2021 | 3.1 | 7.7 | 8.8 | 10.1 | 6.6 |
| 2022 | 2.8 | 7.8 | 8.8 | 10.1 | 6.5 |

** Estimated concentrations shown in this table are model outputs reported within the last five days of each calendar year (e.g., 1999 is the model result on 12/31/1999).*

***Table 4: Grove Pond Well 7 Lower Estimate of PFAS Concentrations***

| | *Annual PFAS Concentration (ng/L)* | | | | |
|---|---|---|---|---|---|
| *Year** | *PFOS* | *PFOA* | *PFHXS* | *PFHXA* | *PFHPA* |
| 1999 | 2.4 | 5.6 | 5.5 | 9.9 | 20.6 |
| 2000 | 2.6 | 5.7 | 5.0 | 8.4 | 18.6 |
| 2001 | 2.9 | 5.9 | 5.0 | 8.0 | 17.4 |
| 2002 | 3.3 | 6.3 | 6.0 | 9.2 | 16.4 |
| 2003 | 3.8 | 6.8 | 8.2 | 12.6 | 16.3 |
| 2004 | 4.4 | 7.0 | 9.3 | 14.6 | 16.9 |
| 2005 | 4.6 | 7.3 | 9.7 | 15.9 | 17.3 |
| 2006 | 4.9 | 7.6 | 10.2 | 17.4 | 17.6 |
| 2007 | 5.3 | 7.5 | 11.7 | 18.8 | 17.8 |
| 2008 | 5.3 | 7.4 | 12.8 | 19.8 | 18.1 |
| 2009 | 5.2 | 7.5 | 13.5 | 20.9 | 18.8 |
| 2010 | 5.3 | 8.5 | 12.4 | 21.9 | 20.2 |
| 2011 | 6.9 | 8.3 | 14.0 | 20.8 | 20.3 |
| 2012 | 6.6 | 8.4 | 14.3 | 19.6 | 20.2 |
| 2013 | 6.5 | 9.5 | 15.1 | 24.7 | 24.1 |
| 2014 | 8.1 | 9.9 | 13.3 | 20.9 | 22.2 |
| 2015 | 9.4 | 8.3 | 9.8 | 13.8 | 13.3 |
| 2016 | 7.0 | 8.0 | 9.6 | 12.2 | 10.3 |
| 2017 | 5.7 | 8.2 | 9.7 | 12.2 | 9.8 |
| 2018 | 5.4 | 8.7 | 9.7 | 12.8 | 10.4 |
| 2019 | 5.9 | 9.1 | 9.8 | 13.3 | 10.7 |
| 2020 | 6.4 | 9.8 | 10.1 | 14.0 | 11.6 |
| 2021 | 7.6 | 9.5 | 9.7 | 13.2 | 10.4 |
| 2022 | 7.0 | 9.5 | 9.6 | 13.2 | 10.3 |

** Estimated concentrations shown in this table are model outputs reported within the last five days of each calendar year (e.g., 1999 is the model result on 12/31/1999).*

***Table 5: Grove Pond Well 8 Lower Estimate of PFAS Concentrations***

*Annual PFAS Concentration (ng/L)*

| *Year** | *PFOS* | *PFOA* | *PFHXS* | *PFHXA* | *PFHPA* |
|---|---|---|---|---|---|
| 1999 | 5.0 | 7.7 | 4.5 | 8.2 | 20.3 |
| 2000 | 5.3 | 8.0 | 3.8 | 6.8 | 19.0 |
| 2001 | 5.9 | 8.4 | 3.6 | 6.4 | 18.4 |
| 2002 | 6.6 | 9.0 | 4.5 | 8.2 | 18.2 |
| 2003 | 7.8 | 9.6 | 7.3 | 13.3 | 19.0 |
| 2004 | 9.1 | 9.9 | 8.5 | 15.7 | 19.9 |
| 2005 | 9.6 | 10.1 | 9.0 | 16.8 | 19.8 |
| 2006 | 10.0 | 10.2 | 9.7 | 18.2 | 19.8 |
| 2007 | 10.6 | 10.4 | 11.3 | 20.6 | 20.8 |
| 2008 | 11.0 | 10.6 | 13.2 | 23.2 | 22.0 |
| 2009 | 11.5 | 10.9 | 14.8 | 25.2 | 23.5 |
| 2010 | 12.1 | 11.1 | 13.4 | 23.8 | 23.1 |
| 2011 | 13.4 | 11.5 | 16.7 | 27.4 | 26.3 |
| 2012 | 14.2 | 12.0 | 18.6 | 29.1 | 28.8 |
| 2013 | 15.2 | 12.6 | 18.5 | 31.0 | 30.6 |
| 2014 | 16.7 | 13.1 | 17.7 | 30.0 | 30.9 |
| 2015 | 18.7 | 12.1 | 14.4 | 24.6 | 26.0 |
| 2016 | 18.4 | 11.6 | 12.9 | 23.1 | 23.7 |
| 2017 | 17.6 | 11.9 | 12.5 | 23.2 | 23.2 |
| 2018 | 17.8 | 12.5 | 12.6 | 23.7 | 23.8 |
| 2019 | 19.2 | 13.2 | 12.7 | 23.2 | 23.7 |
| 2020 | 20.5 | 14.2 | 13.3 | 23.1 | 24.4 |
| 2021 | 22.6 | 14.0 | 12.5 | 23.4 | 23.6 |
| 2022 | 22.5 | 14.0 | 12.4 | 23.4 | 23.5 |

** Estimated concentrations shown in this table are model outputs reported within the last five days of each calendar year (e.g., 1999 is the model result on 12/31/1999).*

***Table 6: Grove Pond Well 1 Upper Estimate of PFAS Concentrations***

*Annual PFAS Concentration (ng/L)*

| *Year** | *PFOS* | *PFOA* | *PFHXS* | *PFHXA* | *PFHPA* |
|---|---|---|---|---|---|
| 1999 | 1.0 | 4.6 | 9.6 | 10.2 | 18.0 |
| 2000 | 1.0 | 4.6 | 8.8 | 8.1 | 14.6 |
| 2001 | 1.1 | 5.5 | 12.0 | 9.5 | 14.2 |
| 2002 | 1.2 | 7.8 | 17.6 | 12.4 | 15.1 |
| 2003 | 1.5 | 10.9 | 22.8 | 16.0 | 16.7 |
| 2004 | 2.0 | 12.3 | 25.3 | 18.0 | 18.0 |
| 2005 | 2.2 | 12.9 | 24.2 | 17.3 | 17.7 |
| 2006 | 2.3 | 13.8 | 22.9 | 17.1 | 17.5 |
| 2007 | 2.6 | 16.5 | 26.4 | 23.7 | 22.4 |
| 2008 | 3.6 | 17.7 | 26.7 | 25.2 | 23.0 |
| 2009 | 4.3 | 18.3 | 26.5 | 26.0 | 23.0 |
| 2010 | 4.7 | 15.2 | 19.9 | 16.6 | 13.7 |
| 2011 | 4.0 | 19.8 | 29.2 | 30.3 | 24.7 |
| 2012 | 5.5 | 21.5 | 31.2 | 32.1 | 26.0 |
| 2013 | 6.3 | 20.0 | 25.8 | 30.1 | 19.1 |
| 2014 | 5.6 | 19.6 | 25.5 | 29.9 | 16.2 |
| 2015 | 5.1 | 21.2 | 29.5 | 22.9 | 13.7 |
| 2016 | 4.4 | 24.6 | 37.3 | 23.6 | 15.8 |
| 2017 | 4.2 | 26.8 | 39.1 | 23.4 | 16.5 |
| 2018 | 4.2 | 27.4 | 37.8 | 22.3 | 16.1 |
| 2019 | 4.1 | 27.4 | 34.6 | 20.7 | 15.0 |
| 2020 | 4.2 | 27.0 | 33.4 | 21.8 | 14.7 |
| 2021 | 4.3 | 29.4 | 37.1 | 23.0 | 16.3 |
| 2022 | 4.6 | 29.6 | 37.2 | 23.0 | 16.4 |

** Estimated concentrations shown in this table are model outputs reported within the last five days of each calendar year (e.g., 1999 is the model result on 12/31/1999).*

***Table 7: Grove Pond Well 2 Upper Estimate of PFAS Concentrations***

| | *Annual PFAS Concentration (ng/L)* | | | | |
|---|---|---|---|---|---|
| *Year** | *PFOS* | *PFOA* | *PFHXS* | *PFHXA* | *PFHPA* |
| 1999 | 3.2 | 10.5 | 14.0 | 24.3 | 46.2 |
| 2000 | 3.4 | 10.3 | 13.4 | 20.9 | 41.4 |
| 2001 | 3.7 | 10.4 | 12.4 | 17.1 | 35.9 |
| 2002 | 4.1 | 11.4 | 14.7 | 17.0 | 33.6 |
| 2003 | 5.1 | 13.9 | 19.7 | 19.8 | 32.6 |
| 2004 | 6.1 | 17 | 25.7 | 26.2 | 33.2 |
| 2005 | 6.5 | 18.2 | 28.3 | 29.5 | 34.4 |
| 2006 | 6.9 | 19.1 | 27.8 | 30.2 | 34.3 |
| 2007 | 7.5 | 20.0 | 27.8 | 32.2 | 34.2 |
| 2008 | 7.9 | 21.4 | 34.8 | 40.0 | 37.8 |
| 2009 | 8.1 | 21.9 | 36.2 | 41.9 | 38.2 |
| 2010 | 8.5 | 22.5 | 34.5 | 43.0 | 38.7 |
| 2011 | 9.3 | 20.4 | 25.2 | 34.3 | 29.3 |
| 2012 | 10.4 | 24.6 | 38.1 | 45.6 | 41.6 |
| 2013 | 11 | 26.0 | 40.0 | 48.0 | 43.6 |
| 2014 | 13.3 | 26.7 | 34.4 | 56.3 | 44.1 |
| 2015 | 14.3 | 26.2 | 30.3 | 55.6 | 38.3 |
| 2016 | 9.3 | 22.3 | 26.6 | 36.7 | 19.4 |
| 2017 | 6.8 | 24.2 | 33.8 | 28.2 | 16.9 |
| 2018 | 5.8 | 25.5 | 35.0 | 26.9 | 16.7 |
| 2019 | 5.4 | 25.5 | 33.5 | 26.6 | 16.3 |
| 2020 | 5.3 | 25.2 | 30.5 | 29.5 | 16.1 |
| 2021 | 5.7 | 25.3 | 30.0 | 37.9 | 19.5 |
| 2022 | 5.7 | 27.4 | 33.4 | 29.8 | 17.9 |

** Estimated concentrations shown in this table are model outputs reported within the last five days of each calendar year (e.g., 1999 is the model result on 12/31/1999).*

***Table 8: Grove Pond Well 6 Upper Estimate of PFAS Concentrations***

| | *Annual PFAS Concentration (ng/L)* | | | | |
|---|---|---|---|---|---|
| *Year** | *PFOS* | *PFOA* | *PFHXS* | *PFHXA* | *PFHPA* |
| 1999 | 5.1 | 14.7 | 17.1 | 30.2 | 59.9 |
| 2000 | 5.4 | 15.2 | 16.5 | 26.1 | 54.2 |
| 2001 | 6.0 | 16.3 | 18.1 | 24.8 | 50.6 |
| 2002 | 6.9 | 18.7 | 22.8 | 28.1 | 47.6 |
| 2003 | 8.3 | 21.6 | 29.9 | 37.0 | 47.0 |
| 2004 | 9.9 | 22.7 | 33.0 | 41.5 | 48.3 |
| 2005 | 10.4 | 23.7 | 33.2 | 44.3 | 48.9 |
| 2006 | 11.1 | 24.6 | 33.9 | 47.9 | 49.3 |
| 2007 | 11.9 | 24.7 | 40.2 | 52.7 | 49.5 |
| 2008 | 11.6 | 24.9 | 42.6 | 55.1 | 50.0 |
| 2009 | 11.3 | 25.6 | 42.7 | 58.3 | 52.1 |
| 2010 | 11.6 | 26.7 | 35.0 | 56.6 | 50.9 |
| 2011 | 15.0 | 28.2 | 45.0 | 57.9 | 55.2 |
| 2012 | 14.7 | 29.2 | 46.9 | 57.8 | 56.3 |
| 2013 | 14.7 | 32.4 | 46.1 | 73.2 | 66.8 |
| 2014 | 19.2 | 33.4 | 41.7 | 67.4 | 61.7 |
| 2015 | 22.3 | 27.6 | 31.9 | 46.4 | 32.7 |
| 2016 | 15.0 | 27.0 | 34.9 | 36.4 | 24.0 |
| 2017 | 10.8 | 28.0 | 35.8 | 35.4 | 23.1 |
| 2018 | 9.4 | 28.9 | 35.3 | 36.9 | 24.4 |
| 2019 | 9.8 | 29.9 | 34.2 | 41.4 | 26.0 |
| 2020 | 10.5 | 31.5 | 34.8 | 50.1 | 31.2 |
| 2021 | 12.6 | 31.3 | 35.2 | 40.6 | 26.3 |
| 2022 | 11.3 | 31.4 | 35.2 | 40.4 | 26.2 |

** Estimated concentrations shown in this table are model outputs reported within the last five days of each calendar year (e.g., 1999 is the model result on 12/31/1999).*

***Table 9: Grove Pond Well 7 Upper Estimate of PFAS Concentrations***

*Annual PFAS Concentration (ng/L)*

| *Year** | *PFOS* | *PFOA* | *PFHXS* | *PFHXA* | *PFHPA* |
|---|---|---|---|---|---|
| 1999 | 9.4 | 22.3 | 21.8 | 39.8 | 82.3 |
| 2000 | 10.2 | 22.9 | 19.9 | 33.8 | 74.2 |
| 2001 | 11.5 | 23.7 | 19.9 | 31.8 | 69.5 |
| 2002 | 13.0 | 25.2 | 23.9 | 36.9 | 65.7 |
| 2003 | 15.3 | 27.1 | 32.8 | 50.6 | 65.1 |
| 2004 | 17.7 | 28.2 | 37.2 | 58.2 | 67.7 |
| 2005 | 18.6 | 29.3 | 38.6 | 63.6 | 69.2 |
| 2006 | 19.8 | 30.3 | 40.8 | 69.6 | 70.5 |
| 2007 | 21.2 | 30.0 | 46.7 | 75.2 | 71.1 |
| 2008 | 21.1 | 29.8 | 51.2 | 79.1 | 72.2 |
| 2009 | 20.9 | 30.2 | 54.0 | 83.6 | 75.4 |
| 2010 | 21.1 | 34.1 | 49.6 | 87.7 | 80.8 |
| 2011 | 27.4 | 33.4 | 56.1 | 83.2 | 81.1 |
| 2012 | 26.5 | 33.5 | 57.1 | 78.5 | 80.8 |
| 2013 | 26.1 | 38.0 | 60.4 | 98.9 | 96.3 |
| 2014 | 32.3 | 39.8 | 53.2 | 83.5 | 88.7 |
| 2015 | 37.7 | 33.4 | 39.2 | 55.3 | 53.4 |
| 2016 | 28.1 | 32.1 | 38.4 | 48.6 | 41.1 |
| 2017 | 22.7 | 33.1 | 38.7 | 48.6 | 39.3 |
| 2018 | 21.7 | 34.9 | 38.8 | 51.1 | 41.4 |
| 2019 | 23.6 | 36.8 | 39.0 | 53.1 | 42.7 |
| 2020 | 25.7 | 39.4 | 40.3 | 55.9 | 46.3 |
| 2021 | 30.3 | 38.1 | 38.6 | 52.9 | 41.4 |
| 2022 | 27.8 | 38.2 | 38.6 | 52.9 | 41.3 |

** Estimated concentrations shown in this table are model outputs reported within the last five days of each calendar year (e.g., 1999 is the model result on 12/31/1999).*

***Table 10: Grove Pond Well 8 Upper Estimate of PFAS Concentrations***

*Annual PFAS Concentration (ng/L)*

| *Year** | *PFOS* | *PFOA* | *PFHXS* | *PFHXA* | *PFHPA* |
|---|---|---|---|---|---|
| 1999 | 19.9 | 31.0 | 17.8 | 32.8 | 81.3 |
| 2000 | 21.0 | 32.1 | 15.1 | 27.2 | 76.1 |
| 2001 | 23.4 | 33.5 | 14.4 | 25.8 | 73.6 |
| 2002 | 26.4 | 35.9 | 18.2 | 33.0 | 72.9 |
| 2003 | 31.2 | 38.6 | 29.1 | 53.3 | 76.1 |
| 2004 | 36.4 | 39.8 | 34.1 | 63.0 | 79.4 |
| 2005 | 38.2 | 40.3 | 35.9 | 67.3 | 79.1 |
| 2006 | 40.0 | 40.9 | 38.8 | 72.8 | 79.4 |
| 2007 | 42.3 | 41.6 | 45.1 | 82.4 | 83.1 |
| 2008 | 43.9 | 42.5 | 53.0 | 92.8 | 88.1 |
| 2009 | 46.1 | 43.5 | 59.4 | 100.9 | 93.9 |
| 2010 | 48.6 | 44.3 | 53.6 | 95.2 | 92.4 |
| 2011 | 53.7 | 46.0 | 66.7 | 109.6 | 105.1 |
| 2012 | 56.9 | 47.9 | 74.6 | 116.3 | 115.1 |
| 2013 | 60.6 | 50.4 | 74.2 | 124.0 | 122.5 |
| 2014 | 66.7 | 52.5 | 71.0 | 119.9 | 123.7 |
| 2015 | 74.7 | 48.3 | 57.5 | 98.2 | 104.1 |
| 2016 | 73.7 | 46.7 | 51.7 | 92.4 | 94.7 |
| 2017 | 70.5 | 47.5 | 50.0 | 92.7 | 93.0 |
| 2018 | 71.4 | 50.2 | 50.6 | 94.8 | 95.2 |
| 2019 | 76.7 | 53.0 | 50.9 | 92.6 | 94.9 |
| 2020 | 82.2 | 56.8 | 53.2 | 92.6 | 97.8 |
| 2021 | 90.3 | 56.0 | 49.8 | 93.6 | 94.3 |
| 2022 | 90.1 | 56.0 | 49.6 | 93.7 | 94.1 |

** Estimated concentrations shown in this table are model outputs reported within the last five days of each calendar year (e.g., 1999 is the model result on 12/31/1999).*

***Table 11: Grove Pond Well 1 Recommended Estimate of PFAS Concentrations***

| | *Annual PFAS Concentration (ng/L)* | | | | |
|---|---|---|---|---|---|
| *Year** | *PFOS* | *PFOA* | *PFHXS* | *PFHXA* | *PFHPA* |
| 1999 | 0.7 | 2.9 | 6.0 | 6.4 | 11.3 |
| 2000 | 0.7 | 2.9 | 5.5 | 5.1 | 9.1 |
| 2001 | 0.7 | 3.5 | 7.5 | 6.0 | 8.9 |
| 2002 | 0.8 | 4.9 | 11.0 | 7.8 | 9.5 |
| 2003 | 1.0 | 6.8 | 14.3 | 10.0 | 10.5 |
| 2004 | 1.3 | 7.7 | 15.8 | 11.3 | 11.3 |
| 2005 | 1.4 | 8.1 | 15.2 | 10.8 | 11.1 |
| 2006 | 1.5 | 8.6 | 14.3 | 10.7 | 11.0 |
| 2007 | 1.6 | 10.3 | 16.5 | 14.8 | 14.0 |
| 2008 | 2.3 | 11.1 | 16.7 | 15.8 | 14.4 |
| 2009 | 2.7 | 11.4 | 16.6 | 16.3 | 14.4 |
| 2010 | 3.0 | 9.5 | 12.5 | 10.4 | 8.6 |
| 2011 | 2.5 | 12.4 | 18.3 | 19.0 | 15.5 |
| 2012 | 3.5 | 13.4 | 19.5 | 20.1 | 16.3 |
| 2013 | 4.0 | 12.5 | 16.2 | 18.8 | 12.0 |
| 2014 | 3.5 | 12.3 | 16.0 | 18.7 | 10.1 |
| 2015 | 3.2 | 13.2 | 18.5 | 14.3 | 8.6 |
| 2016 | 2.8 | 15.4 | 23.3 | 14.8 | 9.9 |
| 2017 | 2.7 | 16.7 | 24.5 | 14.6 | 10.3 |
| 2018 | 2.6 | 17.1 | 23.6 | 14.0 | 10.1 |
| 2019 | 2.6 | 17.1 | 21.7 | 13.0 | 9.4 |
| 2020 | 2.7 | 16.9 | 20.9 | 13.6 | 9.2 |
| 2021 | 2.7 | 18.3 | 23.2 | 14.4 | 10.2 |
| 2022 | 2.9 | 18.5 | 23.3 | 14.4 | 10.3 |

** Estimated concentrations shown in this table are model outputs reported within the last five days of each calendar year (e.g., 1999 is the model result on 12/31/1999).*

***Table 12: Grove Pond Well 2 Recommended Estimate of PFAS Concentrations***

| | *Annual PFAS Concentration (ng/L)* | | | | |
|---|---|---|---|---|---|
| *Year** | *PFOS* | *PFOA* | *PFHXS* | *PFHXA* | *PFHPA* |
| 1999 | 2.0 | 6.6 | 8.8 | 15.2 | 28.9 |
| 2000 | 2.1 | 6.5 | 8.4 | 13.1 | 25.9 |
| 2001 | 2.3 | 6.5 | 7.8 | 10.7 | 22.5 |
| 2002 | 2.6 | 7.1 | 9.2 | 10.6 | 21.0 |
| 2003 | 3.2 | 8.7 | 12.3 | 12.4 | 20.4 |
| 2004 | 3.8 | 10.6 | 16.1 | 16.4 | 20.8 |
| 2005 | 4.1 | 11.4 | 17.7 | 18.5 | 21.5 |
| 2006 | 4.3 | 11.9 | 17.4 | 18.9 | 21.5 |
| 2007 | 4.7 | 12.5 | 17.4 | 20.1 | 21.4 |
| 2008 | 5.0 | 13.4 | 21.8 | 25.0 | 23.7 |
| 2009 | 5.1 | 13.7 | 22.7 | 26.2 | 23.9 |
| 2010 | 5.3 | 14.1 | 21.6 | 26.9 | 24.2 |
| 2011 | 5.8 | 12.8 | 15.8 | 21.5 | 18.3 |
| 2012 | 6.5 | 15.4 | 23.8 | 28.5 | 26.0 |
| 2013 | 6.9 | 16.3 | 25.0 | 30.0 | 27.3 |
| 2014 | 8.3 | 16.7 | 21.5 | 35.2 | 27.6 |
| 2015 | 9.0 | 16.4 | 19.0 | 34.8 | 24.0 |
| 2016 | 5.8 | 13.9 | 16.7 | 23.0 | 12.1 |
| 2017 | 4.3 | 15.1 | 21.1 | 17.7 | 10.6 |
| 2018 | 3.7 | 15.9 | 21.9 | 16.8 | 10.5 |
| 2019 | 3.4 | 15.9 | 21.0 | 16.7 | 10.2 |
| 2020 | 3.3 | 15.7 | 19.1 | 18.5 | 10.1 |
| 2021 | 3.6 | 15.8 | 18.8 | 23.7 | 12.2 |
| 2022 | 3.6 | 17.1 | 20.9 | 18.6 | 11.2 |

** Estimated concentrations shown in this table are model outputs reported within the last five days of each calendar year (e.g., 1999 is the model result on 12/31/1999).*

***Table 13: Grove Pond Well 6 Recommended Estimate of PFAS Concentrations***

| | *Annual PFAS Concentration (ng/L)* | | | | |
|---|---|---|---|---|---|
| *Year** | *PFOS* | *PFOA* | *PFHXS* | *PFHXA* | *PFHPA* |
| 1999 | 3.2 | 9.2 | 10.7 | 18.9 | 37.5 |
| 2000 | 3.4 | 9.5 | 10.3 | 16.3 | 33.9 |
| 2001 | 3.8 | 10.2 | 11.3 | 15.5 | 31.6 |
| 2002 | 4.3 | 11.7 | 14.3 | 17.6 | 29.8 |
| 2003 | 5.2 | 13.5 | 18.7 | 23.2 | 29.4 |
| 2004 | 6.2 | 14.2 | 20.6 | 26.0 | 30.2 |
| 2005 | 6.5 | 14.8 | 20.8 | 27.7 | 30.6 |
| 2006 | 7.0 | 15.4 | 21.2 | 30.0 | 30.8 |
| 2007 | 7.5 | 15.4 | 25.1 | 33.0 | 31.0 |
| 2008 | 7.3 | 15.6 | 26.6 | 34.5 | 31.3 |
| 2009 | 7.1 | 16.0 | 26.7 | 36.5 | 32.6 |
| 2010 | 7.3 | 16.7 | 21.9 | 35.4 | 31.8 |
| 2011 | 9.4 | 17.6 | 28.2 | 36.2 | 34.5 |
| 2012 | 9.2 | 18.3 | 29.3 | 36.2 | 35.2 |
| 2013 | 9.2 | 20.3 | 28.8 | 45.8 | 41.8 |
| 2014 | 12.0 | 20.9 | 26.1 | 42.2 | 38.6 |
| 2015 | 14.0 | 17.2 | 20.0 | 29.0 | 20.5 |
| 2016 | 9.4 | 16.9 | 21.8 | 22.8 | 15.0 |
| 2017 | 6.8 | 17.5 | 22.4 | 22.1 | 14.5 |
| 2018 | 5.9 | 18.0 | 22.1 | 23.1 | 15.3 |
| 2019 | 6.1 | 18.7 | 21.4 | 25.9 | 16.3 |
| 2020 | 6.6 | 19.7 | 21.8 | 31.3 | 19.5 |
| 2021 | 7.9 | 19.5 | 22.0 | 25.4 | 16.5 |
| 2022 | 7.1 | 19.6 | 22.0 | 25.3 | 16.4 |

** Estimated concentrations shown in this table are model outputs reported within the last five days of each calendar year (e.g., 1999 is the model result on 12/31/1999).*

***Table 14: Grove Pond Well 7 Recommended Estimate of PFAS Concentrations***

| | *Annual PFAS Concentration (ng/L)* | | | | |
|---|---|---|---|---|---|
| *Year** | *PFOS* | *PFOA* | *PFHXS* | *PFHXA* | *PFHPA* |
| 1999 | 5.9 | 14.0 | 13.7 | 24.9 | 51.5 |
| 2000 | 6.4 | 14.3 | 12.5 | 21.1 | 46.4 |
| 2001 | 7.2 | 14.8 | 12.5 | 19.9 | 43.5 |
| 2002 | 8.2 | 15.8 | 15.0 | 23.1 | 41.1 |
| 2003 | 9.6 | 17.0 | 20.5 | 31.6 | 40.7 |
| 2004 | 11.1 | 17.6 | 23.3 | 36.4 | 42.3 |
| 2005 | 11.6 | 18.3 | 24.2 | 39.8 | 43.3 |
| 2006 | 12.4 | 19.0 | 25.5 | 43.5 | 44.1 |
| 2007 | 13.3 | 18.8 | 29.2 | 47.0 | 44.5 |
| 2008 | 13.2 | 18.6 | 32.0 | 49.5 | 45.2 |
| 2009 | 13.1 | 18.9 | 33.8 | 52.3 | 47.1 |
| 2010 | 13.2 | 21.3 | 31.0 | 54.8 | 50.5 |
| 2011 | 17.2 | 20.9 | 35.1 | 52.0 | 50.7 |
| 2012 | 16.6 | 21.0 | 35.7 | 49.1 | 50.5 |
| 2013 | 16.3 | 23.8 | 37.8 | 61.8 | 60.2 |
| 2014 | 20.2 | 24.9 | 33.3 | 52.2 | 55.5 |
| 2015 | 23.6 | 20.9 | 24.5 | 34.6 | 33.4 |
| 2016 | 17.6 | 20.1 | 24.0 | 30.4 | 25.7 |
| 2017 | 14.2 | 20.7 | 24.2 | 30.4 | 24.6 |
| 2018 | 13.6 | 21.8 | 24.3 | 32.0 | 25.9 |
| 2019 | 14.8 | 23.0 | 24.4 | 33.2 | 26.7 |
| 2020 | 16.1 | 24.6 | 25.2 | 35.0 | 29.0 |
| 2021 | 19.0 | 23.8 | 24.2 | 33.1 | 25.9 |
| 2022 | 17.4 | 23.9 | 24.1 | 33.1 | 25.8 |

** Estimated concentrations shown in this table are model outputs reported within the last five days of each calendar year (e.g., 1999 is the model result on 12/31/1999).*

***Table 15: Grove Pond Well 8 Recommended Estimate of PFAS Concentrations***

| | *Annual PFAS Concentration (ng/L)* | | | | |
|---|---|---|---|---|---|
| *Year** | *PFOS* | *PFOA* | *PFHXS* | *PFHXA* | *PFHPA* |
| 1999 | 12.5 | 19.4 | 11.2 | 20.5 | 50.8 |
| 2000 | 13.2 | 20.1 | 9.5 | 17.0 | 47.6 |
| 2001 | 14.7 | 21.0 | 9.0 | 16.1 | 46.0 |
| 2002 | 16.5 | 22.5 | 11.4 | 20.6 | 45.6 |
| 2003 | 19.5 | 24.1 | 18.2 | 33.3 | 47.6 |
| 2004 | 22.8 | 24.9 | 21.3 | 39.4 | 49.7 |
| 2005 | 23.9 | 25.2 | 22.5 | 42.1 | 49.5 |
| 2006 | 25.0 | 25.6 | 24.3 | 45.5 | 49.6 |
| 2007 | 26.5 | 26.0 | 28.2 | 51.5 | 52.0 |
| 2008 | 27.5 | 26.6 | 33.1 | 58.0 | 55.1 |
| 2009 | 28.8 | 27.2 | 37.1 | 63.1 | 58.7 |
| 2010 | 30.4 | 27.7 | 33.5 | 59.5 | 57.8 |
| 2011 | 33.6 | 28.8 | 41.7 | 68.5 | 65.7 |
| 2012 | 35.6 | 30.0 | 46.6 | 72.7 | 72.0 |
| 2013 | 37.9 | 31.5 | 46.4 | 77.5 | 76.6 |
| 2014 | 41.7 | 32.8 | 44.4 | 75.0 | 77.3 |
| 2015 | 46.7 | 30.2 | 36.0 | 61.4 | 65.1 |
| 2016 | 46.1 | 29.2 | 32.3 | 57.8 | 59.2 |
| 2017 | 44.1 | 29.7 | 31.3 | 58.0 | 58.1 |
| 2018 | 44.6 | 31.4 | 31.6 | 59.3 | 59.5 |
| 2019 | 48.0 | 33.1 | 31.8 | 57.9 | 59.3 |
| 2020 | 51.4 | 35.5 | 33.3 | 57.9 | 61.1 |
| 2021 | 56.5 | 35.0 | 31.2 | 58.5 | 59.0 |
| 2022 | 56.3 | 35.0 | 31.0 | 58.6 | 58.8 |

** Estimated concentrations shown in this table are model outputs reported within the last five days of each calendar year (e.g., 1999 is the model result on 12/31/1999).*

**Digital Attachment 1: Previous Study Reports**